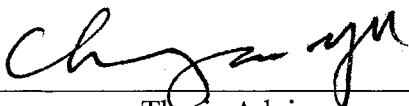STUDY ON PROTEIN-QUINONE

INTERACTION

By

TONG XIE

Bachelor of Science
Zhongshan University
Guangzhou, China
1990

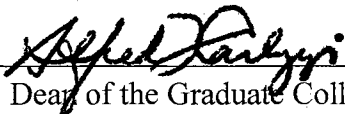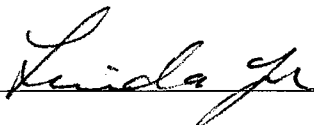Master of Science
Zhongshan University
Guangzhou, China
1993

Submitted to the Faculty of the
Graduate College of the
Oklahoma State University
in partial fulfillment of
the requirements for
the Degree of
DOCTOR OF PHILOSOPHY
May, 2001

STUDY ON PROTEIN-QUINONE

INTERACTION

Thesis Approved:

_____
Thesis Advisor

_____

_____

_____

_____
Dean of the Graduate College

ACKNOWLEDGEMENTS

TABLE OF CONTENTS

LIST OF TABLES

LIST OF FIGURES

LIST OF SCHEMES

NOMENCLATURE

ADP	adenosine diphosphate
APDP	N-[4-(p-azidosalicylamido)butly]-3'(2'-pyridyldithio)propionamide
ATP	adenosine triphosphate
Azido-Q	3-azido-2-methyl-5-methoxy-6-geranyl-1,4-benzoquinone
3-azido-Q_0C_{10}	3-azido-2-methoxy-5-methyl-6-decyl-1,4-benzoquinone
5-azido-Q_0C_{10}	5-azido-2,3-dimethoxy-6-decyl-1,4-benzoquinone
s-BDNP	2-sec-butyl-4,6-dinitrophenol
5-Br-Q_0C_{10}	5-bromo-2,3-dimethoxy-6-decyl-1,4-benzoquinone
BSA	bovine serum albumin
CcO	cytochrome c oxidase
5-Cl-Q_0C_{10}	5-chloro-2,3-dimethoxy-6-decyl-1,4-benzoquinone
cyt.	cytochrome
DBMIB	dibromothymoquinone, 2,5-dibromo-3-methyl-6-isopropylbenzoquinone
DTT	dithiothreitol
EDTA	ethylenedinitrilo-tetraacetic acid, disodium
EPR	electron paramagnetic resonance
ER	endoplasmic reticulum
$FADH_2$	flavin adenine dinucleotide, reduced form
FCCP	carbonycyanide-p-trifluoromethoxyl phenydrazone
GSH	glutathione (reduced form)
HPLC	high performance liquid chromatography

HQNO	heptylhydroxyquinoline-N-oxide
HRMS	high resolution mass spectrometry
kDa	kilodalton
MQ	menaquinone
NADH	nicotinamide adenine dinucleotide, reduced form
NQR	NADH-ubiquinone reductase
O.D.	optical density
PAGE	polyacrylamide gel electrophoresis
Pi, P	phosphate
PQ	plastoquinone
PDI	Protein Disulfide Isomerase
Q, UQ	ubiquinone
Q_0	2,3-dimethoxy-5-methyl-1,4-benzoquinone
Q_0C_{10}	2,3-dimethoxy-5-methyl-6-decyl-1,4-benzoquinone
$Q_0C_{10}Br$	2,3-Dimethoxy-5-methyl-6-(10-bromo)-decyl-1,4-benzoquinone
QCR	quinol cytochrome c reductase
RCR	respiratory control ratio
SCR	succinate cytochrome c reductase
SDS	sodium dodecylsulfate
SMP	submitochondrial particles
SQR	succinate ubiquinone reductase
TTFA	2-thenoyltrifluoroacetone
TLC	thin layer chromatography
UHDBT	5-n-undecyl-6-hydroxy-4,7-dioxobenzothiazole
UV	ultra violet

PART I

INTERACTION OF 5-HALO-UBIQUINONE DERIVATIVES WITH

MITOCHONDRIAL ELECTRON TRANSFER SYSTEM

CHAPTER I

INTRODUCTION

Mitochondrial Respiratory Chain

All living organisms continuously dissipate free energy to develop and maintain their highly ordered structures. This energy is supplied by their environment, such as food, substrates and other metabolites. A main form of energy in the cell is the energy-rich compound adenosine triphosphate (ATP), which in turn, can supply the energy for most of the energy-requiring processes elsewhere in the cell. A substantial part of the ATP present in most cells is synthesized in a process called oxidative phosphorylation. Mitochondrion is a specialized organelle whose primary function is oxidative phosphorylation.

Oxidative phosphorylation is carried out by a coupling reaction of two multienzyme complexes localized in the inner membrane of mitochondria of eukaryotic cells, in the thylakoid membrane of chloroplasts, in the plasma membrane of respiring prokaryotes or in the specialized membranes of photosynthetic bacteria. One multienzyme complex, known as the respiratory or electron transfer chain, catalyzes the exergonic oxidation of NADH or succinate by oxygen. The other multienzyme complex is the ATP synthetase complex, which catalyzes the endergonic synthesis of ATP from ADP and inorganic phosphate.

Components of the Respiratory Chain and Their Functions

The mitochondrial electron transfer chain, also called respiratory chain of mammalian mitochondria because of the final acceptor oxygen, is an assembly of more than twenty discrete carriers of electrons, which are mainly grouped into four multisubunit complexes: NADH-ubiquinone reductase (NQR, Complex I), succinate-ubiquinone reductase (SQR, Complex II),

ubiquinol-cytochrome c reductase (QCR, Complex III, cytochrome bc_1 complex), and

cytochrome c oxidase (CcO, Complex IV) (1). These four enzymes and ATP synthase (ATPase,

Complex V) are located in the mitochondrial inner membrane and account for most of its

membrane mass. Each complex in the electron transfer chain consists of several protein subunits

that are associated with a variety of redox active prosthetic groups with successively increasing

midpoint potentials (2).

Over the past two decades, investigators have been making much progress on the

mechanistic study of electron transfer and oxidative phosphorylation based on the availability of

biochemical studies of several complexes (3~8). The recent advances in the 3-dimentional X-ray

crystal structures have provided a final push in the study of these reactions. The arrangement of

these complexes and the agents that transfer electrons between them are illustrated in Scheme 1.1.

NADH and succinate, which are derived from the TCA cycle, β-oxidation of fatty acids

and amino acid oxidation, are oxidized by Complex I and Complex II to form NAD^+ and

fumarate, respectively, and to reduce ubiquinone. The electrons released from ubiquinol are

transferred to Complex III then Complex IV and finally to molecular oxygen. The electron

transfer through Complex I, Complex III, and Complex IV generates a membrane potential and

proton gradient that is used by ATP synthase to synthesize ATP.

Table 1.1 summarizes the characteristics of the mitochondrial complexes.

In the electron-transport process, electrons are transferred from NADH and $FADH_2$ (high

reducing condition) to O_2 *via* protein-bound redox centers. Coenzyme Q or ubiquinone, which is

ubiquitous in respiring organisms, carries electron from Complex I and II to Complex III, while

cytochrome c carries of electron from Complex III to Complex IV.

Respiratory Control and the Concept of Coupling

Since molecular oxygen acts as the final electron acceptor in the mitochondrial

respiratory chain, the oxygen electrode has long been the most versatile tool for investigating the

I

Intermembrane
space

$2H^+$

Matrix
NADH
$+H^+$

$2e^-$

NAD$^+$

II

$2e^-$

succinate   fumarate

III

$4H^+$

Cyt c

Q

$2e^-$

$4H^+$

$1/2O_2 + 2H^+$

IV

$2H^+$

$2e^-$

H_2O

V

H^+

$++++$

ADP +Pi   ATP
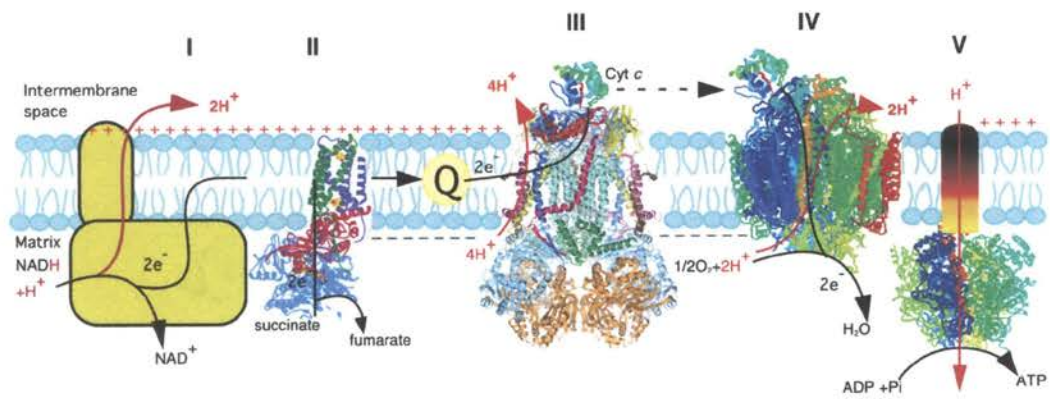
Scheme 1.1. Mitochondrial Respiratory Chain

4

Table 1.1. Characters of Some Components in the Bovine Heart Mitochondrial Membrane

Component	Concentration range (nmol/mg protein)	Molecular weight (Da)	No. of poly-peptides	Prosthetic groups	Midpoint potential (mV) [12]
NADH		709			−315
Complex I (NQR)	0.06~0.13	907,000[5]	43	FMN	−245~−335
				[2Fe-2S]N-1a	−375
				[2Fe-2S]N-1b	−250
				[2Fe-2S]N-2	−150
				[4Fe-4S]N-3,4	−250
				[4Fe-4S]N-5,6	−260
Succinate		118			30
Complex II (SQR)	0.19	127,000	5	FAD	−40
				[2Fe-2S] S-1	$0^{(63)}$
				[4Fe-4S] S-2	$−270^{(63)}$
				[3Fe-4S] S-3	$130^{(64)}$
				b_{560}	$−185^{(62)}$
ubiquinone	6~8	863			65
Complex III (QCR)	0.25~0.53	248,000[6]	11	b_{562} (b_H)	+30
				b_{566} (b_L)	−30
				c_1	230
				[2Fe-2S]	280
cytochrome c	0.8~1.02	12,327	1	c	235
Complex VI (CcO)	0.6~1	204.005[7]	13	a	210
				Cu_A	245
				Cu_B	340
				a_3	385
O_2		32			815
ATP synthetase	0.52~0.54	600,000[8]	14		
phospholipid	440~587				

proton (moves with an electron) circuit in the mitochondrial electron transfer system. The electrode directly determines only the rate of a single reaction ($O_2 + 4e^- + 2H^+ \rightarrow 2H_2O$), which is the final transfer of electrons to O_2. However, information on many other mitochondrial processes can be obtained simply by altering the incubation conditions so that the desired process becomes a significant step in determining the overall reaction rate.

The oxygen uptake trace shown in Figure 1.1 is typical of measurements made with a Clark oxygen electrode. The respiratory states in mitochondrial studies are explained below according to the order of addition of agents during an experiment (9):

State 1: mitochondria alone (in the presence of Pi, Mg^{2+})

State 2: substrate added, respiration low due to lack of ADP

State 3: a limited amount of ADP added, allowing rapid respiration

State 4: all ADP converted to ATP, respiration slows

State 5: anoxia

Only the terms "state 3" and "state 4" continue to be commonly used in the 1990s. The ratio of the state 3 to state 4 respiration is the respiratory control ratio (RCR), which provides a measure of the coupling status of the mitochondria. In poorly coupled or uncoupled mitochondria, state 4 respiration is high, and RCR approaches a value of 1.

The dependence of substrate oxidation on the presence of a phosphate acceptor indicates that, in coupled mitochondria, electron transfer and ATP synthesis are geared to each other. Unless the energy released during electron transport is used in some energy-dependent process such as ATP synthesis or ion transport, oxidation of substrate is limited. Therefore, the true index of coupling is the "state 4" respiration which shows how readily the oxidative energy can be dissipated when it is not being utilized. In perfectly coupled mitochondria, this rate is expected to be zero (10).

The foregoing thermodynamic studies suggest that oxidation of NADH, FADH$_2$, and ascorbate by O_2 are associated with the synthesis of three, two, and one ATP molecules,

State 1   State 2   State 3   State 4   State 5
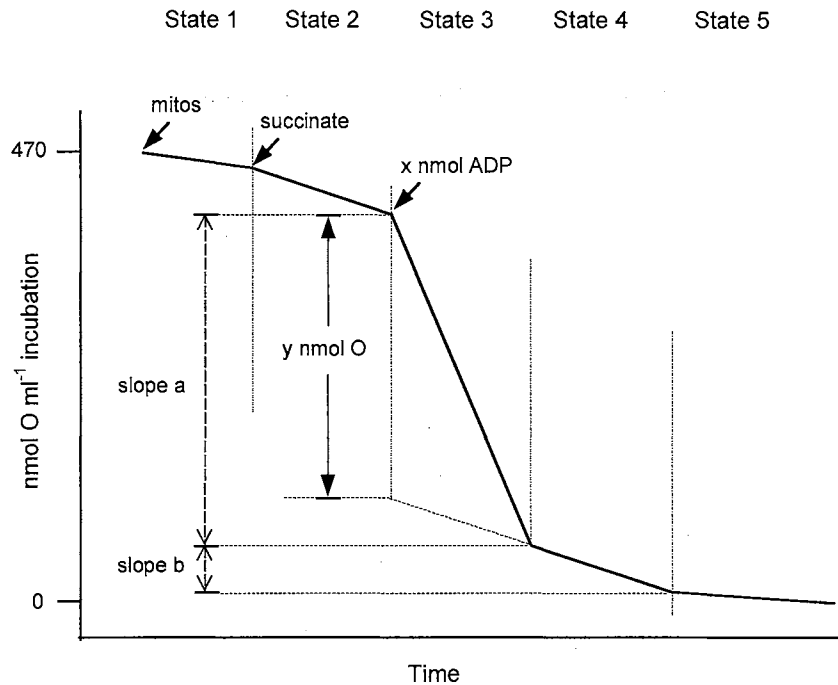
Figure 1.1. <u>Respiratory States and Determination of P/O Ratio.</u> Mitochondria were added to an oxygen-electrode chamber containing phosphate buffer, followed by succinate as substrate. A limited amount of ADP is added, which allows the ATP synthase to synthesize ATP coupled to proton re-entry across the membrane. When ADP is exhausted, respiration slows and finally anoxia is attained. The controlled respiration prior to addition of ADP, which is strictly termed "state 2", is functionally the same as state 4, and the latter term is usually used for both states. The respiratory control ratio is calculated by state 3 respiration divided by state 4 respiration, which is slope a/slope b in the figure. The oxygen uptake during the accelerated state 3 respiration due to the known amount of ADP can be quantified allowing a P/O ratio to be calculated. It is x/y (moles ATP synthesized per mol O uptake) in the figure.

respectively. This stoichiometry, called the P/O ratio, has been confirmed experimentally through O_2 uptake by resting and active mitochondria (Figure 1.1).

Chemical Structure and Physical Properties of Coenzyme Q Homologs

The naturally occurring quinones belong to the class of benzoquinones and naphthoquinones. Chemically the quinone molecules can be considered as two parts. The quinone ring is active in oxidation-reduction and acid-base reactions. The polyisoprenoid chain is responsible for the hydrophobic properties.

Coenzyme Q or ubiquinone (2,3-dimethoxy-5-methyl-6-polyprenyl-1,4-benzoquinone) is uniquely designed as an electron and proton carrier within the lipid phase of membrane. It freely diffuses through the membrane because of the hydrophobic nature of the isoprenoid tail. This side chain in the 6 position of the benzoquinone ring ranges from 6 to 10 isoprenoid units, mainly Q_6 in yeast, Q_8 in some bacteria, and Q_{10} in many vertebrates (Scheme 1.2a) (11). Most respiratory chain dehydrogenases transfer reducing equivalents to ubiquinone (UQ, in mitochondria), menaquinone (MQ, in fermentative bacteria) or plastoquinone (PQ, in chloroplast) (Scheme 1.2a).

Ubiquinone (UQ) undergoes a $2H^+ + 2e^-$ reduction to form ubiquinol (UQH$_2$). The quinone can exist in three different redox states: quinol, semiquinone, and quinone. In each of these redox states, the quinone species can be protonated/deprotonated with one or two protons (12). Studies on the rate of oxidation of quinol by artificial or biological electron acceptors have led to a scheme where the quinol is first deprotonated to the quinol anion followed by oxidization to the semiquinone. Thus, the quinol oxidation proceeds *via* a sequence of alternating deprotonation and oxidation steps, of which the deprotonation steps are assumed to be non-rate-limiting. The first deprotonation step is likely to occur in a more hydrophilic environment. When the quinol is bound to an enzyme, stabilization of the intermediate QH⁻ (transiently in the course of oxidation of quinol) would favor oxidation of quinol (13,14)(Scheme 1.2b).

8

a. Structure of ubiquinone and related redox carriers

| Ubiquinone | Menaquinone | Plastoquinone |

$$R = -(CH_2 - CH = \underset{\underset{CH_3}{|}}{C} - CH_2)_nH, \qquad n = 6 \sim 10$$
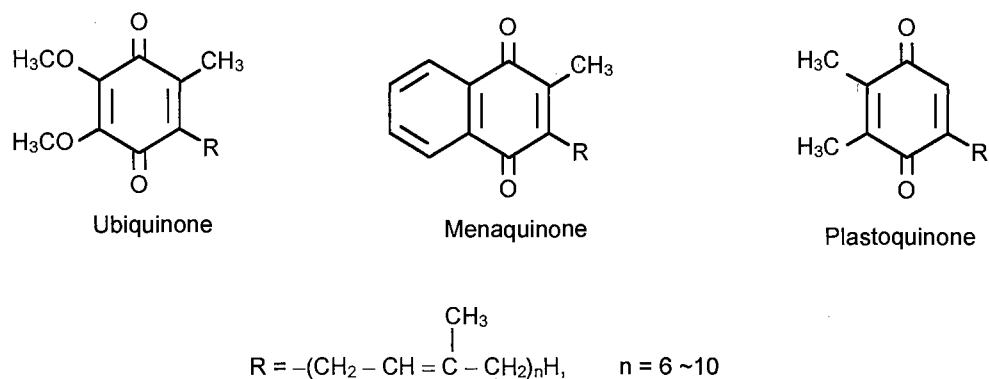
b. Ubiquinone function as an electron and hydrogen carriers

| Ubiquinone (oxidized) | Ubisemiquinone anion | Ubiquinol (reduced) |
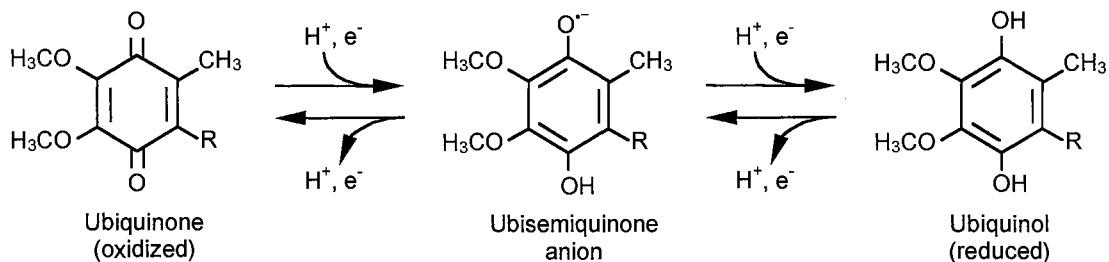
Scheme 1.2. <u>Structure and Function of Ubiquinone and Related Redox Carriers</u>

9

A traditional approach in studying the sequence of the electron transfer chain carriers has been to measure their midpoint or standard oxidation-reduction potentials which allows them to be placed on an electropotential scale. Information about the midpoint potentials of the carriers is also useful in establishing the spans that are capable of yielding sufficient energy for ATP synthesis (Table 1.1).

Midpoint potentials of the various coenzyme Q homologs can be determined by polarography or by reductive titration. There is variation in the values reported from pure compounds and for quinones in various organelles, as shown in Table 1.2. The most frequently quoted midpoint potential value for isolated coenzyme Q is +104 mV to +112 mV (54). For beef heart submitochondrial particles, it is +65 mV (46); for plant mitochondria, +70 mV (55); and for the ubiquinone/ubiquinol couple in *Rhodopseudomonas* it is +92 mV (56). The semiquinone forms of many substituted benzoquinones give high midpoint potentials (52). In the case of semiquinones, the midpoint potential of the radical forms may be lowered to a more normal level by stabilization through binding to a corresponding apolipoprotein (51).

Structural Requirement for Q as Electron Transfer Intermediate

The availability of a reconstitutively active PL- and Q-depleted SQR, QCR and CcO provided us with the opportunity to study the role of ubiquinone in these complexes using synthetic Q analogs and quinone-like inhibitors. One of the approaches of studying Q-protein interactions and Q-binding sites of the Q-mediated electron transfer complexes is to elucidate the structural requirements for Q using various synthetic Q-derivatives with variations in the length and saturation of the isoprenoid side chain and quinone nucleus (15). The structural requirements for Q to serve as an electron donor and acceptor differ significantly. Over the past 20 years, our lab has systematically synthesized various Q as electron acceptors, donors, and mediators in an attempt to understand the structural requirements for the Q function in the mitochondrial electron transfer chain (16).

10

Table 1.2. Midpoint Potential of Coenzyme Q Homologs
and Related Compounds

Source of quinone	Redox couple or conditions	Midpoint potential	Ref.
mitochondria	Ubiquinone/ubiquinol	$E_{m(7.0)}$ = +104 mV	45
Submitochondrial particles	Ubiquinone/ubiquinol	$E_{m(7.0)}$ = +65 mV	46
Synthetic ubiquinones	Polarography	$E_{m(7.4)}$ = +98 mV	47
	Reductive titration	$E_{m(7.0)}$ = +112 mV	48
QCR (Complex III)	Ubiquinol/ubiquinone	E_m = +30 mV	
	Ubiquinol/semiquinone	E_m = +300 mV	49
	Ubisemiquinol/ubiquinone	E_m = −300 mV	
SQR (Complex II)	Q/QH$_2$	$E_{m(7.0)}$ = +84 mV	50
	Q$^{\cdot-}$/QH$_2$	$E_{m(7.0)}$ = +204 mV	
SCR	Q/semiquinone	$E_{m(7.4)}$ = +140 mV	51
Synthetic ubiquinol-1	QH$_2$/Q	E_0 = +490 mV	52
	QH$^-$/QH$^{\cdot}$	E_0 = +191 mV	53

$E = E_0 + (RT/nF) \ln([ox]/[red])$

Standard redox potential E_0 is the redox potential when all components are in their standard states.

$E_{h, pH=x} = E_{m, pH=x} + (RT/F) \ln([ox]/[red])$

Mid-point redox potential $E_{m, pH=x}$ is the redox potential when the reduced component is in the same concentration of oxidized component and pH is in certain value.

11

Alkyl Side Chain at 6-Position

The alkyl side chains vary in chain length, degree of saturation, and location of double bonds. When Q is used as an electron acceptor for succinate-ubiquinone reductase, an alkyl side-chain of 6 or more carbons is needed to obtain maximum activity. However, when Q is used as an electron donor for ubiquinol-cytochrome c reductase or mediator in succinate-cytochrome c reductase, an alkyl side-chain of 10 carbons is required for maximum efficacy. Q derivatives with alkyl side chains significantly longer than 10 carbons have less activity. This is due mainly to the lack of a proper dispersion condition for these highly hydrophobic derivatives. (15).

Introduction of one or two isolated double bonds into the alkyl side chain of Q has little effect on electron-transfer activity. The coenzyme Q_1 and Q_2 analogs, 2,3-dimethoxy-5-methyl-6-pentyl-1,4-benzoquinone (Q_0C_5) and 2,3-dimethoxy-5-methyl-6-decyl-1,4-benzoquinone (Q_0C_{10}) were found to be as good in restoring activity as the two coenzyme Q homologues themselves. *Trans* derivatives were found to have slightly higher activity than their *cis*-counterpart.

However, introduction of a conjugated double bond system drastically reduces electron-transfer efficiency, and the effect depends on its location in the alkyl side chain. The flexibility in the portion of the alkyl side chain immediately adjacent to the benzoquinone ring is required for efficient electron-transfer activity of Q (17).

Substitutions at 2, 3, 5-Positions of Benzoquinone Ring

The effect of substituents on the 1,4-benzoquinone ring of Q on its electron-transfer activity was studied by using synthetic derivatives that have a decyl or geranyl side chain at the 6-position and various arrangements of methyl, methoxy, and hydrogen at the 2-, 3- and 5-positions of the benzoquinone ring.

When Q is used as an electron acceptor for succinate-quinone reductase, the methyl group at the 5-position is less important than the methoxy groups at the 2- and 3-positions (17). Replacing the 5-methyl group with hydrogen causes a slight increase in activity. However, replacing one or both of the 2- and 3-methoxy groups with a methyl completely abolishes electron-acceptor activity. Replacing the 3-methoxy group with hydrogen results in a complete loss of electron-acceptor activity, whereas, replacing the 2-methoxy with hydrogen results in 30% of original activity. This suggests that the 3-methoxy group is more critical than the methoxy group at the 2-position.

When Q serves as an electron donor for ubiquinol-cytochrome c, the structural requirements for substituents on the benzoquinone ring are less strict (Table 1.3). All 1,4-benzoquinol derivatives examined show partial activity when used as electron donors. Derivatives that possess one unsubstituted position, show substrate inhibition at high concentrations, a phenomenon not observed with fully substituted derivatives.

A group of 5-hydroxy analogues of coenzyme Q with various side chains were synthesized and tested. More than 50% inhibition of activity on succinoxidase and NADH oxidase systems was reported in many of these hydroxy Q analogues (11,60).

The structural requirements for quinone derivatives to be reduced by succinate-cytochrome c reductase are also less specific than those for succinate-quinone reductase. Replacing one or both methoxy groups at position 2 or 3 with a methyl and keeping the 5-position unsubstituted (plastoquinone derivatives) yields derivatives with no acceptor activity for succinate-Q reductase. However, these derivatives can be reduced by succinate in the presence of succinate-cytochrome c reductase.

Quinone-Like Inhibitors

It is generally assumed that quinone-like inhibitors can fit in the quinone site of Q-binding protein. Certain compounds appear to inhibit ubiquinone function by competing with the

Table 1.3. Comparison of Electron-Transfer Activity of Q-Derivatives

Q derivatives*	R2	R3	R5	R6	Activity (%)		Ref.
					As acceptor for SQR	As donor for QCR	
Q_0C_{10}	MeO	MeO	Me	decyl	100	100	35
Q_2	MeO	MeO	Me	geranyl	100	100	15
1,4-benzoquinone	H	H	H	H	0	0	57
2-Me-Q_0C_{10}	Me	MeO	Me	decyl	0	15	17
3-Me-Q_0C_{10}	MeO	Me	Me	decyl	0	14	17
5-Me-PQ_0C_{10}	Me	Me	Me	decyl	0	20	17
2-H-Q_0C_{10}	H	MeO	Me	decyl	29	54	17
3-H-Q_0C_{10}	MeO	H	Me	decyl	0	27	17
2-H-5-Me-PQ_0C_{10}	H	Me	Me	decyl	32	22	17
3-H-5-Me-PQ_0C_{10}	Me	H	Me	decyl	0	20	17
5-H-Q_0C_{10}	MeO	MeO	H	decyl	117	91	17
2-Me-5-H-Q_0C_{10}	Me	MeO	H	decyl	18	25	17
3-Me-5-H-Q_0C_{10}	MeO	Me	H	decyl	9	23	17
PQ_0C_{10}	Me	Me	H	decyl	0	27	17
3,5-Di-H-Q_0C_{10}	MeO	H	H	decyl	0	6	17
2,5-Di-H-Q_0C_{10}	H	MeO	H	decyl	30	11	17
5-MeO-PQ_0C_{10}	Me	Me	MeO	decyl	0	20	17

quinone for an enzyme active site. s-BDNP(2-sec-butyl-4,6-dinitrophenol) is a well-characterized inhibitor and has been employed to test quinone sites in many different quinone-binding proteins. Piericidin and rotenone are inhibitors for complex I. thenoyltrifluoroacetone (TTFA) and carboxin are inhibitors for complex II. heptylhydroxyquinoline-N-oxide (HQNO) and Antimycin are Q_i site inhibitors for bc_1 complex. stigmatellin and 5-n-undecyl-6-hydroxy-4,7-dioxobenzothiazole (UHDBT) are Q_o site inhibitors for bc_1 complex. The ubiquinone analog dibromothymoquinone, 2,5-dibromo-3-methyl-6-isopropylbenzoquinone (DBMIB), reported to block electron transport in chloroplasts at the level of plastoquinone, was subsequently found to act as a competitive inhibitor in bovine heart mitochondria at the level of the bc_1 cytochromes. Coenzyme Q reversible inhibition of electron transport in *Escherichia coli* by DBMIB has also been shown (11).

All of these inhibitors are antagonists with structural similarities to ubiquinone. However, they cannot function as quinone to transfer electrons. The structures of some of these compounds are shown in Scheme 1.3. Quinone-like inhibitors have been extensively used in the study of Q:protein interactions (18).

Two Mechanisms for Q Function on Electron Transfer

Electron transfer within complexes is ensured by the presence of mobile components shuttling electrons between pairs of fixed redox components. While cytochrome c has been considered as the mobile component between bc_1 complex (Complex III) and cytochrome c oxidase (Complex IV), a common pool of ubiquinone has been postulated to receive electrons from either NADH dehydrogenase (Complex I), succinate dehydrogenase (Complex II) or other mitochondrial flavin-linked dehydrogenase systems to reduce Complex III. Quinone serves as a non-protein electron carrier in the electron transfer system.

It has been proposed that quinone functions as a redox pool which shuttles electrons between complexes and the cytochromes in the mitochondrial electron transport system (19,20).

15
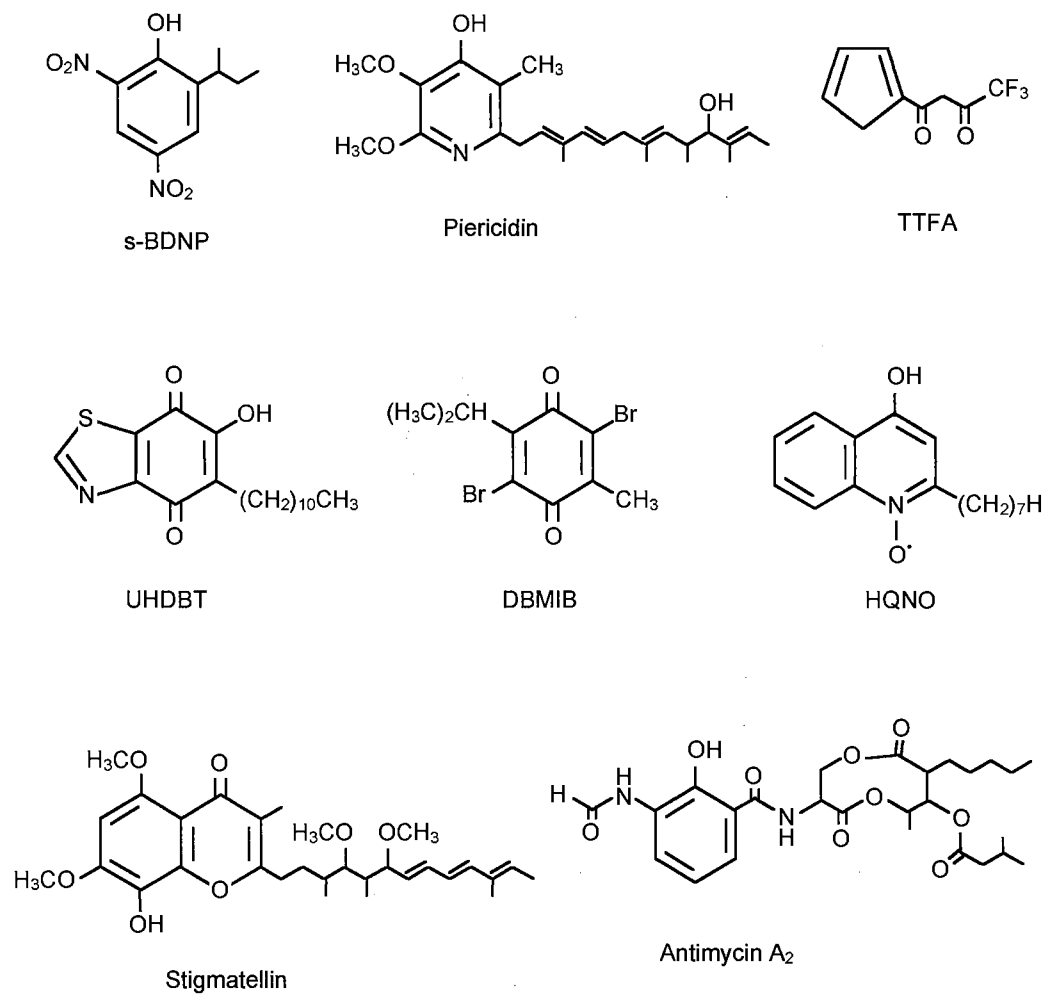
Scheme 1.3. Structural Formula of Inhibitors for Electron Transfer

16

The Q pool hypothesis is based on the following findings of quinone:

1. relatively small molecular size

2. lipophilic nature

3. relative abundance of Q compared to other redox components in the inner mitochondrial membrane (Table 1.1)

4. many enzymes can deliver electrons to quinone whereas quinol is generally dehydrogenated by only one type of enzyme (19)

5. dynamic and kinetics of its oxidation-reduction reaction (21)

This apparent pool behavior implied that ubiquinone is a homogeneous mobile carrier in the hydrocarbon domain of the membrane and that it could shuttle reducing equivalents between spatially separated redox protein complexes.

On the other hand, some studies (22) indicate the heterogeneity in the Q population of the inner mitochondrial membrane. Quinone is proposed to be largely or totally bound as a prosthetic group of specific Q-binding proteins present in the complexes. Therefore, electron transfer occurs by direct collision of prosthetic groups of different complexes. The observed pool behavior in mitochondrial respiratory chain is not due to the free diffusion of ubiquinone molecules, but through stoichiometric complexes between the two enzymes, which are formed and reformed at rates higher than the rate of electron transfer (58,59)

The identification of the Q-binding proteins in mitochondrial NADH-ubiquinone reductase (23), succinate-ubiquinone reductase (24) and ubiquinol-cytochrome c reductase (25) supports the idea that a Q-protein complex (26) is the active species during electron transfer. As an evidence of this view, EPR spectra of native and reconstituted membranes revealed stable forms of ubisemiquinone. Since ubisemiquinone dissimulates rapidly, the long-lasting form must be tightly bound and stabilized by a specific protein. However, protein-bound ubiquinone makes

up only a small portion of the total ubiquinone present in the mitochondrial inner membrane. The quinone contents in SCR, SQR, QCR are reported to be approximately 1:1 molar ratio (26).

The hypotheses that ubiquinone functions as a mobile pool (27) and that Q binds to protein as a prosthetic group (26) are compatible, if bound quinone is capable of equilibrating with the free quinone by both association-dissociation and Q-Q interaction. Both schools of thought regarding the reaction mechanism of Q acknowledge the presence of specific Q-binding sites in electron transfer complexes. Quinone-binding sites are clearly established by X-ray crystallographic studies in cytochrome bc_1 complex (4), and by photo affinity labeling (28,29) and molecular genetic (30,31) approaches in succinate-ubiquinone reductase.

Objective of This Study

The participation of ubiquinone (Q) in mitochondrial electron-transfer chain is well established (32). However, the interaction between Q and protein and the reaction mechanism of Q-mediated electron transfer are not yet fully understood.

In this study, as an effort to understand the reaction mechanism of quinone-mediated electron transfer, we synthesized a series of ubiquinone-derivatives with a bromine or chlorine atom at 5-position and different alkyl side chains at 6-position of a benzoquinone ring [5-halo-2,3-dimethoxy-6-alkyl-1,4-benzoquinone], and compared their chemical properties and electron transfer activities with Q_0C_{10}.

Redox midpoint potential of 5-bromo- and 5-chloro-Q derivatives can be determined from the ratio of reduced and oxidized forms of known Q. The effect on electron transfer by these 5-halo-Q derivatives has been studied among protein complexes in the mitochondrial electron-transfer chain, and was shown to result in a decrease in energy coupling efficiency and lower P/O ratio. These derivatives have also been shown to decrease state 3 respiration of rat liver mitochondria. Details of the interaction of 5-halo-Q derivatives in the electron transfer complexes will be discussed in the later chapters.

CHAPTER II

EXPERIMENTAL PROCEDURES

Materials

Cytochrome c, Type III, from horse heart, and 2,3-dimethoxy-5-methyl-1,4-

benzoquinone (Q_0) and bovine serum albumin were purchased from Sigma; silica gel G thin layer

plates from Analtech; 2,3-dimethoxy-5-methyl-6-decyl-1,4-benzoquinone (Q_0C_{10}) was

synthesized as previously reported (33). Azolectin (crude soybean phospholipids) was a product

of Associate Concentrate and partially purified according to Sone et al (34). Other chemicals

were of the highest purity commercially available.

Membrane proteins were prepared from bovine mitochondria or SMP. Mitochondria

were prepared from fresh rat livers.

Major Equipment for Analysis

Absorption spectra were measured in a Shimadzu spectrophotometer, model 2101PC.

^{1}H NMR spectra were measured in a Varian XL-400 NMR spectrometer.

The molecular weights of the Q derivatives were determined with a V6 ZAB-2SE high

resolution mass spectrometer.

The proton pumping assay was performed using a Beckman model 39849 electrode, and

an Accument Model 10 (Fisher Scientific) pH meter.

The consumption of oxygen was measured by YSI Model 53 Biological Oxygen Monitor.

The Q components of extract from mitochondria were analyzed by Waters'

MILLIPORE* high performance liquid chromatography (HPLC) system.

Synthesis of 5-Bromo-2,3-Dimethoxy-6-Alkyl-1,4-Benzoquinones and

5-Chloro-2,3-Dimethoxy-6-Alkyl-1,4-Benzoquinones

The method used for the synthesis of 5-bromo- and 5-chloro-Q derivatives are

summarized in Scheme 1.4.

5-Bromo-2,3-dimethoxy-6-methyl-1,4-benzoquinone (5-Br-Q_0C_1): To a solution of 2,3-

dimethoxy-5-hydro-6-methyl-1,4-benzoquinone (Q_0 or 5-H-Q_0C_1) (180 mg, 1 mmol) in 5 ml of

acetic acid, hydrobromic acid (5 ml, 48%) in acetic acid was added. The mixture was stirred at

room temperature for 30 min, diluted with 40 ml of water, and extracted with ether. The ether

extract was washed with H_2O and dried over anhydrous Na_2SO_4. One gram of Ag_2O was added

to the dried ether solution and the mixture was stirred for 1 hour at room temperature. The solid

phase was removed by filtration, and the filtrate solution was rotary evaporated. The crude

product was purified by preparative thin layer chromatography (TLC) developed by diethyl ether-

hexane, 1:3. The yield was 92%. 5-Br-Q_0C_1 is red crystalline. m.p 58-60°C. ^{1}H NMR (CDCl$_3$):

2.20 (s, 3H), 4.02 (s, 3H), 4.06 (s, 3H) ppm. Mass spectrometry (MS) (m/z), 260 (M), 262

(M+2); high resolution mass spectrometry (HRMS), 259.9681 (cal. 259.9684).

By using the same method, a series of 5-bromo- and 5-chloro-Q derivatives were

synthesized. Starting materials, such as 2,3-dimethoxy-5-propy-1,4-benzoquinone, 2,3-

dimethoxy-5-pentyl-1,4-benzoquinone, and 2,3-dimethoxy-5-decyl-1,4-benzoquinone, were

prepared according to the methods described previously (21, 22).

5-Bromo-2,3-dimethoxy-6-propyl-1,4-benzoquinone (5-Br-Q_0C_3): Red oil. ^{1}H NMR

(CDCl$_3$): 1.02 (t, 3H), 1.75 (m, 2H), 2.20 (t, 2H), 4.02 (s, 3H), 4.06 (s, 3H) ppm. MS(m/z): 288

(M); 290 (M+2).

5-Bromo-2,3-dimethoxy-6-pentyl-1,4-benzoquinone (5-Br-Q_0C_5): Red oil. 1H NMR

(CDCl$_3$): 0.89 (t, 3H), 1.28-1.75 (m, 6H), 2.20 (t, 2H), 4.02 (s, 3H), 4.06 (s, 3H) ppm. MS(m/z):

316 (M); 318 (M+2).
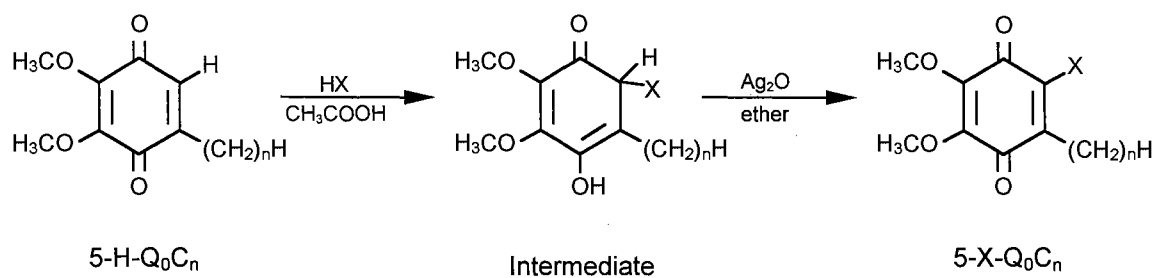
$X =$ Br or Cl

$n =$ 1   (5-Br-Q_0C_1 or 5-Cl-Q_0C_1)

         3   (5-Br-Q_0C_3 or 5-Cl-Q_0C_3)

         5   (5-Br-Q_0C_5 or 5-Cl-Q_0C_5)

      10   (5-Br-Q_0C_{10} or 5-Cl-Q_0C_{10})

Scheme 1.4.   Synthetic Pathway of 5-Bromo- and 5-Chloro-Q Derivatives

21

5-Bromo-2,3-dimethoxy-6-decyl-1,4-benzoquinone (5-Br-Q_0C_{10}): Red oil. ^{1}H NMR (CDCl$_3$): 0.89 (t, 3H), 1.23-1.6 (m, 16H) 2.20 (t, 2H), 4.02 (s, 3H), 4.06 (s, 3H) ppm. MS (m/z): 386 (M); 388 (M+2); HRMS, 386.1098 (cal. 386.1093).

5-Chloro-2,3-dimethoxy-6-methyl-1,4-benzoquinone (5-Cl-Q_0C_1): Red crystalline. ^{1}H NMR (CDCl$_3$): 2.18 (s, 3H), 4.01 (s, 3H), 4.05 (s, 3H) ppm. MS (m/z), 216 (M), 218 (M+2); HRMS, 216.0185 (cal. 216.0190).

5-Chloro-2,3-dimethoxy-6-propyl-1,4-benzoquinone (5-Cl-Q_0C_3): Red oil. ^{1}H NMR (CDCl$_3$): 0.95 (t, 3H), 1.62 (m, 2H) 2.16 (t, 2H), 4.01 (s, 3H), 4.04 (s, 3H) ppm. MS (m/z): 244 (M); 246 (M+2).

5-Chloro-2,3-dimethoxy-6-pentyl-1,4-benzoquinone (5-Cl-Q_0C_5): Red oil. ^{1}H NMR (CDCl$_3$): 0.89 (t, 3H), 1.20-1.62 (m, 6H), 2.15 (t, 2H), 4.01 (s, 3H), 4.04 (s, 3H) ppm. MS (m/z): 272 (M); 274 (M+2).

5-Chloro-2,3-dimethoxy-6-decyl-1,4-benzoquinone (5-Cl-Q_0C_{10}): Red oil. ^{1}H NMR (CDCl$_3$): 0.89 (t, 3H), 1.18-1.60 (m, 16H), 2.14 (t, 2H), 4.01 (s, 3H), 4.04 (s, 3H) ppm. MS(m/z): 342 (M); 344 (M+2).

Enzyme Preparations and Assays

Unless otherwise specified, all the operations were performed at 0~4 °C.

Concentration of cytochrome a, b, and c were determined spectrophotometrically. For cytochrome a, a difference millimolar extinction coefficients of 12 was used for reduced minus oxidized absorbance at 605 nm minus 700 nm. For cytochrome b, a difference millimolar extinction coefficients of 28.5 was used for reduced minus oxidized absorbance at 562 nm minus 575 nm. And for cytochrome c, a difference millimolar extinction coefficients of 18.5 was used for reduced minus oxidized absorbance at 552 nm minus 540 nm (39).

Protein assays were performed according to the Lowry methods in the presence of 1% SDS, using crystalline bovine serum albumin as standard (40).

Succinate Quinone Reductase

Succinate-ubiquinone reductase (SQR), was prepared from succinate-cytochrome c reductase by methods reported previously (22,36). SQR preparation was suspended in 50 mM sodium potassium phosphate buffer, pH 7.8, containing 0.2% sodium cholate and 10% glycerol.

Succinate-Q reductase activity was assayed, at room temperature, for its ability to catalyze TTFA sensitive Q-reduction or Q-stimulated DCIP reduction by succinate, using a Shimadzu UV-2101PC. The reaction mixture used for the Q reduction assay contains 100 μmol of sodium potassium phosphate buffer, pH 7.4, 20 μmol of succinate, 10 μmol of EDTA, 25 nmol of Q_0C_{10} and 0.01% n-dodecyl-β-maltoside in a total volume of 1 ml. The reaction of Q_0C_{10} was followed by measuring the decrease in absorption at 275 nm, using a millimolar extinction coefficient of 12.25 mmol^{-1}cm^{-1}(11). Alternatively, the reaction mixture (1 ml) for Q-stimulated DCIP reduction assay contained 40 μmol of DCIP, 100 μmol of sodium potassium phosphate buffer, pH 7.4, 20 μmol of succinate, 10 μmol of EDTA, 25 nmol of Q_0C_{10} and 0.01% of Triton X-100. The reduction of DCIP was followed by measuring the absorption decrease at 600 nm, using a millimolar extinction coefficient of 21 mmol^{-1}cm^{-1}.

Ubiquinol Cytochrome c Reductase and Succinate Cytochrome c Reductase

Ubiquinol-cytochrome c reductase was prepared from beef heart submitochondrial particles (SMP) as reported previously (36). The final preparation of ubiquinol-cytochrome c reductase was dispensed in 50 mM Tris-Cl buffer, pH 8.0, containing 0.66 M sucrose.

QCR activity assay: an appropriate amount of the bc_1 complex was added to an assay mixture (1 ml) containing 50 mM sodium potassium phosphate buffer, pH 7.0, 1mM EDTA, 100 μmol cytochrome c, and 25 μmol $Q_0C_{10}H_2$ (reduced form Q_0C_{10}) or specified reduced form Q derivative. The activity was determined by measuring the reduction of cytochrome c (an increase in absorbance at 550 nm) in a Shimadzu UV-2101PC spectrophotometer at room temperature. A

millimolar extinction coefficient of 18.5 mmol^{-1}cm^{-1} was used to calculate activity. The nonenzymatic oxidation of reduced Q, determined under the same conditions in the absence of enzyme, was subtracted from the total activity measured with enzyme.

Succinate-cytochrome c reductase (SCR) was prepared from beef heart submitochondrial particles (SMP) as reported previously (35). The method for SCR activity assay was similar to that for QCR activity, except the reduced Q substrate was replaced by 20 mM sodium succinate. The lipid-depleted SCR activity was assayed in the presence of 25 μM oxidized Q derivative, which acts as a mediator for electron transfer.

Cytochrome c Oxidase

Phospholipid-depleted cytochrome c oxidase was prepared from the beef heart SMP as reported previously (37). The final preparation of CcO was dispersed in 50 mM phosphate buffer, pH 7.4, containing 1.5% sodium cholate and stored in -80 °C until use.

CcO activity assay: the depleted CcO was reconstituted with asolectin in 1:100 ratio (w/w, protein:phospholipids) before the assay. An appropriate amount of the CcO was added to an assay mixture (1 ml) containing 50 mM sodium potassium phosphate buffer, pH 7.0; 1mM EDTA; 0.1% dodecyl maltoside; 100 μmol reduced cytochrome c. The activity was determined by measuring the oxidation of reduced form of cytochrome c^{red} (a decrease in absorbance at 550 nm) in a Shimadzu UV-2101PC spectrophotometer at room temperature. A millimolar extinction coefficient of 18.5 mmol^{-1}cm^{-1} was used to calculate the enzymatic activity.

An alternative method to assay the CcO activity is to measure the oxygen consumption of the enzymatic reaction system. The assay mixture contained 50 mM sodium potassium phosphate buffer, pH 7.4; 0.2 mM EDTA; 20 μM cytochrome c; and 30 mM sodium ascorbate in total volume of 1.3 ml. The reconstituted CcO/phospholipids was added into the assay mixture at room temperature with stirring. The specific activity was about 15~20 nmol O$_2$ consumed/s/nmol heme a.

<u>Intact Mitochondria</u>

Intact mitochondria were prepared from fresh rat liver and assayed by reported methods based on differential centrifugation (38). The final preparation of mitochondria was dispensed in 10 mM Tris-Cl buffer, pH 7.4, containing 250 mM of sucrose and 15 mM of EDTA.

Midpoint Potentials and Relative Hydrophobicity

The midpoint potentials of Q derivatives were determined from the ratio of reduced and oxidized forms of Q_0 and a given derivative in the system containing the given derivative and Q_0H_2 after a short exposure to pH 12 followed by neutralization with acid under anaerobic condition (17). The buffer system used was 50 % ethanol in 50 mM phosphate pH 7.0. Midpoint potential of 110 mV was used for Q_0 in the calculations.

The relative hydrophobicity of Q derivatives were determined by the R_f of thin layer chromatography using hexane/diethyl ether (4:1) mixture as developing solvent system.

Preparation of bc_1-phospholipid Vesicles

The bc_1-phospholipid (PL) vesicles were prepared by cholate dialysis method (41). The acetone-washed asolectin, 40 mg/ml, in 50 mM sodium potassium phosphate buffer, pH 7.4, containing 1.5% sodium cholate, was sonicated until clear and used for preparation of protein-PL vesicles. One ml of phospholipid solution was added to a protein solution containing 1 mg bc_1 and 1.5% sodium cholate. The PL-protein mixture was incubated for 30 min on ice, then dialyzed against 50 mM sodium potassium phosphate buffer, pH 7.4 (100× sample volumes), for 20 hours at 4 °C, with two changes of buffer. The bc_1 vesicles preparation was stored at 0 °C and its integrity was good within 48 hours.

Proton Pumping Assay for bc_1 Vesicles

The proton pumping assay was performed using a Beckman model 39849 electrode, and an Accument Model 10 (Fisher Scientific) pH meter. The bc_1 complex was incorporated into azolectin phospholipid vesicles (liposomes) (41). The bulk-phase proton gradient generated by protein-PL vesicles was determined with a pH electrode (for outward proton ejection) (42). The reaction mixture, in a final volume of 1.2 ml, contained 150 mM KCl, 5 mM MgCl$_2$, 10 μM cytochrome c, 1 μg valinomycin, 15 μM Q$_0$C$_{10}$H$_2$ or specified Q in reduced form; and 30 μl bc_1 vesicles (1 mg protein/ml). Electron flow was initiated by the addition of 5 nM of K$_3$[Fe(CN)$_6$]. The oxidized form of cytochrome c serves as an electron acceptor in the system. After pH equilibrium was reached, the uncoupler FCCP was added to render the liposome membrane freely permeable to protons and a second aliquot of ferricyanide was added. The protons released under these conditions are the "scalar" protons released by oxidation of reduced Q, as no contribution from the accumulation of vectorially translocated protons is possible in the presence of FCCP. One nmol HCl was added to the assay system as a pH standard. The resulting H$^+$/e$^-$ ratio was measured according to the pH changes by ferricyanide before and after the addition of FCCP.

Measurement of Oxygen Uptake and Determination of P/O for Mitochondria

The oxygen uptake in the presence of Q-derivatives was measured by SQR and CcO, using succinate as substrate. The reaction mixture, in a final volume of 1.3 ml, contained 50 μmol of Na/K phosphate buffer, pH 7.4; 10 μmol succinate; 500 nmol EDTA; 0.2% sodium cholate; 100 nmol cytochrome c; 30 nmol of Q-derivative and 0.2 mg CcO. The reaction was started by the addition of SQR (24 μg).

For P/O ratio determination, 1.3 ml assay mixture, contained 225 μmol sucrose; 20 μmol Na/K phosphate buffer, pH 7.4; 20 μmol KCl; 5 μmol MgCl$_2$; 1 μmol EDTA; and 1.3 μg BSA. Intact mitochondria preparation was incubated with specified quinone for 3 minutes at room

temperature. One mg (100ul, 10 mg/ml) protein of mitochondria was added for each assay. The state 4 and state 3 of respiration were stimulated by the additions of 30 μmol succinate, pH 7.4 and 250 nmol ADP, respectively.

Identification of Quinone Extracted from Mitochondria

The quinone species contained in rat liver mitochondria were identified and quantified by high performance liquid chromatography (HPLC).

Quinone content from certain mitochondrial membrane was extracted by following a published procedure (44). Methanol (−20 °C) was added to 2 ml of mitochondria (50 mg/ml) to yield a final volume of 10 ml and the mixture was sonicated immediately to denature the protein. Ubiquinone was extracted with 4×15 ml of hexane. The extracted sample in hexane was dried by rotary evaporation and re-dissolved in 0.5 ml of 95% ethanol. Coenzyme Q_{10} was extracted from control bovine mitochondrial membranes following the same method.

The sample in 95% ethanol was filtered through a 0.2 μm membrane, and loaded onto a Microsorb-MV® reverse phase column (C8, 5 μm). Synthetic Q_0C_{10}, 5-chloro-Q_0C_{10} and native coenzymes Q_{10} were used as standard quinone compounds for HPLC. Ubiquinones were eluted from the column with a linear gradient ranging from 90% to 100% methanol (v/v). The flow rate was 0.8 ml/min. The ubiquinone species contained in rat liver mitochondria was identified and quantified based on the retention time and peak area of known standard coenzyme Qs.

CHAPTER III

RESULTS AND DISCUSSION

Structures and Properties of 5-Bromo- and 5-Chloro-Q Derivatives

Scheme 1.4 shows the chemical structures of 5-bromo- and 5-chloro-Q derivatives. The spectroscopic properties of 5-bromo- and 5-chloro-Q derivatives are similar to those of 5-methyl-Q, but with small red shifts in both oxidized forms and reduced forms (Table 1.4).

The midpoint potentials (E_m) of 5-bromo- and 5-chloro-Q were found to be 142 mV and 148 mV, respectively, whereas E_m is 110 mV for the 5-hydro-Q counterpart and 100 mV for the 5-methyl-Q counterpart (Table 1.4). Little differences of E_m were obtained in Q derivatives with different length of alkyl side chain at 6- position. Introduction of an electron withdrawing group such as bromine or chlorine atom to the benzoquinone ring results in stabilization of the reduced form of the derivatives and thus increases the redox mid-point potential.

The relatively high midpoint potential of 5-halo-Q makes it easier to be reduced than native ubiquinone Q_{10} or the control Q_0C_{10}. Its reduced form would be more stable.

5-Bromo- and 5-Chloro-Q Derivatives as Electron Acceptors for SQR

Table 1.5 summarizes the maximum electron-acceptor activities of 5-bromo- and 5-chloro-Q derivatives, as compared to that of Q_0C_{10}. When Q derivatives serve as the electron acceptors for SQR, the halo- group substituted at 5-position decreased the quinone reduction rate. Even though the reduction rate is lower, the equilibrium concentrations are the same as the Q_0C_{10} control. This result agrees with the data of the 5-halo-Q's midpoint potential.

Table 1.4. Comparison of Characteristics of 5-Halo-Q Derivatives

Q-Derivatives	MW	R_f[1]	Wavelength (nm)[2]		Midpoint Potential [3] (mV)
			oxi	red	
Q_0 (5-H-Q_0C_1)	182	0.348	268.5	289.5	110
Q_0C_5 (5-Me-Q_0C_5)	238	0.414	279.0	291.0	100
Q_0C_{10} (5-Me-Q_0C_{10})	308	0.466	279.5	291.5	100
Q_0Br (5-Br-Q_0C_1)	260	0.361	293.0	297.5	
5-Br-Q_0C_3	288	0.415	295.2	298.0	142
5-Br-Q_0C_5	316	0.460	296.0	298.0	
5-Br-Q_0C_{10}	386	0.511	296.0	296.5	
Q_0Cl (5-Cl-Q_0C_1)	216	0.355	284.5	296.5	
5-Cl-Q_0C_3	244	0.417	287.0	296.0	148
5-Cl-Q_0C_5	272	0.457	288.0	298.0	
5-Cl-Q_0C_{10}	342	0.505	288.5	298.0	

1. R_fs were determined by TLC (thin layer chromatography), using hexane-ether, 4:1 as the developing solvent system.

2. The spectral measurements for Q derivatives were performed in 95% ethanol. The reduced form spectra were obtained after a few grain of $NaBH_4$ added.

3. The redox potentials were determined following the method described in "Experimental Procedures" of Chapter II.

Table 1.5. Comparison of Electron Transfer Activity of 5-Halo-Q Derivatives

Q-Derivatives	as Acceptor for SQR, %[1]	as Donor to cytochrome c[2], μM/min		as Mediator for SCR, %[5]
		Nonenzymatic[3] (absence of QCR)	Enzymatic[4] (presence of QCR)	
Q_0C_{10}	100	0.14	6.39	100
5-Br-Q_0C_1	22	4.10	0	52
5-Br-Q_0C_3	34	3.42	2.57	54
5-Br-Q_0C_5	39	2.43	4.38	57
5-Br-Q_0C_{10}	54	0.36	8.02	60
5-Cl-Q_0C_1	26	15.32	0	55
5-Cl-Q_0C_3	42	11.31	1.08	61
5-Cl-Q_0C_5	54	9.10	4.50	68
5-Cl-Q_0C_{10}	73	1.54	7.69	84

1. The electron-acceptor activities of Q-derivatives were measured by SQR using succinate as substrate. The reaction mixture, in a final volume of 1.0 ml, contained 50 mM of Na/K phosphate buffer, pH 7.4; 20 μmol succinate; 0.5 μM EDTA; 0.5% sodium cholate and 30 nmol of oxidized Q-derivative. The reduction of Q-derivative was spectrophotometrically followed by the decrease in the absorption at 278 nm for Q_0C_{10}, at corresponding wavelength for 5-halo-Q according to Table 1.4, after the addition of 1.2 μg SQR. The activity of Q_0C_{10} was considered as 100%.

2. The electron-donor activities were measured following the oxidation of reduced Q derivatives by cytochrome c.

3. Nonenzymatic oxidation of reduced Q-derivatives was measured by cytochrome c reduction in the absence of protein complex. The reaction mixture, in a final volume of 1.0 ml, contained 100 mM of Na/K phosphate buffer, pH 7.0; 0.3 μM EDTA; 100 μM cytochrome c. The interaction was measured by following the reduction of cytochrome c at 550 nm, after 25 nmol of reduced Q-derivative was added.

4. Enzymatic oxidation of reduced Q-derivatives by cytochrome c was measured by QCR. The assay mixture is the same as that used for nonenzymatic activity assay. QCR (1.2 μg) was added to the mixture, then reduced Q-derivative was added to start the reduction of cytochrome c. This activity is the difference between the total activity and the activity in nonenzymatic assay.

5. The method for SCR activity assay is described in the Experimental Procedures in Chapter II.

All the halo-Q derivatives show partial electron acceptor activities regarding the presence of alkyl side chain at 6-position of the benzoquinone ring. The electron acceptor activity increases slightly as size of 6-alkyl group increases. A long alkyl side chain does help the Q get close to the reaction center of SQR which is a membrane protein and should be surrounding by detergent or phospholipids.

Interaction of Reduced 5-Bromo and 5-Chloro-Q Derivatives with Cytochrome c

Unlike the ubiquinone Q_0C_{10}, which show little direct interaction with cytochrome c, 5-halo-Q derivatives with an alkyl side chain of less than five carbons equilibrate with cytochrome c freely in the absence of an electron transfer protein complex. The equilibrium is redox state and concentration dependent. Since the midpoint redox potentials of 5-halo-Q derivatives are lower than that of cytochrome c (235 mV), the following reaction is favored on the reduction of cytochrome c. As expected, the reaction is pH dependent. When pH is lower than 7, very little 5-halo-QH_2 is oxidized by cytochrome c.

$$5\text{-X-}QH_2 \;+\; 2\,\text{cyt.}c^{3+} \;\rightleftharpoons\; 5\text{-X-}Q \;+\; 2\,\text{cyt.}c^{2+} \;+\; 2\,H^+$$
$$X = \text{Br or Cl}$$
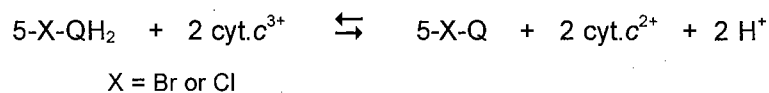
5-Halo-Q derivatives with an alkyl side chain of more than five carbons show little direct interaction with cytochrome c, but significantly increase the oxidation by cytochrome c in the presence of ubiquinol-cytochrome c reductase. The interactions between 5-halo-Q derivatives and cytochrome c in the absence and presence of QCR are shown in Table 1.5. The mediator activity of Q derivatives for SCR results from the sum of SQR, QCR and the nonenzymatic electron transfer.

Figure 1.2 shows the concentration dependent oxidation of reduced halo-Q derivatives by cytochrome c catalyzed by QCR. Unlike the normal enzymatic reaction when using Q_0C_{10} as electron donor, which has a hyperbolic curve, the QCR activity increased with increasing concentrations of 5-halo-Q derivatives, reached a maximum and then decreased.

31
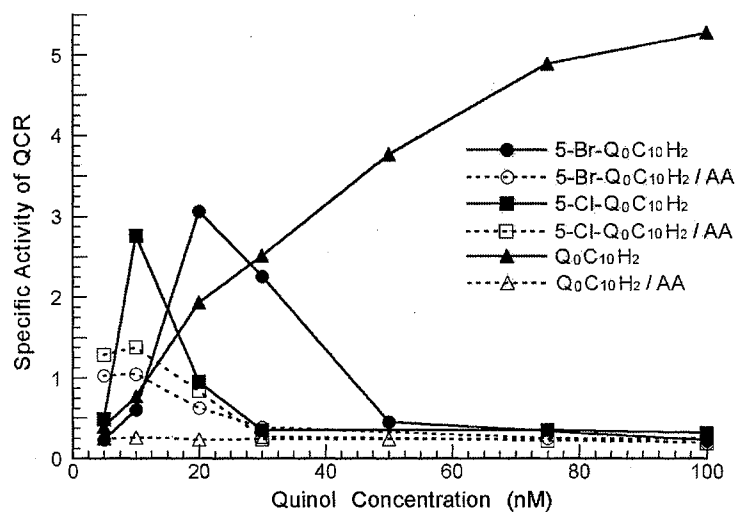
Figure 1.2. <u>Effect on QCR Activity by Quinol Concentration.</u> Assay mixture contained 100 mM Na/K phosphate buffer, pH 7.4; 100 µM cytochrome c and indicated concentration of quinol in 1.0 ml. The reduction of cytochrome c was followed at 550 nm. The reaction was started by the additions of 2 µg QCR containing 0.01% sodium cholate. Solid line corresponds to the assay with indicated quinone, and the dot line corresponds to the assay with indicated quinone and antimycin A.

At high concentration of reduced derivatives virtually no oxidation was observed. This substrate inhibition is an intriguing phenomenon.

It should be mentioned that this enzymatic electron-transfer reaction is partially sensitive to antimycin A, which is a Q_i site inhibitor for bc_1 complex (Figure 1.2). The sensitivity increased as the concentration of 5-halo-QH_2 increased.

5-Bromo- and 5-Chloro-Q Derivatives Act as Electron Mediators between SQR and CcO in the Electron Transfer Chain

The following pathway shows how in the presence of 5-halo-Q derivative, electron is transferred from succinate to oxygen in the presence of SQR and CcO, bypassing QCR.

$$\text{Succinate} \xrightarrow{\text{SQR}} \text{native Q} \xrightarrow{\text{QCR}} \text{cyt.}c \xrightarrow{\text{CcO}} O_2$$

$$\text{Succinate} \xrightarrow{\text{SQR}} \text{5-X-Q} \longrightarrow \text{cyt.}c \xrightarrow{\text{CcO}} O_2$$
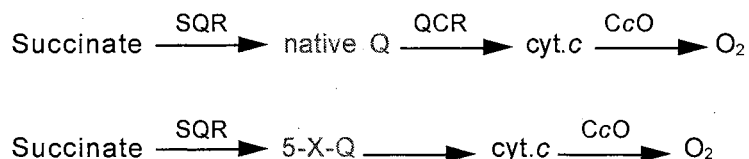
This bypassing function can be explained by the following observations.

The proton pumping activity in the cytochrome bc_1 region decreases when reduced 5-halo-Q derivatives is used as substrate (Table 1.6).

According to the protonmotive Q cycle pathway of electron transfer and proton translocation in the cytochrome bc_1 complex, when one electron is transferred to cytochrome c, two protons are released to the outer, positive side of the membrane and one molecule of ubiquinol is converted to ubisemiquinone at center N. This proton pumping function of bc_1 complex in vesicles results in a H^+/e^- ratio of 2.0.

The H^+/e^- value measured by $Q_0C_{10}H_2$, which serves as the control, indicates that the proton pumping activity of bc_1 complex in vesicles is 2. However, when 5-halo-QH_2 is used as the substrate for proton pumping assay, the H^+/e^- ratio dropped to about 1. This indicates that only one proton is pumped out when an electron is transferred.

Table 1.6. Proton Pumping Activity (H^+/e^- ratio) of Cytochrome bc_1 Vesicles

Reduced Q-derivatives	Proton pumping activity (H^+/e^-)
$Q_0C_{10}H_2$	2.01
5-Br-$Q_0C_1H_2$	1.03
5-Br-$Q_0C_{10}H_2$	1.07
5-Cl-$Q_0C_1H_2$	1.07
5-Cl-$Q_0C_{10}H_2$	1.19

The method of proton pumping assay for cytochrome bc_1 liposomes is described in "Experimental Procedures" of Chapter II. Reduced form specified QH_2, 15 μM, was added as electron donor. The ratio of the pH changes produced by the addition of equal amounts of ferricyanide, in the absence and presence of FCCP was taken as a measure of the H^+/e^- ratio for electron flow through the bc_1 complex.

The observation that oxidation of reduced 5-halo-Q derivatives in bc_1-phospholipid vesicles doesn't pump extra protons out from the vesicles supports the hypothesis that 5-halo-Q bypass the function of QCR.

An electron transfer system of SQR and CcO, in the absence of QCR is then reconstituted for the assay. Table 1.7 summarizes the oxygen uptake rates in the electron-transfer chain from SQR to CcO in the presence or absence of cytochrome c, using 5-halo-Q derivatives as an electron mediator.

The QCR bypassing ability of 5-halo-Q derivatives in the electron-transfer chain depends on the length of the side chain in the derivatives. Derivatives with an alkyl side chain of less than five carbons show significant bypassing function. The compounds with an alkyl side chain of ten carbons have much less bypass activities.

The reconstituted respiratory system has a much higher oxygen uptake rate in the presence of $5\text{-Br-}Q_0C_1$ or $5\text{-Cl-}Q_0C_1$ than other derivatives with longer 6-alkyl groups (Table 1.7). This is consistent with the higher rates observed for the electron transfer from reduced Q to cytochrome c (Table 1.5). We found that reduced form of $5\text{-halo-}Q_0C_n$ can be oxidized by oxygen either in the absence or in the presence of CcO in the reaction mixture. The former oxidation was not sensitive to cyanide.

The direct interaction between $5\text{-halo-}Q_0C_nH_2$ and oxygen is pH dependent. Figure 1.3 shows the effect of pH on O_2-uptake rate of SQR reduced $5\text{-Cl-}Q_0C_1$. The electron transfer from $5\text{-Cl-}Q_0C_1H_2$ to oxygen in presence of CcO is a pH insensitive enzymatic reaction in the range of pH 7.0 to 7.5. However, in the absence of CcO, the reaction is pH sensitive because it is a non-enzymatic reaction. Because reduced form 5-halo-Q is more stable at low pH, the O_2-uptake is relatively slow when pH value is lower than 6.5.

The electrons transferred from $5\text{-halo-}Q_0C_nH_2$ to molecule oxygen may take either or both of the following two pathways: The first pathway is part of the normal respiratory sequence, and is catalyzed by cytochrome c oxidase. In the second pathway, the electron goes to oxygen directly through a non-enzymatic reaction. This pathway allows the electron

Table 1.7. Oxygen Uptake Rates in the Electron-Transfer from SQR to CcO

Q-Derivatives	O_2 Up-take [ΔO nmol/min]	
	absence of cytochrome c	presence of cytochrome c
Q_0	1.20	2.30
Q_0C_{10}	0.65	1.77
5-Br-Q_0C_1	25.56	55.23
5-Br-Q_0C_3	–	20.32
5-Br-Q_0C_5	3.53	19.98
5-Br-Q_0C_{10}	1.53	8.59
5-Cl-Q_0C_1	24.97	66.09
5-Cl-Q_0C_3	–	23.45
5-Cl-Q_0C_5	2.64	18.21
5-Cl-Q_0C_{10}	1.65	8.99

The oxygen uptake in the presence of Q-derivatives was measured by SQR and CcO, using succinate as substrate. The reaction mixture, in a final volume of 1.3 ml, contained 50 mM of Na/K phosphate buffer, pH 7.4; 10 mM succinate; 0.5 mM EDTA, 0.2% sodium cholate, 100 µM cytochrome c, 30 nmol of Q-derivative and 0.2 mg CcO. The consummation of oxygen was measured by YSI Model 53 Biological Oxygen Monitor at room temperature with stirring. The reaction was started by the addition of 24 µg SQR.
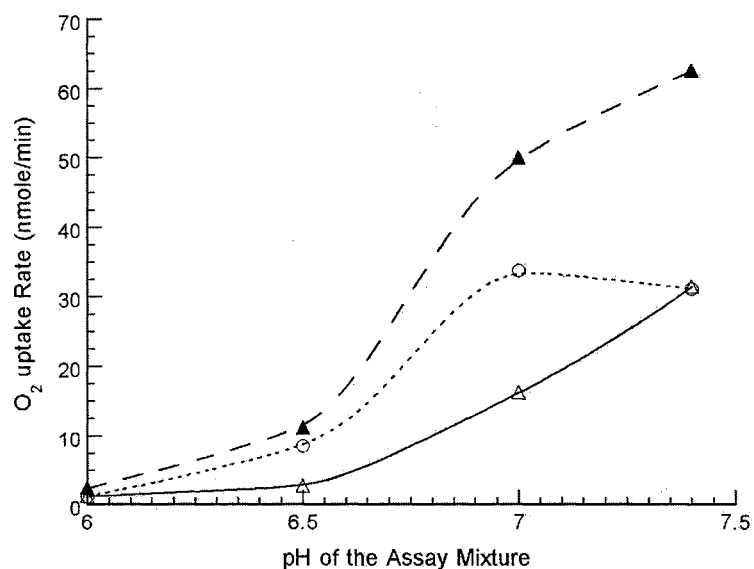
Figure 1.3. <u>pH Effect on the O_2-Uptake Rate of SQR Reduced 5-Cl-Q_0C_1.</u> The assay
conditions are the same as those described in Table 1.7. ▲ − − − − The reaction
system containing SQR, cytochrome c, CcO, and 5-Cl-Q_0C_1. The rate of O_2-uptake
is the sum of enzymatic and nonenzymatic reactions between reduced 5-Cl-$Q_0C_1H_2$
and oxygen. △ ——— The reaction system containing SQR and 5-Cl-Q_0C_1, but
absence of cytochrome c and CcO. That is a nonenzymatic reaction between
reduced 5-Cl-$Q_0C_1H_2$ and oxygen. O ·········· The difference of ▲ and △, which
indicates the pure enzymatic reaction between reduced 5-Cl-$Q_0C_1H_2$ and oxygen

transfer in respiratory chain bypass both QCR and CcO in the presence of 5-halo-Q.

$$5\text{-}X\text{-}Q_0C_nH_2 \longrightarrow \text{cyt. } c \xrightarrow{\ C c O\ } O_2 \quad \text{(cyanide sensitive, pH independent)}$$
$$5\text{-}X\text{-}Q_0C_nH_2 \longrightarrow O_2 \quad \text{(cyanide insensitive, pH dependent)}$$
$$X = \text{Br or Cl}$$
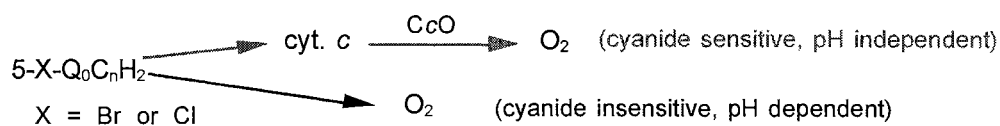
Effect of 5-Bromo- and 5-Chloro-Q Derivatives on
State 3 Respiration of Mitochondria

Compared to the control Q_0C_{10}, the oxygen uptake trace for intact mitochondria in the presence of 5-halo-Q_0C_{10} shows a higher state 4 respiratory and longer time for the state 3. As a result, more oxygen uptake for certain amounts of ATP synthesis. The electrons derived from NADH or succinate are bypassing ubiquinol-cytochrome c reductase region of respiratory chain and thus less energy is conserved, leading to a larger oxygen consumption in stimulation of respiration upon the addition of ADP.

In mitochondria, the low P/O ratio indicates that more oxygen or more energy is consumed in order to synthesize certain amounts of ATP. According to our oxygen uptake measurement for intact rat liver mitochondria, the P/O ratio decreased as the concentration of 5-halo-Q derivatives increases (Figure 1.4). Supported by this observation, we conclude that the presence of 5-halo-Q causes "energy leak" in the mitochondrial respiratory chain.

In Vivo Effect of 5-Cl-Q_0C_{10} on Energy Metabolism

The hypothesis that of 5-halo-Q bypasses QCR was supported by the above data conducted *in vitro*. For further confirmation, some *in vivo* experiments were performed. Twelve newborn rats were divided into 3 groups to study their energy metabolism by the growth rate analysis. Table 1.8 compares the growth rate in body weights of rats fed on none, Q_0C_{10} and 5-Cl-Q_0C_{10}. This experiment resulted in the following observations:

    1. Growth rate of rat fed with Q_0C_{10} is about the same as that of the control rat.

    2. Rat fed with 5-Cl-Q_0C_{10} had less body weight than the control.
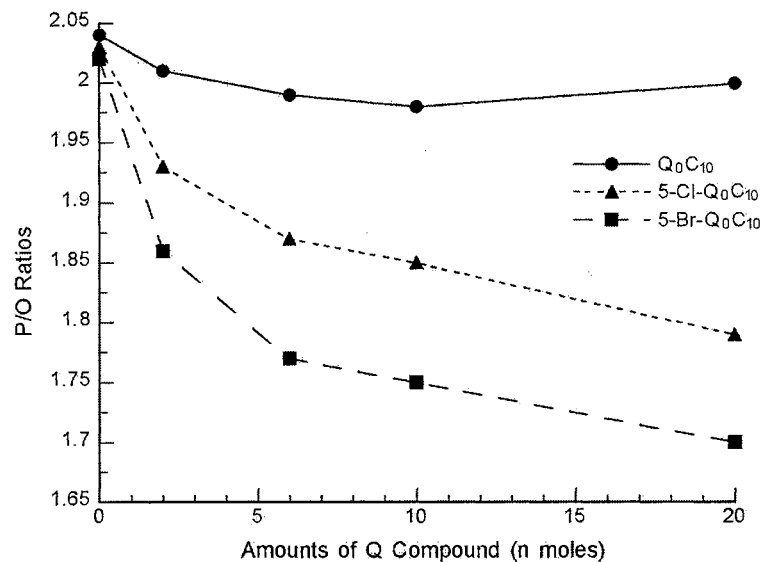
Figure 1.4. <u>The Effect of Quinone Concentration on the P/O Ratios of Mitochondria.</u>
Mitochondria were prepared from fresh rat liver, according to methods in "Experimental Procedures". 1.3 ml assay mixture, contained 225 µmol sucrose, 20 µmol Na/K phosphate buffer, pH 7.4, 20 µmol KCl, 5 µmol $MgCl_2$, 1 µmol EDTA, 1.3 µg BSA. The consumption of oxygen was measured by YSI Model 53 Biological Oxygen Monitor at room temperature with stirring. After 3 minutes incubation with quinone in the indicated amounts, 1 mg (100ul, 10 mg/ml) protein of mitochondria was added for each assay. The state 2 (state 4) respiration was stimulated by the additions of 30 µmol succinate, pH 7.4; and the state 3 respiration was stimulated by the additions of 250 nmole ADP after state 2 was stable.

Table 1.8. Effect on Body Weight of Rat Fed with 5-Cl-Q_0C_{10}

| Sex | Number of days fed with Q | Feeding Compound | | | | | |
| | | Control | | Q_0C_{10} | | 5-Cl-Q_0C_{10} | |
		Weight (g)	growth rate (%)	Weight (g)	growth rate (%)	Weight (g)	growth rate (%)
Female	0	60.5		61.5		58.8	
	10	94.5	56.2	93.0	51.2	91.5	55.6
	20	130.6	59.7	130.4	60.8	123.5	54.4
	40	185.0	89.9	185.5	89.6	176.2	89.6
Male	0	59.8		65.8		62.0	
	10	106.8	78.6	113.0	71.7	102.5	64.0
	20	176.5	116.6	190.8	118.2	153.0	81.5
	40	275.7	165.9	296.8	161.1	247.5	151.6

The rats for feeding treatment were 3-week old. Coarse feed was soaked in an EtOH solution of Q_0C_{10} or 5-Cl-Q_0C_{10} for 10 min to be saturated, then dried by air. Every pellet contained 0.5 μmol (0.2 mg) Q. Each rat was fed 8~10 pellets of fodder per day. Body weights were measured in the morning before feeding, using a digital scale. The growth rate was calculated by body weight increase divided by the initial body weight.

3. $5\text{-Cl-}Q_0C_{10}$ effect on male rat is higher than that on female rat.

4. $5\text{-Cl-}Q_0C_{10}$ effect is more significant in the first 20-day of feeding

In order to prove that the energy metabolism change is due to feeding of $5\text{-Cl-}Q_0C_{10}$, quinones were extracted by organic solvent from the liver mitochondria of these rats and were analyzed by HPLC. Figure 1.5 shows that the Q compound in the diet had been absorbed into the rate liver mitochondria without change in form. Based on the type of feeding, either Q_0C_{10} or $5\text{-Cl-}Q_0C_{10}$ was detected in the HPLC profile of Q extracted from liver mitochondria of the rats fed with corresponding Q. Even though the Q_0C_{10} and $5\text{-Cl-}Q_0C_{10}$ did not resolve very well under the conditions the HPLC was run, they were clearly different from the native Q_{10}.

The *in vivo* results indicate that $5\text{-Cl-}Q_0C_{10}$ can be absorbed by rat liver mitochondria. The presence of this $5\text{-Cl-}Q_0C_{10}$ compound in mitochondria could induce an "energy leak" in the energy metabolism. This indicates that less ATP is synthesized for same amount of energy consumed, or production of same amount of ATP requires more energy to be converted. As a result, the body weight of rats decreases with the same calories uptake.

Summary

In summary of this study, there are several findings on the interaction of 5-halo-ubiquinone derivatives with mitochondrial electron transfer system. First, synthetic 5-halo-Q_0C_n has higher midpoint potential than its Q_0C_n counterpart. Due to this relatively high midpoint potential, 5-halo-Q_0C_n has electron acceptor activity for SQR with a lower efficacy. The SQR reduced 5-halo-$Q_0C_nH_2$ can directly transfer electron to the electron terminal acceptor oxygen, bypassing protein complex QCR and CcO. This bypassing effect of 5-halo-ubiquinone derivatives decreases as the length of alkyl side chain at position 6 increases. Finally, the bypass ability of 5-halo-Q leads to a low P/O ratio for mitochondrial oxidative phosphorylation. The results from *in vivo* experiment support the idea that 5-halo-quinone have the bypass effect on the energy metabolism.

41
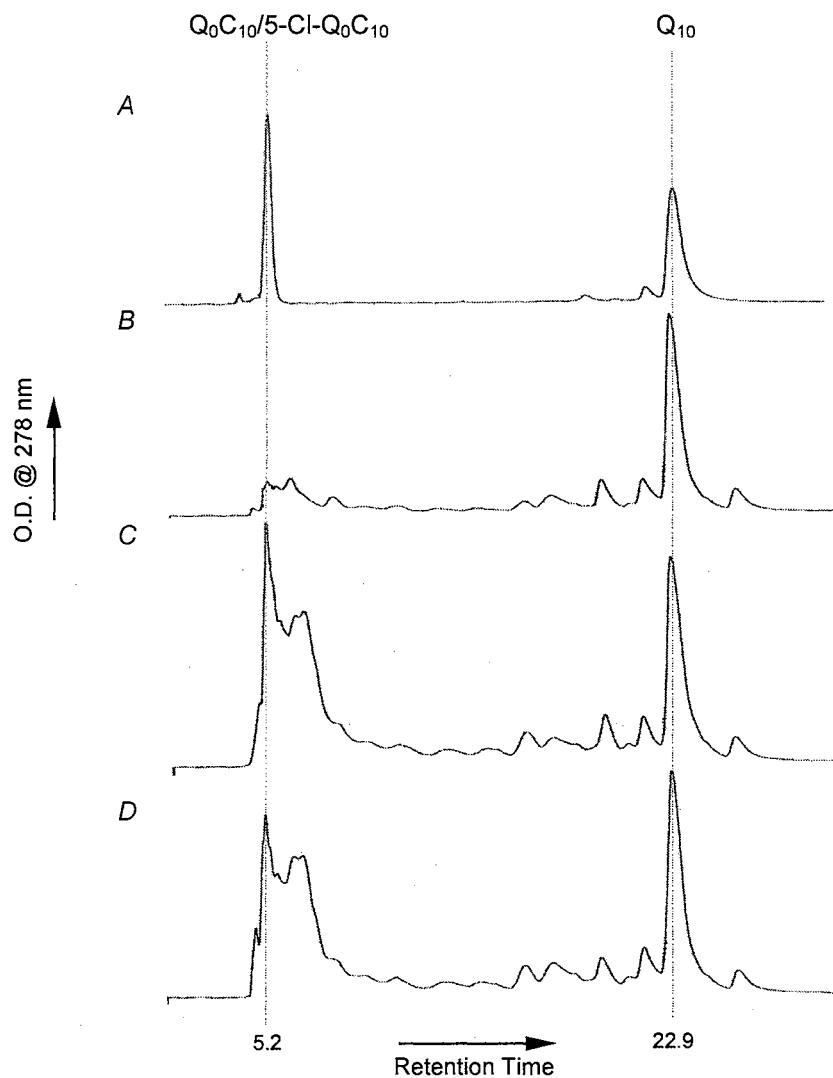
Figure 1.5. <u>Determination of Quinone Content in the Mitochondrial Extraction by HPLC.</u>
Mitochondria from rat liver, fed with different Q compounds, were extracted with
organic solvents as described in "Experimental Procedures" of Chapter II. The
purified quinones or mitochondria extraction was injected into a reverse phase C8-
HPLC column. Pure Q_0C_{10}, 5-Cl-Q_0C_{10} and Q_{10} served as standards. Profile A is a
mixture of these three standards. Profile B, C, and D are extract of liver
mitochondria from rat fed with no Q, Q_0C_{10}, and 5-Cl-Q_0C_{10}, respectively.

42

References

1. Trumpower B.L. and Gennis, R.B. (1994) *Annu. Rev. Biochem.* **63**, 675~716

2. Nicholls D. G. and Ferguson S. J. (1992) *Bioenergetics 2*, 107~140

3. Brandt, U. (1997) *Biochim. Biophys. Acta*, **1318**, 79~91

4. Hägerhäll, C. (1997) *Biochim. Biophys. Acta*, **1320**, 107~141

5. Fearnley, I.M. and Walker, J.E. (1992) *Biochim. Biophys. Acta*, **1140**, 105~134

6. Xia, D., Yu, C.A., Kim, H., Xia, J.Z., Kachurin, A.M., Zhang, L., Yu. L., and Deisenhofe, J. (1997), *Science*, **277**, 60~66

7. Tsukihara, T., Aoyama, H., Yamashita, E., Tomiraki, T., Yamguchi, H., Shinzawa-Itoh, K., Nakashima, R., Yaono, R., and Yoshikawa, S. (1996) *Science*, **272**, 1136~1144.

8. Abrahams, J.P., Leslie, G.W., Lutter, R., and Walker, J.E. (1994) *Nature*, **370**, 621~633

9. Chance, B. and Williams, G.R.(1956) *Adv. Enzymol.* **17**, 65~134

10. Tzagoloff, A. (1982) *Mitochondria*, Plenum Press. 131~156

11. Lenaz, G. (1985) *Coenzyme Q*, John Wiley & Sons, Inc.1~144

12. Voet, D. and Voet, J.G. (1995) *Biochemistry*, John Wiley & Sons, Inc. 563~596

13. Gutman, M. (1980) *Biochim. Biophys. Acta*, **594**, 53~84

14. Rich, P.R. (1984) *Biochim. Biophy. Acta*, **768**, 53~79

15. Yu, C.A., Gu, L.Q., Lin, Y., and Yu, L. (1985) *Biochemistry*, **24**, 3897~3902

16. Yu, C.A. and Yu, L. (1993) *J. Bioenerg. Biomemgr.*, **23**, 259~273

17. Gu, L.Q., Yu. L., and Yu, C.A. (1990) *Biochim. Biophys. Acta*, **1015**, 482~492

18. Von Jagow, G. and Link, T.A. (1986) *Method Enzymol*, **126**, 253~271

19. Green, D.E. (1962) *Comp.Biochem. Physiol.* **4**, 81~122

20. Gupte, S., Wu, E.S., Hoechli, L. Hoechli, M., Jacobson, K., Sowers, A.E. and Hackenbrock, C. R. (1984) *Proc. Natl. Acad. Sci. USA*, **81**, 2606~2610

21. Kroger, A. and Klingenberg, M. (1973) *Eur. J. Biochem.*, **34**, 358~368

22. Yu, L. and Yu, C.A. (1982) *J. Biol. Chem.*, **257**, 2016~2021

23. Ragan, C.I. and Cottingham, I.R. (1985) *Biochim. Biophys. Acta*, **811**, 13~31

24. Miki, T., Yu, L., and Yu, C.A. (1992) *Arch. Biochem. Biophys.*, **293**, 61~66

25. Yu, L., Yang, F.D., and Yu, C.A. (1985) *J. Biol. Chem.*, **260**, 963~973

26. Yu, C.A., and Yu, L. (1981) *Biochim. Biophys. Acta*, **639**, 99~128

27. Kroger, A. and Klingenberg, M. (1973) *Eur. J. Biochem.*, **34**, 358~368

28. Lee, G.Y., He, D.Y., Yu, L., and Yu, C.A. (1995) *J. Biol. Chem.*, **270**, 6193~6198

29. Shenoy, S.K., Yu, L., and Yu, C.A. (1997) *J. Biol. Chem.*, **272**, 17867~17872

30. Yang, X., Yu, L., He, D.Y., and Yu, C.A. (1998) *J. Biol. Chem.*, **273**, 31916~31923

31. Shenoy, S.K., Yu, L., and Yu, C.A. (1999) *J. Biol. Chem.*, **274**, 8717~8722

32. Crane, F.L. (1977) *Ann. Rev. Biochem.*, **46**, 439~469

33. Yu, C.A., and Yu, L. (1982) *Biochemistry*, **21**, 4096~4101

34. Sone, N., Yoshida, M., Hirata, H., and Kagawa, Y. (1977) *J. Biochem. (Tokyo)* , **81**, 519~528

35. Yu, L., and Yu, C.A. (1982) *J. Biol. Chem.*, **257**, 10215~10221

36. Yu, C.A., and Yu, L. (1980*) Biochim. Biophys. Acta,* **591**, 409~420

37. Yu, C.A., Yu, L., and King, T.E. (1975) *J. Biol. Chem.*, **250**, 1383~1392

38. Harmon, H. J. & Crane, F.L. (1976) *Biochim. Biophys. Acta*, **440**, 45~58

39. Berden, J.A. and Slater, E.C. (1970) *Biochim. Biophys. Acta*, **216**, 237~249

40. Lowry, O.H. Rosebrough, N.J., Farr, A.L. and Randall, R.J. (1951) *J. Biol. Chem.*, **193**, 265~275

41. Racker, E. and Kandrach, A. (1973) *J. Biol. Chem.*, **248**, 5841~5847

42. Guner, S., Robertson, D.E., Yu, L., Qiu, Z-H., Yu, C.A., and Knaff, D.B. (1991) *Biochim. Biophys. Acta,* **1058**, 269~279

43. Yu, L., Yang, F.D. and Yu, C.A. (1985) *J. Biol. Chem.*, **260**, 963~973

44. Redfearn, E.R. (1967) *Methods Enzymol.* **X**, 381~384

45. Morton, R.A. (1971) *Biol. Rev. Cambridge Philos. Soc.*, **46**, 47~96

46. Urban, P.F. and Klingenberg, M. (1969) *Eur. J. Biochem.*, **9**, 519~525

47. Moret, V., Pinanomti, S., and Fornasari, E, (1961) *Biochim. Biophy. Acta*, **54**, 381~383

48. Schnarf, U. (1966) *Dissertation*, ETH, Zurich, Np. 3871

49. Nelson, B.C., Norling, B., Persson, B. and Ernster, L. (1972). *Biochim. Biophy. Acta*, **267**, 205~210

50. DeVries, S., Berden, J.A., and Slater, E.C. (1980) *FEBS Lett.*, **122**, 143~148

51. Salerno, J.C. and Ohnishi, T. (1980) *Biochem. J.*, **192**, 769~781

52. Rich, P.R., and Bendall, D.S. (1980) *Biochim. Biophy. Acta*, **592**, 506~518

53. Rich, P.R. (1981) *Biochim. Biophy. Acta*, **637**, 29~33

54. Glover, J. and Threlfall, D.R. (1962) *Biochem. J.*, **85**, 14~15

55. Storey, B.T. (1973) *Biochim. Biophy. Acta*, **292**, 592~603

56. Takamiya, K. and Dutyon, P. (1979) *Biochim. Biophy. Acta*, **546**, 1~16

57. Yu, C.A. and Yu, L. (1982) *Biochemistry* **19**, 5715~5720

58. Heron, C., Ragan, C.I. and Trunpower, B.L. (1978) *Biochem. J.*, **174**, 791~800

59. Yu, C.A., Yu, L. and King, T.E. (1974) *J. Biol. Chem.*, **249**, 4905~4910

60. Catlin, J.C., Daves, G.D., Jr., and Folkers, K. (1971) *J. Med. Chem.*, **14**, 45~48

61. Smith, L.A. and Lester, R.L. (1961) *Biochim. Biophy. Acta*, **48**, 547~551

62. Yu, L., Xu, J-X., Haley, P.E. and Yu, C.A. (1987) *J. Biol. Chem.*, **262**, 1137~1143

63. Ohnishi, T., Salerno, J.C., Winter, D.B., Lim, J., Yu, C.A., Yu, L. and King, T.E. (1976) *J. Biol. Chem.*, **251**, 2094~2104

64. Ackrell, B.A.C., Kearney, E.B., Mims, W.B., Peisach, J. and Beinert, H. (1984) *J. Biol. Chem.*, **259**, 4015~4018

PART II

STUDIES ON QUINONE BINDING DOMAIN OF DSBB

CHAPTER IV

INTRODUCTION

Disulfide Bonds Formation during Protein Folding

The three-dimensional structure of a biologically active protein is most likely in its energetically favorable conformation, and is determined by its amino-acid sequence. Many proteins can fold correctly on their own or with the help of molecular chaperones. However, presence of disulfide bonds in a protein can interfere in this process. The proper folding and stability of a large number of proteins depends on the formation of disulfide bonds.

Disulfide bonds play a number of different roles in protein structure and activity. Although proteins can form disulfide bonds spontaneously in the presence of oxygen or in thiol/disulfide redox buffers, these *in vitro* processes are often slow and prone to errors (1,2). In contrast, disulfide bond formation *in vivo* is generally fast and accurate, occurring on a time scale of seconds rather than minutes or hours, which is the case *in vitro* (3). Indeed, it is now known that, a number of disulfide bond proteins (Dsb) catalyze the oxidation, reduction, and isomerization of disulfide bonds *in vivo* in newly exported proteins in both eukaryotes and prokaryotes (4). DsbB is one of these disulfide forming enzymes and is located in the inner bacterial membrane.

The formation of stable disulfide bonds in proteins takes place in specific compartments in the cell. In prokaryotes, disulfides form in the rather oxidizing environment of the *E.coli* periplasm (5); in eukaryotes, disulfide bonds are introduced into soluble proteins (or soluble portions of membrane proteins) at the endoplasmic reticulum (6). The cytoplasm of either eukaryotes or prokaryotes, which is in a reducing environment, does not contain proteins with stable disulfide bonds (6,7). Nevertheless, a number of cytoplasmic reductases go through cycles of oxidation and reduction of cysteine pairs as part of their

enzymatic activity (8,9).

Thioredoxin (Figure 2.1) is one of the best characterized redox proteins, containing two redox-active half-cysteine residues (C32, C35) in an exposed active center, which can be re-reduced by thioredoxin reductase and NADPH (10). Thioredoxin is a small 12 kDa ubiquitous protein, present in the cytoplasm of *E. coli*, and evolutionarily conserved in both eukaryotes and prokaryotes. Thioredoxin serves as a model for our understanding of *E. coli* Dsb proteins. Despite the lack of sequence homology, all of these redox proteins involved in the disulfide bond formation contains an active site that is similar to thioredoxin.

In eukaryotes, disulfide bonds are introduced into proteins in the endoplasmic reticulum (ER). There are a number of oxidoreductases with thioredoxin-like domains in the ER. One of the most prominent and best characterized reductase of these enzymes is Protein Disulfide Isomerase (PDI), a 57 kDa protein with two thioredoxin-like domains. It has been shown to catalyze disulfide bond formation *in vitro* (1,11) and to be essential for efficient disulfide bond formation *in vivo* (12). PDI is also capable of the disulfide bond breakage and rearrangement during the folding of proteins translocated into ER (13).

Redox Proteins in *E. coli* for Disulfide Bond Formation

In *Escherichia coli* (*E. coli*), a family of redox proteins are involved in the folding of transported proteins containing disulfide bonds. Such redox proteins are located in the cytoplasmic membranes or in the periplasm and their active site is always facing the periplasm. Most of these proteins are called Dsb's for disulfide bond proteins (4).

Almost all the enzymes involved in the formation, reduction, and isomerization of disulfide bonds belong to a class of enzymes with features similar to their prototype, thioredoxin. In common, these enzymes have the active motif containing two vicinal cysteines, Cys-X-Y-Cys (where X, Y denote any amino acid), and they can exist either in the reduced form, Dsb-$(SH)_2$, or in the oxidized form Dsb-S_2 with an intramolecular disulfide bond established between both half cysteine residues (4). As Scheme 2.1 shows, oxidation and
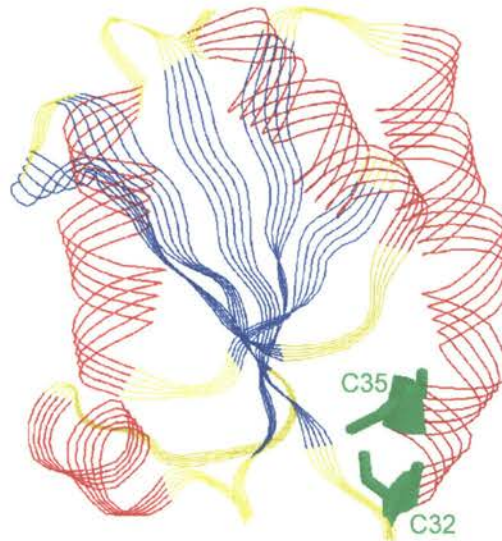
Molecular Weight	11720
Number of Residues	105
Number of Alpha	5
Content of Alpha	39.05%
Number of Beta	6
Content of Beta	28.57%

Sequence and secondary structure

```
  1  MVKQIESKTA FQEALDAAGD KLVVVDFSAT WCGPCKMIKP FFHSLSEKYS
        EEEE SHHH HHHHHHTTT SEEEEEEE T T HHHHHTHH HHHHHHHH T

 51  NVIFLEVDVD DCQDVASECE VKCMPTFQFF KKGQKVGEFS GANKEKLEAT
     TEEEEEEETT TTHHHHHHTT    SSSEEEEE ETTEE EEEE S   HHHHHHH

101  INELV
     HHHTT
```

Figure 2.1. Sequence Detail and Three Dimensional X-Ray Structure of Oxidized
Thioredoxin (Brookhaven Code: 1ERU). Symbols in secondary structure: H-
Alpha helix; G-310 helix; I-Pi helix; B-Beta bridge; E-Extended strand; T-Beta
turn; S-Bend region; C-Random coil.

Disulfide Bond Formation/Reduction
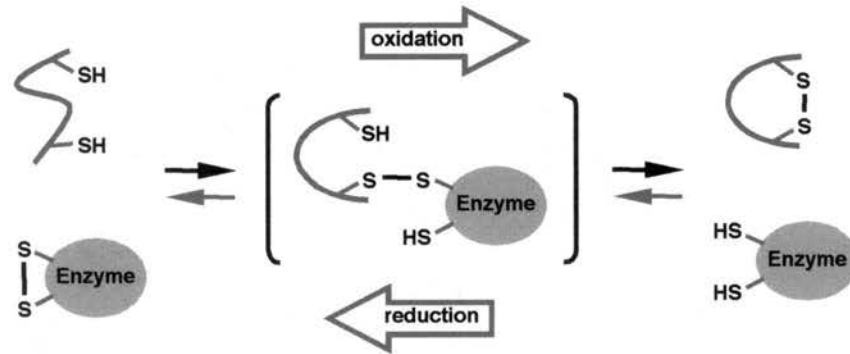
Disulfide Bond Isomerization
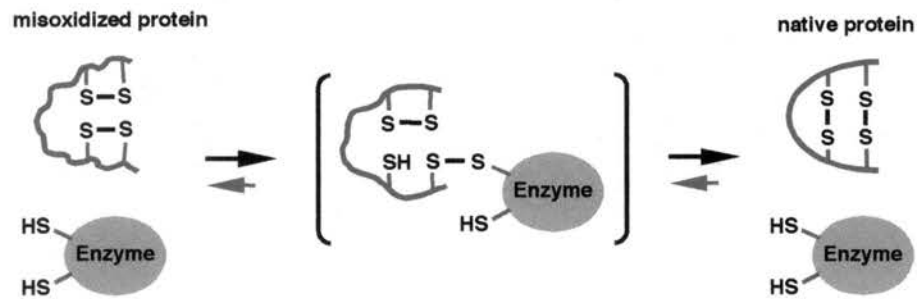
Scheme 2.1. <u>Enzymatic Disulfide Bond Oxidation, Reduction, and Isomerization</u>. Disulfide
bond oxidation, reduction, and isomerization are thought to proceed *via* a
mixed disulfide intermediate between the enzyme and the substrate protein.
The enzyme is shown as a round *disc*, the substrate protein is depicted as a
simple *line*.

reduction of disulfide bonds is mediated by thiol-disulfide exchange between the active site cysteines of the enzyme and cysteines in the target protein (14).

Scheme 2.2 illustrates the disulfide bond formation and isomerization by Dsb enzymes of *E.coli in vivo*. Table 2.1 summarizes the characteristics of the members of thioredoxin super-family in *E. coli*. (4,14).

While many of the thiol redox components of the *E coli* cytoplasm were identified initially *via* biochemical studies, nearly all of the thiol redox components of cell envelope were discovered through genetic analysis. The first of these to be identified was the periplasmic thiol-disulfide oxidoreductase DsbA, which is responsible for the formation of disulfide bonds in newly translocated proteins (3).

DsbA is a soluble periplasmic enzyme that serves as a potent catalyst for protein and peptide cysteine oxidation. Once it has transferred its disulfide bond to a substrate, DsbA is rapidly reoxidized by the membrane protein DsbB. The oxidation of protein cysteines by DsbA is very rapid but often results in the formation of incorrect disulfide bonds (15).

The rearrangement of nonnative disulfides is catalyzed primarily by the dimeric periplasmic enzyme DsbC. DsbC is a 23 kDa homodimer and has both protein disulfide isomerase and chaperone activity. The 1.9 Å resolution crystal structure of oxidized DsbC where both Cys-X-X-Cys active sites form disulfide bonds has been reported (16). The molecule consists of separate thioredoxin-like domains joined *via* hinged linker helices to an N-terminal dimerization domain (Figure 2.2). The hinges allow relative movement of the active sites, and a broad uncharged cleft between them may be involved in peptide binding and DsbC foldase activities.

For DsbC to be able to catalyze disulfide bond isomerization, its active site Cys-X-Y-Cys sequence must be present in the dithiol form. This dithiol motif requires continuous reduction for activity. Genetic evidence suggests that the source of periplasmic reducing power resides within the cytoplasm, provided by thioredoxin (*trxA*) and thioredoxin reductase (*trxB*) (14). Cytoplasmic electrons donated by thioredoxin are thought to be transferred into
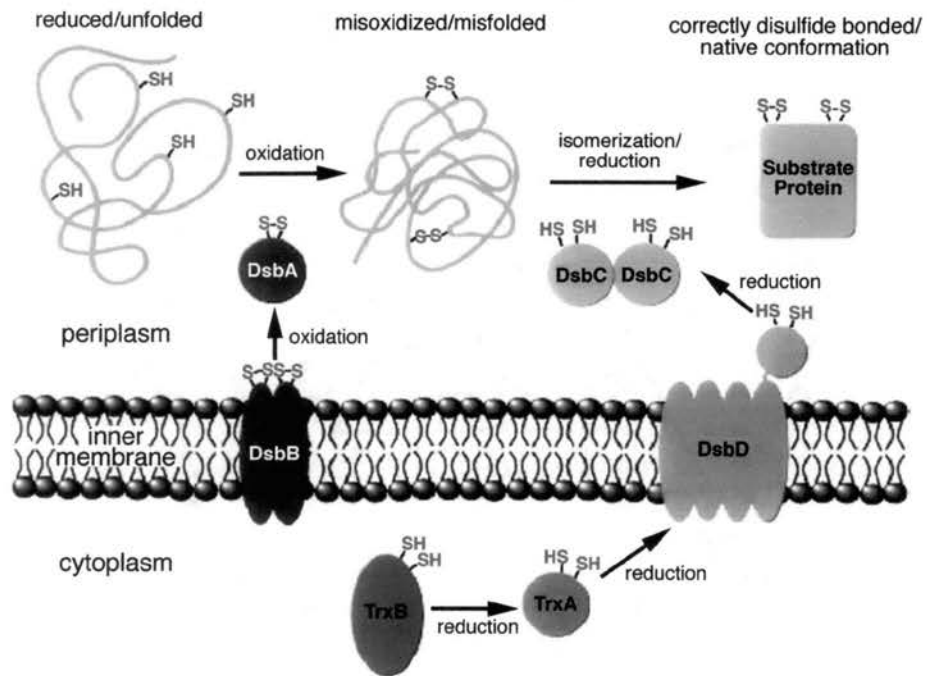
Scheme 2.2. Model of Disulfide Bond Formation and Isomerization by Various Dsb
Enzymes in the Periplasm of *E. coli*

Table 2.1. Various Redox Proteins of *E. coli.* (4)

gene name	protein name	MW (kDa)	cellular location	function	redox potential (pH7, 30°C)	thiol/disulfide active motif [4,59]
dsbA	DsbA	21	periplasm	oxidant	-89 mV [56]	Cys-Pro-His-Cys
dsbB	DsbB	20.1	inner membrane	oxidant		Cys-Val-Leu-Cys
dsbC	DsbC	2×23	periplasm	disulfide isomerase	-96 mV [57]	Cys-Gly-Tyr-Cys
dsbD (dipZ)	DsbD (DipZ)	53	inner membrane	reductant cyt.c biogenesis		Cys-Val-Ala-Cys
dsbE (ccmG)	DsbE (CcmG)	20	periplasm	reductant cyt.c maturation		Cys-Pro-Thr-Cys
dsbG	DsbG	25.7	periplasm	reductant disulfide isomerase		Cys-Pro-Tyr-Cys
trxA	Thioredoxin	12	cytoplasm	reductant	-270 mV [58]	Cys-Gly-Pro-Cys
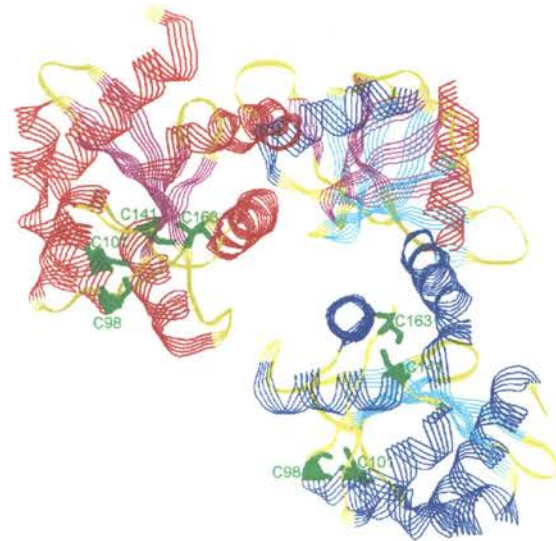
Molecular Weight		23445	
Number of Residues		216	
Number of Alpha	9(a)		8(b)
Content of Alpha	36.11%		37.50%
Number of Beta	11(a)		11(b)
Content of Beta	21.30%		20.83%

Sequence and secondary structure

```
1     DDAAIQQTLA KMGIKSSDIQ PAPVAGMKTV LTNSGVLYIT DDGKHIIQGP
a        HHHHHHHH HTT   BSEEE E SSTTEEEE EETTEEEEEE TTS    EEES
b        HHHHHHHH HHT   BSEEE E SSTTEEEE EETTEEEEEE TTS    EE


51    MYDVSGTAPV NVTNKMLLKQ LNALEKEMIV YKAPQEKHVI TVFTDITCGY
a       EE SSSS E EHHHHHHTHH HHGGGGGSEE E    TT   EEE EEEE TT HH
b       EE SSSS E EHHHHHHHHH HHHGGGG EE E    SS SEEE EEEE TT HH


101   CHKLHEQMAD YNALGITVRY LAFPRQGLDS DAEKEMKAIW CAKDKNKAFD
a     HHHHHTTHHH HHHTTEEEEE EE   TT SSS HHHHHHHHHH TSSSHHHHHH
b     HHHHHHTHHH HHHTTEEEEE EE   TTTTTS HHHHHHHHHH TSSSHHHHHH


151   DVMAGKSVAP ASCDVDIADH YALGVQLGVS GTPAVVLSNG TLVPGYQPPK
a     HHHTT       S  HHHH HHHHHHHT  SSSEEE TTS  EEES    HH
b     HHHTT       S  HHHH HHHHHHHT  SSSEEE TTS  EEES    HH


201   EMKEFLDEHQ KMTSGK
a     HHHHHHHHHH HHHHTT
b     HHHHHHHHHH HHHTTT
```

Figure 2.2. <u>Sequence Detail and Three Dimensional X-Ray Structure of DsbC (Brookhaven Code: 1EEJ</u>). Symbols in secondary structure: H-Alpha helix; G-310 helix; I-Pi helix; B-Beta bridge; E-Extended strand; T-Beta turn; S-Bend region; C-Random coil.

the periplasm *via* the membrane protein DsbD. Based on the membrane topological analysis, the N- and C-terminal domains of DsbD are positioned in the periplasmic space, connected by eight transmembrane segments. Electron transfer was shown to require five cysteine sulphydryls of DsbD. The membrane-embedded disulfides of DsbD accept electrons from cytoplasmic thioredoxin and transfer them to the C-terminal periplasmic dithiol motif of DsbD (17).

Besides DsbA, DsbB, DsbC, DsbD, two more Dsb proteins were identified and characterized recently. DsbE was shown to be membrane bound, facing the periplasm with its C-terminal, hydrophilic domain. While DsbD is essential for maintaining cytochrome *c* apoproteins in the correct conformations for the covalent attachment of heme groups to the appropriate pairs of cysteine residues (18), DsbE plays an important role in cytochrome *c* maturation in *E. coli*. A reducing function for the two cysteine residues in the active-site motif (CXYC) is suggested in a pathway for maturation of *c*-type cytochromes (19).

As a periplasm protein homologue of DsbC, DsbG is an inefficient catalyst of disulfide rearrangement. It functions primarily as a periplasmic disulfide isomerase with narrower substrate specificity than DsbC. It is reported that DsbG functions predominantly either as a reductant or as a catalyst for disulfide isomerization (20).

The efficiency with which these enzymes perform their various functions is determined by a number of factors, including the redox potential of the active site disulfide bond, which reflects whether an enzyme is more reducing or oxidizing, and the ability of the enzyme to bind to polypeptides (Table 2.1).

DsbA-DsbB System in Disulfide Bond Formation

In *E. coli*, disulfides form in the rather oxidizing environment of the periplasm. The oxidizing power of the periplasm originates from the DsbA-DsbB system. DsbA and DsbB constitute a redox couple involved in the formation of disulfide bonds. As the major pathway for stable disulfide bond formation, the DsbA-DsbB system has drawn much attention in the

field. Much progress has been made in the understanding of these redox proteins through various approaches. Regarding their biochemical and biological activities, the roles of these enzymes in cell physiology are determined (21).

<u>DsbA</u>

Studies with purified DsbA *in vitro* show that it is a potent oxidizing disulfide catalyst required for disulfide bond formation in secreted proteins. This property is consistent with the high redox potential of its active site disulfide bond. DsbA is a small soluble protein, which contains a thioredoxin-fold with a highly unstable disulfide bond. DsbA acts by transferring its active site disulfide bond very rapidly to folding proteins. This leads to the oxidation of the target protein and the reduction of the active site CXXC motif of DsbA.

The availability of a 1.7Å resolution crystal structure for DsbA (Figure 2.3) has led to an abundance of information concerning the mechanism of DsbA action (22). Three unique features on the active site surface of the DsbA molecule — a groove, hydrophobic pocket, and hydrophobic patch — form an extensive uncharged surface surrounding the active disulfide, which could participate in the binding or stabilization of peptide (23).

The active site of DsbA is similar to that of mammalian protein disulfide isomerases, and includes a reversible disulfide bond formed from cysteines separated by two residues (Cys30-Pro31-His32-Cys33). Unlike most protein disulfides, the active-site disulfide of DsbA is highly reactive and the oxidized form of DsbA is much less stable than the reduced form at physiological pH. His32, one of the two residues between the active-site cysteines, is critical to the oxidizing power of DsbA and to the relative instability of the protein in the oxidized form. Mutation of this single residue to tyrosine, serine, or leucine results in a significant increase in stability (of approximately 5-7 kcal/mol) of the oxidized His32 variants relative to the oxidized wild-type protein. Despite the dramatic changes in stability, the structures of all three oxidized DsbA His32 variants are very similar to the wild-type oxidized structure, including conservation of solvent atoms near the active-site residue,
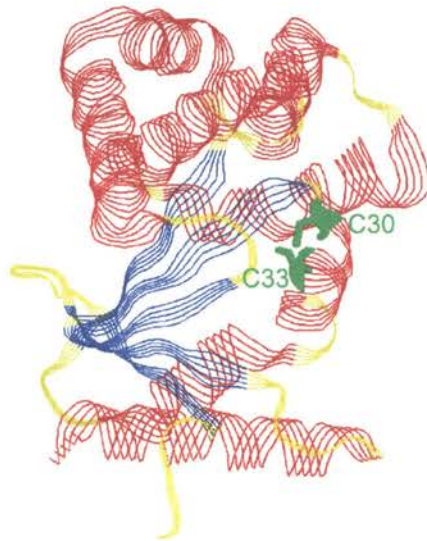
Molecular Weight	21116
Number of Residues	189
Number of Alpha	9
Content of Alpha	49.74%
Number of Beta	5
Content of Beta	10.58%

Sequence and secondary structure

```
1    AQYEDGKQYT TLEKPVAGAP QVLEFFSFFC PHCYQFEEVL HISDNVKKKL
       BTTTEE E SS   TT      SEEEEE TT  HHHHHHHHTT  HHHHHHTTT

51   PEGVKMTKYH VNFMGGDLGK DLTQAWAVAM ALGVEDKVTV PLFEGVQKTQ
     TTT   EEEEE   SSSSHHHHH HHHHHHHHHH HHTTHHHHTH HHHHHHHTS

101  TIRSASDIRD VFINAGIKGE EYDAAWNSFV VKSLVAQQEK AAADVQLRGV
       SHHHHHH HHHHTT   HH HHHHHHHTHH HHHHHHHHHH HHHHTT   SS

151  PAMFVNGKYQ LNPQGMDTSN MDVFVQQYAD TVKYLSEKK
     SEEEETTTEE E GGGS   SS HHHHHHHHHH HHHHHHT
```

Figure 2.3. <u>Sequence Detail and Three Dimensional X-Ray Structure of Oxidized DsbA (Brookhaven Code: 1FVK)</u>. Symbols in secondary structure: H-Alpha helix; G-310 helix; I-Pi helix; B-Beta bridge; E-Extended strand; T-Beta turn; S-Bend region; C-Random coil.

Cys30. These results show that the His32 residue does not exert a conformational effect on the structure of DsbA. The destabilizing effect of His32 on oxidized DsbA is therefore most likely electrostatic in nature (24).

Although the redox potentials of DsbA and DsbC are comparable, −89 mV and −96 mV, respectively; under steady state conditions in the periplasm, DsbA is oxidized, whereas DsbC is almost exclusively reduced. The thiol group of Cys30, the accessible thiol in the redox active site, ionizes with a very low pK_a value of 3.5 (26), although the pK_a of a normal cysteine is about 8.7. His32, within DsbA's di-thiol active site motif Cys30-Pro-His-Cys33, contributes to lowering the pK_a value of DsbA (25). This low pK_a also originates in part from the location of the accessible cysteine Cys30 near an α helix (22) and the dipole of this α helix stabilizes the negative charge of the thiolate anion (27).

After transferring the disulfide bond from its active site to the target protein, DsbA is in reduced state and the active site disulfide bond must be reoxidized in order for DsbA to catalyze another round of disulfide bond formation. Reoxidation of DsbA is performed by the integral membrane protein DsbB (Scheme 2.2).

DsbB

DsbB is a 20.1 kDa membrane protein with 176 amino acid residues. It spans the membrane four times and both the N-and C-termini of the protein are in the cytoplasm (28). Mutation analysis shows that of the six cysteine residues in DsbB, two pairs are located in the two periplasm domains of the protein. These four of the six cysteines are essential for DsbB activity, whereas the remaining two are not. The pair of cysteines in the first periplasmic domain is organized in a Cys41-Val-Leu-Cys44 motif, whereas the second pair of cysteines is Cys104-Cys30, separated by a 26-amino acid spacer (Scheme 2.3).

The proposed role of DsbB as an oxidant of DsbA is supported by the following findings of:

   a. DsbA accumulates in the reduced state in a *dsbB* mutant (29),

```
        10        20        30        40        50        60        70
         |         |         |         |         |         |         |
MLRFLNQCSQGRGAWLLMAFTALALELTALWFQHVMLLKPCVLCIYERCALFGVLGAALIGAIAPKTPLR
CEEEECCCCCCCHHHHHHHHHHHHHHHHHHHHHHHHCCCHHEEHHHHHHHHHHHHHHHHHHHHHCCCCCCCHH

YVAMVIWLYSAFRGVQLTYEHTMLQLYPSPFATCDFMVRFPEWLPLDKWVPQVFVASGDCAERQWDFLGL
HHHHHHHHHHHHCCCCEEEEEEEEEECCCCCCCCCCEHHCCCCCCCCCCCCCCEEEEECCCHHHHHHHHHCCC

EMPQWLLGIFIAYLIVAVLVVISQPFKAKKRDLFGR
CHHHHHHHHHHHHHHHHHHHHHHHHCCCCHHHHHHCCC
```

Sequence length: 176

Alpha helix (H):   95 is 53.98%
Extended strand (E):   21 is 11.93%
Random coil (C):   60 is 34.09%

Scheme 2.3.   Membrane Topology of Oxidized DsbB and Its Secondary Structure

Prediction by Hierarchical Neural Network Method (Guermeur, 1997)

b. A mixed disulfide-bonded complex formed between DsbB and DsbA (30).

A mixed disulfide between DsbA-Cys30:DsbB-Cys104 could be readily trapped *in vivo* using various mutant DsbA and DsbB proteins. The mixed disulfide species is very transient but can be stabilized when Cys33 of DsbA and Cys130 of DsbB are substituted for Ala (Scheme 2.4). On the other hand, mutation in Cys104 of DsbB disrupts the formation of this mixed disulfide complex between DsbA and DsbB. Cys104 was shown to form a reversible disulfide bond with Cys130, which is the one responsible for recycling DsbA (31). The Cys104:Cys130 linkage is reoxidized intra-molecularly by the N-terminally located Cys41-Val-Leu-Cys44 thioredoxin-like motif of the DsbB protein.

The *in vivo* redox states of the four essential cysteine residues of DsbB are disulfide-bonded by Cys41-Cys44 and Cys104-Cys130. The Cys41-Cys44 disulfide is preserved in the absence of Cys104-Cys130, but the Cys104-Cys130 disulfide is not formed effectively in the absence of the Cys41-Cys44 disulfide bond (39).

Electron Transfer Chain Participates in Disulfide Bond Formation

Formation of a disulfide bond from the thiol (-SH) groups of two cysteine residues generates two electrons and changes the covalent structure of the polypeptide chain. These disulfide bonds cannot be spontaneously formed unless the protein interacts with an oxidant that accepts the electrons (32). The compelling experimental evidence in bacteria shows that, oxidative protein folding is coupled to the electron-transport chain (33).

In the model pathway for disulfide bond formation, DsbA randomly transfers its extremely reactive catalytic disulfide bond to folding proteins, and is itself recovered as an oxidant by disulfide exchange with inner membrane protein DsbB (34). There remains the question of how oxidized membrane-located DsbB protein is regenerated.

Recently, molecular oxygen was found to act as the final electron acceptor for DsbB-catalyzed protein folding *in vitro* (35). However, DsbB, which lacks cofactors such as haems or flavins, can not be oxidized directly by oxygen. The haem-containing cytochrome *bd* or
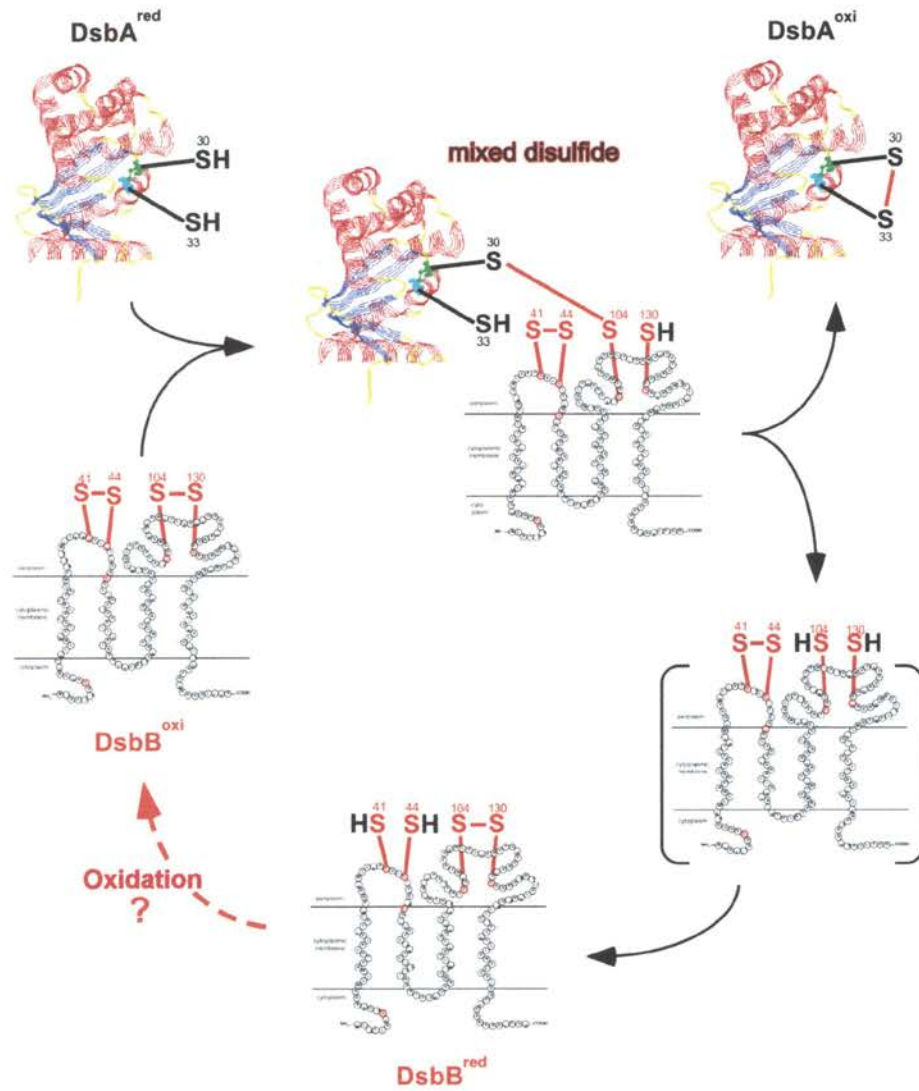
Scheme 2.4. Reoxidation of Reduced DsbA-$(SH)_2$ by Oxidized DsbB-S_2

bo oxidase complex is found to be associated with DsbB and crucial for its activity (33). It is a hint that disulfide formation is linked to the electron-transfer chain.

Genetic studies also suggest that DsbB is oxidized by passing electrons to the respiratory chain. DsbA accumulates in the reduced form in strains depleted for ubiquinone and menaquinone and at late stages of the depletion, forms a disulfide-bonded complex with DsbB. This is followed by reduction of the bulk of DsbA molecules. It suggests that the respiratory electron transfer chain participates in the oxidation of DsbA, by acting primarily on DsbB (36).

It is reported that the Cys41-Cys44 disulfide bond in the membrane integrated DsbB cannot be reduced by treatment with DTT (39). A structural and/or functional basis should exist for this DTT resistance of Cys41-Cys44. The Cys41-Cys44 region of DsbB may be masked or buried in a respiration-dependent manner. Alternatively, the effect could be more functional, where this pair of cysteines are subjected to a very strong oxidation mechanism coupled with respiration; whenever they are reduced, they are oxidized back immediately. The finding that the oxygen is required for DTT resistance of the Cys41-Cys44 disulfide bond supports the latter idea (39).

Quinones are ubiquitous hydrogen and electron carriers in the electron transport chain (PART I, CHAPTER I). In *E. coli* cells, ubiquinone-40 (Q_8) is the predominant species under aerobic condition, whereas menaquinone-40 (vitamin K12) functions mainly under anaerobic condition (60).

Regarding the oxidative pathway, it has been shown that components of the electron transport chain serve as DsbB's immediate electron acceptors (35). By reconstituting the DsbA-DsbB system with purified components *in vitro*, it is reported that ubiquinone serves as DsbB's immediate electron acceptor (33). Ubiquinones are then reoxidized by terminal oxidases such as cytochrome *bd* and *bo* oxidase which finally transfer electrons onto oxygen. In the aerobic electron transfer chain of *E.coli*, *bo*-type ubiquinol oxidase is expressed under high oxygen tension, and *bd*-type ubiquinol oxidase predominates under low oxygen tension.

These two haem-containing oxidases, which can restore DsbB activity, though structurally unrelated, catalyze the two-electron oxidation of ubiquinol-40 and four-electron reduction of dioxygen to produce water (37). The idea that the ubiquinone acts as an electron carrier in the DsbB reoxidation is also supported by the phenomenon that low ubiquinone content in *E.coli* causes thiol hypersensitivity (38).

The observation that menaquinones act as DsbB′s electron acceptor suggested that disulfide bonds could form under anaerobic condition. The existence of this alternative pathway became evident when a strain of *E. coli* lacking both terminal oxidases and grown in the absence of oxygen showed no defects in disulfide-bond formation. It turns out that oxidized menaquinone, which can replace ubiquinone under anaerobic condition and transports electrons to alternative electron acceptors such as fumarate or nitrate, can oxidize DsbB directly, albeit with a lower efficiency than ubiquinone. This menaquinone pathway also allows disulfide bond to be formed in strains that lack ubiquinone (33,39).

Ubiquinone and menaquinone are probably the only oxidants in the *E. coli* inner membrane that can directly oxidize DsbB. Strains lacking ubiquinone and menaquinone show a strong defect in disulfide bond formation (39).

The electron-flow pathways for oxidative protein folding under aerobic and anaerobic conditions are illustrated in Scheme 2.5. The reaction of DsbA with folding polypeptide involves two electrons and occurs *via* disulfide interchange reactions. The same process applies to the oxidation of DsbA by DsbB. Molecular oxygen acts as the final electron acceptor for DsbB-catalysed protein folding under aerobic condition (40).

In biological systems, the most extensively disulfide chemistry study is the chemistry of disulfide exchange. Little information is available describing their ultimate source. DsbB possesses a novel catalytic activity, which to our knowledge has not yet been fully described. It catalyzes the formation of a disulfide using oxidized quinones as an electron acceptor. Eventually, molecular oxygen acts as the final electron acceptor for DsbB-catalyzed protein folding.
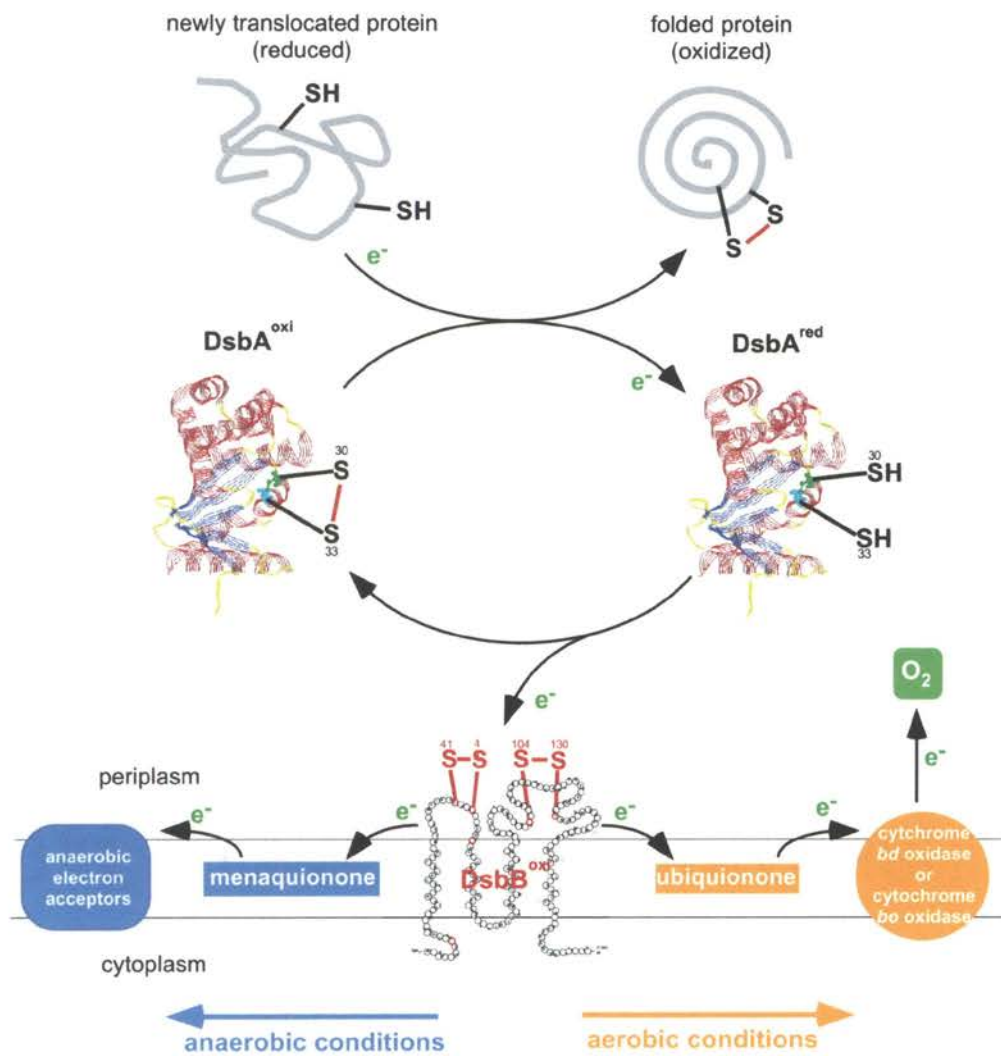
Scheme 2.5. <u>DsbB Links Disulfide Bond Formation to Electron Transport</u>

Objective of This Study

The goal of this study is to understand the ubiquinone-mediated electron transfer reaction in disulfide bond formation. The active species of ubiquinone in electron transfer is proposed to be a protein-bound quinone entity (65). The identification of quinone binding domain of DsbB could explain the mechanism of DsbB reduction and the pathway of disulfide bond formation.

To date, a number of quinone-binding proteins in the electron transfer system have been extensively studied in several labs including ours. Quinone binding sites have been clearly established by X-ray crystallographic studies of cytochrome bc_1 complex (41) and fumarate:quinone reductase (64), by photo-affinity labeling (43,44) and molecular genetic approaches in succinate-ubiquinone reductase (45,46).

The studies on quinone reduction activity of DsbB, the quinone analogues inhibition on DsbB activity and the identification of quinone component in pure DsbB provide us lots information of the function and structure of quinone in disulfide formation.

The availability of azido-Q derivatives in our laboratory enabled us to study the quinone:protein interaction and to identify the quinone binding domain in DsbB by the photoaffinity labeling approach. The successful isolation of the azido-Q linked peptide(s) from an azido-Q labeled protein relies on the susceptibility of isolated protein toward proteolytic enzyme digestion and separation of proteolytic peptides by high performance liquid chromatography (HPLC).

Furthermore, simulation of Q binding pocket for DsbB using a known quinone protein as the modeling template will facilitate our identification of the quinone binding domain of this protein.

CHAPTER V

EXPERIMENTAL PROCEDURES

Materials

The ubiquinone derivatives, 2,3-dimethoxy-5-methyl-6-decyl-1,4-benzoquinone (Q_0C_{10}),

2,3-dimethoxy-5-methyl-6-(10-bromo)-decyl-1,4-benzoquinone ($Q_0C_{10}Br$) and radioactive azido-

Q derivatives, 3-azido-2-methoxy-5-methyl-6-geranyl-1,4-benzoquinone ($[^3H]3-N_3-5-MeO-PQ_2$)

and 5-azido-2,3-dimethoxy-6-decyl-1,4-benzoquinone ($[^3H]5-N_3-Q_0C_{10}$) were synthesized in our

laboratory according to previously reported methods (47,48).

Sodium cholate was obtained from Sigma and re-crystallized from methanol. n-Dodecyl-

β-D-maltoside was from Anatrace. Insta-gel liquid scintillation cocktail was from Packard

Instrument Co. Crosslinker N-[4-(p-azidosalicylamido)butly]-3'(2'-pyridyldithio)propionamide

(APDP) was from Pierce Co. Other chemicals were of the highest purity commercially available.

Preparation and Purification of Proteins

DsbA was purified from periplasmic extracts of the DsbA-overproducing strain JCB607

using Resource Q anion exchange chromatography (Amersham Pharmacia Biotech), essentially

as described previously (22,49). The purity of DsbA was >98% as judged by Coomassie-stained

gels. DsbA was reduced by incubation with 10 mM DTT for 20 min on ice. Excess DTT was

removed by PD-10 (Amersham Pharmacia biotech) gel filtration in 20 mM Hepes, pH 7.5, 0.5

mM EDTA. The thiol content was measured with dithiobisnitrobenzoic acid (DTNB) (50).

DsbA was >95% reduced and stored at −70 °C until use.

DsbB was purified from membranes prepared from the DsbB overexpression strain

WM76 of *E.coli*. The membranes were solubilized in 1% n-dodecyl maltoside. The His-tagged

DsbB was then bound to a nickel-nitrilotriacetic acid column that had been equilibrated with 50 mM sodium phosphate, pH 8.0, 300 mM NaCl, 0.02% n-dodecyl maltoside by passing the solubilized membranes over the column at a flow rate of 0.2 ml/min. The column was washed with the same buffer containing 50 mM imidazole. DsbB was eluted with a linear imidazole gradient ranging from 50 to 300 mM. Fractions containing DsbB were pooled and loaded directly onto a hydroxyapatite column equilibrated with 50 mM sodium phosphate, pH 6.2, 100 mM NaCl, and 0.1% n-dodecyl maltoside. DsbB was eluted from the column with a linear gradient in a buffer that contained 300 mM NaCl, 0.1% n-dodecyl maltoside, and sodium phosphate ranging in concentration from 50 to 500 mM. Fractions containing purified DsbB were concentrated to 5 mg/ml and dialyzed against 10 mM Hepes, pH 7.5, 50 mM NaCl. The protein was stored at −70 °C without loss of activity for more than 6 months. The DsbB concentration was determined after reduction of protein-bound quinone with $NaBH_4$ using the extinction coefficient of $\varepsilon_{276} =$ 46.5 mM^{-1} (33).

Enzymatic Activity Assay for DsbB

DsbB activity was monitored for its ability to transfer electron from DsbA to ubiquinone in 50 mM sodium phosphate pH 6.0, 300 mM NaCl, 0.1% dodecyl-maltoside at 25°C. DsbA in reduced form was added as a substrate. Reoxidation of DsbA was measured with a fluorescence spectrophotometer as described before (35). The reduction of quinone was measured spectrophotometricaly. Ubiquinone (Q_0C_{10}) reduction was followed at 275 nm with extinction coefficients of 12.25 mM^{-1} (60). The reaction was started by the addition of a small volume of DsbB. The concentration of DsbB was between 0.5 nM and 5 nM and was linear to the initial velocity over this range of enzyme concentration.

For steady state kinetics, initial rates were derived from the linear decrease of either fluorescence of $DsbA^{red}$ or absorbance of ubiquinone. The rates were transformed into nmole DsbA/sec or nmole quinone/sec and plotted against the concentration of substrate. The data were

fitted to a hyperbola, and V_{max} and K_m values were obtained from the fit of Michaelis-Menten equation. For steady state kinetics, initial rates were derived from the linear decrease of either fluorescence of DsbA or ubiquinone.

Identification of Ubiquinone Bound to DsbB

Spectral Measurement

Absorbance of DsbB was recorded from 240 nm to 390 nm in 50 mM sodium phosphate, pH 6.0, 300 mM NaCl and 0.1% n-dodecyl maltoside. Protein bound ubiquinones were reduced by adding a few grains of solid sodium borohydride to the cuvette and mixing thoroughly. After 5 min incubation at room temperature, the reduced spectrum was recorded from 240 to 390 nm. Employing an absorption coefficient of $\Delta\varepsilon_{275} = 12.25$ mM^{-1} (60), the amount of bound ubiquinone was calculated.

High Performance Liquid Chromatography (HPLC) Analysis

The quinone species bound to DsbB was identified and quantified by HPLC after organic solvent extraction. Methanol (-20 °C) was added to 1.4 ml of DsbB (4.4 mg/ml) to yield a final volume of 10 ml and vortexed immediately. Ubiquinone was extracted with 4×15 ml of hexane. The sample was dried by rotary evaporation of the solvent and re-dissolved in 0.5 ml of 95% ethanol, filtered through a 0.2-μm membrane, and loaded onto a Microsorb-MV® reverse phase column (C8, 5 μm). Coenzymes Q_1, Q_2, Q_8, and Q_{10} were used as standard quinone compounds for HPLC. Coenzymes Q_8, Q_{10} were extracted from *E. coli* membranes and bovine mitochondria respectively by following a published procedure (51). Ubiquinones were eluted from the column with a linear gradient of methanol ranging from 90 to 100% (v/v). The flow rate was 0.8 ml/min. The ubiquinone species bound to DsbB was identified and quantified based on the retention time and peak area of known standard coenzyme Qs.

Titration of the DsbB's Ubiquinone-binding Site with Exogenous Quinone

The method for DsbB's quinone-binding site titration was based on the previous report (46). Purified DsbB was washed with 10 volumes of titration buffer containing 50 mM K^+/Na^+ phosphate, pH 7.4, 1.0% sodium cholate prior to quinone titration. This is done by repeating concentration/dilution using Centricon-10. Titration experiments were performed in a total volume of 1 ml at a DsbB concentration of 0.50 mg/ml (25 µM). 2,3-Dimethoxy-5-methyl-6-(10-bromo)-decyl-1,4-benzoquinone ($Q_0C_{10}Br$) was added stepwise in 1 µl volumes from a 5 mM stock solution in EtOH. After the addition of each µl of quinone solution, the sample was incubated for 15 min at room temperature, and the spectra were recorded from 240 nm to 340 nm. The absorbance change at 280 nm upon addition of $Q_0C_{10}Br$ was plotted against the concentration of quinone added to the cuvette. A same titration procedure in the absence of DsbB was performed as a negative control and showed basically the same change in absorbance for each µl of added quinone.

Photo-affinity Labeling of DsbB with [³H]Azido-Q

The photo-affinity labeling reaction for DsbB was carried out according to the previously reported methods (52). DsbB (400 µl, 2.6 mg/ml), in 50 mM K^+/Na^+ phosphate buffer, pH 7.4, containing 1.0 % sodium cholate was incubated with 20 µl [³H]5-N_3-Q_0C_{10} or [³H]3-N_3-5-MeO-PQ_2 (in 95% ethanol, 5 molar excess to DsbB) at 0 °C for 1 hour in dark. The specific radioactivity of azido-Q used was 6×10^3 cpm/nmol in the labeling buffer. This mixture was transferred to an illuminating apparatus made from two quartz glasses sandwiched with a Teflon ring. The assembly was immersed in ice-water to maintain the temperature at 0 °C. The sample was then illuminated with long wavelength UV light (Spectroline EN-14, 365 nm long wavelength, 23 watts) for 7 minutes at a distance of 4 cm from the light source. The DsbB activity was assayed before and after the illumination.

To determine the amount of [^{3}H]azido-Q incorporated into DsbB, the illuminated

[^{3}H]azido-Q treated sample was spotted onto a 3M paper and developed with a mixture of

chloroform and methanol (2:1, v/v) to resolve non-protein bound [^{3}H]azido-Q. The paper was cut

into small strips and subjected to liquid scintillation counting. The radioactivity incorporation in

DsbB was determined by the cpm number of the protein origin.

To remove the unbound [^{3}H]azido-Q, the labeling reaction mixture was eluted through a

gel filtration chromatography in the presence of 1.0 % sodium cholate, and washed with 15

volumes of cold buffer containing 50 mM K$^+$/Na$^+$ phosphate buffer, pH 7.4, 1.0 % sodium

cholate using Certricon-10 through repetitive dilution/concentration. Estimation of the

scintillation counting showed that the majority of radioactivity in the labeled DsbB retentate came

from the [^{3}H]-Q bound protein and not the free form [^{3}H]-Q.

Protease Digestion of the [^{3}H]Azido-Q Labeled DsbB

The digestion reaction mixture was set up with 1 mg/ml of [^{3}H]-Q bound protein in 50

mM K$^+$/Na$^+$ phosphate buffer, pH 7.4, containing 1.0 % sodium cholate, 1.0 M urea, 100 mM

(NH$_4$)$_2$CO$_3$, 1 mM EDTA, 0.2% SDS. Protease V8 (V8:DsbB 1:50, w/w) or trypsin

(trypsin:DsbB 1:50, w/w) was added into the reaction mixture. The reaction mixture was then

incubated at 37 °C for 40 hours. The digested products from labeled DsbB were subjected to

16% high resolution SDS-PAGE to check the digestion patterns of the DsbB protein.

Isolation of Ubiquinone-Binding Peptides

The protease digested [^{3}H]azido-Q label DsbB was mixed with same volume of 90%

CH$_3$CN (acetonitrile), 0.1% TFA (trifluoroacetic acid) in H$_2$O, incubated at 37 °C for 30 minutes.

The sample was centrifuge at 13K rpm for 1 minute. The radioactivity of the supernatant and

precipitate were checked to determine the recovery. One hundred μl of supernatant was injected

onto a Supelcosil LC-308 reversed phase HPLC column (C8, 5 μm particles, 300 Å pores, 4.6

mm ID, 25 cm length). The separation was achieved with a linear gradient formed from 0.1%

TFA in H$_2$O and 90% CH$_3$CN in H$_2$O containing 0.1% TFA in 50 minutes and continued with

90% CH$_3$CN in H$_2$O containing 0.1% TFA for 15 minutes, with a flow rate of 1.0 ml/min. One

ml fractions were collected in 1.0 ml (1 tube per minute). The absorbance from 200 nm to 400

nm was recorded by Waters 996 Diode Array Detector. The radioactivity of each fraction was

measured by liquid scintillation counting. Peaks with high absorbance and/or specific

radioactivity were collected, dried, and subjected to amino acid sequencing and mass

spectrometry analysis.

Crosslinking of DsbB by APDP

Cleavable, photoreactive, heterobifunctional crosslinker APDP (N-[4-(p-

azidosalicylamido)butly]-3'(2'-pyridyldithio)propionamide) was dissolved in dry DMSO to make

a 20 mM stock solution. The APDP working solution was prepared by mixing APDP stock with

same volume of PBS (20 mM sodium phosphate, 150 M NaCl, pH 7.2). APDP was kept in dark

during all steps until exposing to UV to finish the photo-affinity labeling.

DsbB (1 mg/ml), was reduced with 1 % (v/v) β-mercaptoethanol in 50 mM sodium

phosphate, pH 6.2, 100 mM NaCl, and 0.1% n-dodecyl maltoside. Excess β-mercaptoethanol

was removed by a 2 ml Pierce desalting column pre-equilibrated with 50 mM sodium phosphate,

pH 6.2, 100 mM NaCl, and 0.1% n-dodecyl maltoside.

Reduced DsbB was incubated with 5 molar excess APDP on ice for 2 hours and then

shifted to 37 °C for 15 minutes. The reaction mixture was illuminated with long wavelength UV

for 7 minutes at a distance of 4 cm at room temperature. The illuminated samples were applied to

SDS-PAGE (12 % acrylamide, 3 % bis-acrylamide:acrylamide). Same sample treated with 0.5 %

β-mercaptoethanol served as the no linking control.

CHAPTER VI

RESULTS AND DISCUSSION

Ubiquinone-Dependent Disulfide Bond Formation

The ultimate source of oxidizing equivalents for the formation of disulfide bonds in the prokaryote *E. coli* originates in the electron transport system (33,39). By reconstituting the DsbA-DsbB system *in vitro*, we demonstrated that DsbB is reoxidized by quinones. It is suggested that ubiquinones function as the electron acceptors of DsbB under aerobic growth while under anaerobic condition, menaquinones reoxidize DsbB.

Enzymatic activity of DsbB can be measured based on the observation that reduced DsbA has an about 3-fold higher tryptophan fluorescence than the oxidized form of the protein (57). This provides a convenient way to follow the oxidation or reduction of DsbA in solution (23,25).

Since quinones are proposed to serve as the second substrate of DsbB, quinones should get reduced during the course of the reaction. To demonstrate this, we decided to monitor the reaction by simply following the absorption change between ubiquinone and its corresponding ubiquinol ($\Delta\varepsilon_{275} = 12.25$ mM^{-1}). Figure 2.4 shows that DsbB efficiently reduces Q_0C_{10} as measured by the absorbance change at 275 nm. No reduction of ubiquinone is observed in the absence of DsbB. Only when DsbB is added to the reaction mixture in catalytic amounts, reduction of ubiquinone was observed. Enzymatic activities were derived from the initial slopes of absorbance decrease. For ubiquinone reduction we observed an activity of 278 nmol of ubiquinone per nmol of DsbB per min. This activity agrees well with the activity derived from the fluorescence assay measured under the same conditions (35). Thus, this new assay can be employed to determine the activity of DsbB.
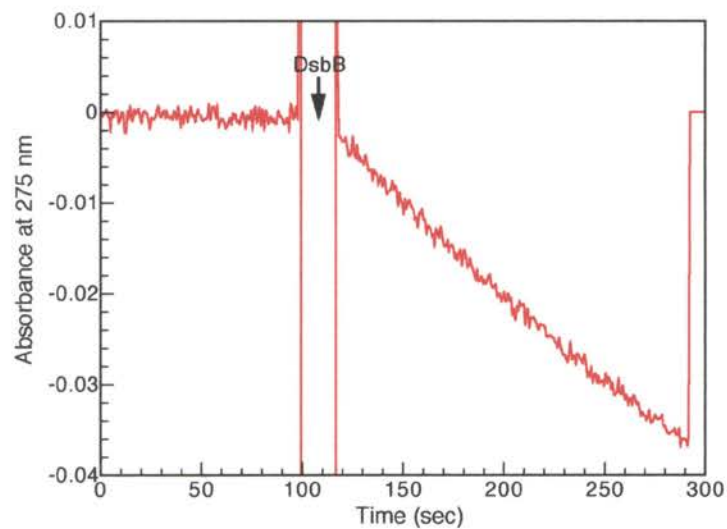
Figure 2.4. <u>Quinone Reductase Activity Assay for DsbB</u>. Assay mixture contains 50 mM
sodium phosphate, pH 6.0, 300 mM NaCl and 0.1% n-dodecyl maltoside, 0.5
mM EDTA in 1 ml. DsbA^{red} (10 μM) and Q_0C_{10} (20 μM) were added as reaction
substrates. DsbB (1 nM) was added to start the enzymatic reaction.

In order to characterize the ubiquinone reductase activity of DsbB, we measured initial velocities of ubiquinone reduction at various concentrations of Q_0C_{10}. The concentration of DsbA was held constant at 20 μM, whereas the concentration of the quinone was varied (Figure 2.5A). To obtain kinetic constants the curves were fitted to the Michaelis-Menten equation. When Q_0C_{10} was used as a substrate, the apparent K_m was 2.0 μM, whereas V_{max} was 5.0 nmol of DsbA per nmol of DsbB/sec. Under saturating concentrations of Q_0C_{10} (25 μM) and in the presence of 0.1 % dodecyl maltoside, an apparent K_m value of DsbA^{red} for the highly purified system was determined to be 3.1 μM in our reconstituted system (Figure 2.5B). The apparent k_{cat}/K_m values for ubiquinone is 3×10^6 M^{-1}sec^{-1}, making quinones very specific substrates for DsbB. To our knowledge, DsbB has an undescribed enzymatic activity; it catalyzes the formation of a disulfide bond by the reduction of ubiquinone.

DsbB is considered the major source of disulfides in prokaryotes, because mutations in *dsbB* result in severe defects in disulfide bond formation (35). The other Dsb proteins have important roles in disulfide exchange, but none seem to actually create disulfides *de novo*. We did not observe spontaneous reaction of DsbA and ubiquinone under our assay conditions. The reaction between thiols and quinones is rather complex as the redox reaction competes with arylation of the thiol groups. DsbB is capable of accelerating the redox reaction specifically and very efficiently.

Quinone Analogue 5-Halo-Q Inhibits DsbB Activity

Study of quinone:protein interaction in DsbB with various Q-derivative could generate lots of information on the structural specificity of the Q-binding site in the protein. The lack of good inhibitors for the DsbB has hampered attempts to discern a common mechanism of quinone interaction and the identification of binding sites utilizing site-directed mutagenesis. The quinone reduction assay for DsbB not only provides us a good method to study the kinetic properties of DsbB, but also allows us to discover the effect of quinone like compounds on DsbB's function.
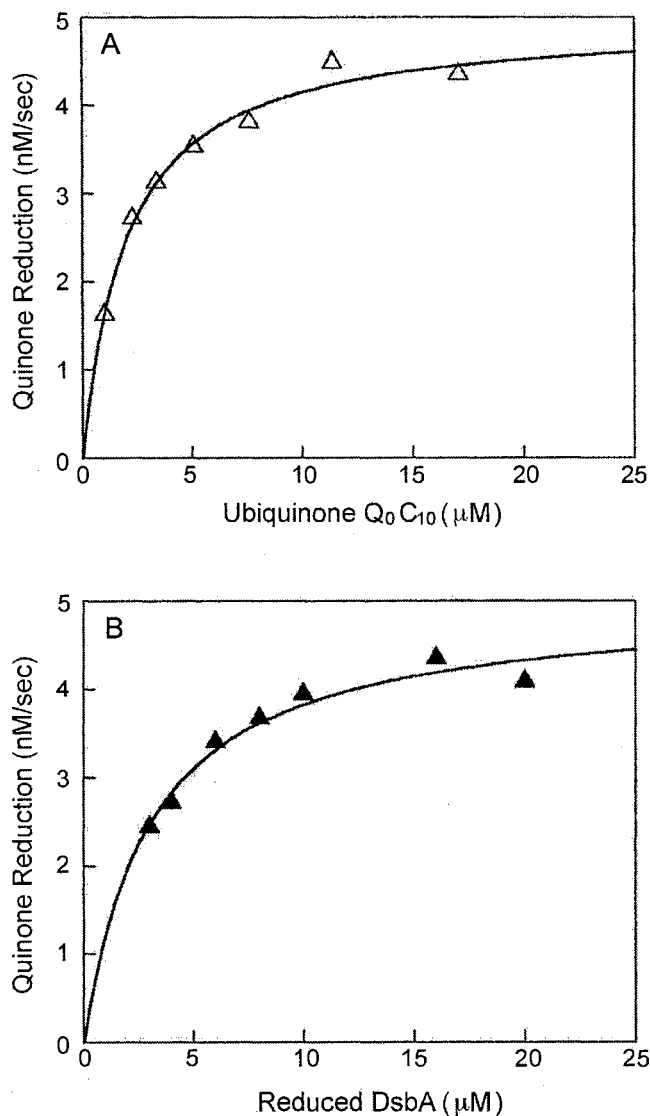
Figure 2.5. Kinetic Properties of DsbB Determined by the Quinone Reduction Assay.

A, initial velocities of DsbB-catalyzed quinone reduction were measured at 275 nm. The assay buffer is described in Figure 2.4, includes 20 μM reduced DsbA. Q_0C_{10} was added to the indicated concentrations. To start the reaction, DsbB was added to a final concentration of 1 nM. The data were fitted to a hyperbola using Sigma Plot. The apparent values for $K_m(Q_0C_{10})$ = 2.0 μM and V_{max} = 5.0 nmol of $DsbB^{red}$ per nmol of DsbB/s were calculated from the fit. B, initial velocities of quinone reduction were determined under saturating concentrations of Q_0C_{10} (25 μM). Increasing amounts of reduced DsbA were added, and the reaction was started by the addition of DsbB to 1 nM. The apparent $K_m(DsbA)$ is 3.1 μM, and V_{max} is 5.0 nmol of ubiquinone per nmol of DsbB/s.

75

A series of inhibitors for other quinone binding proteins had been tested in the DsbA-DsbB-Q enzymatic system. We checked the effect of the following compounds: 2-sec-butyl-4,6-dinitrophenol (s-BDNP), 2-thenoyltrifluoroacetone (TTFA), 5-*n*-undecyl-6-hydroxy-4,7-dioxobenzothiazole (UHDPT), stigmatellin, heptylhydroxyquinoline-*N*-oxide (HQNO), piericidin A, antimycin A, and 5-halo-2,3-dimethoxy-6-decyl-1,4-benzoquinone. They are well characterized and have been employed to test quinone sites in many quinone binding proteins such as electron transfer complexes (Part I, Scheme 1.3). Among them, 5-Br-Q_0C_{10} and 5-Cl-Q_0C_{10} showed the most significant inhibitory effect on DsbB activity.

The inhibition measurements were performed at 20 μM Q_0C_{10}, which corresponds to 10×K_m. This result prompted us to investigate 5-halo-Q's mode of inhibition when using Q_0C_{10} as a substrate. Table 2.2 indicates that V_{max} remains unchanged while the apparent K_m for Q_0C_{10} increases from 2.03 μM to about 5.50 μM or 9.60 μM in the presence of 10 μM 5-Br-Q_0C_{10} or 5-Cl-Q_0C_{10} respectively compared to the absence of inhibitor. The inhibition constants K_i were calculated to be 5 μM and 2 μM for 5-Br-Q_0C_{10} and 5-Cl-Q_0C_{10}, respectively.

Therefore, the inhibition by either 5-Cl-Q_0C_{10} or 5-Br-Q_0C_{10} is competitive. The lower K_i value of 5-Cl-Q_0C_{10} suggests that it is a stronger inhibitor than 5-Br-Q_0C_{10}. A point to note here is that all concentrations that were used in the calculation are apparent values. Since DsbB is a membrane protein and quinone has a hydrophobic tail that can freely diffuse through the membrane, it is hard to know the localized concentration of quinone around the active site of DsbB.

The strong inhibitory effect of the ubiquinone analogue 5-halo-Q demonstrates that DsbB contains a highly specific ubiquinone-binding site. 5-Halo-Q competes with Q_0C_{10} for binding at DsbB's quinone site. As a quinone analogue, 5-halo-Q_0C_{10} serves as electron acceptor with reduced efficacy for SQR in respiratory chain (Part I, Table 1.5). This suggests that quinone-binding site and its mechanism of DsbB is similar to that of SQR. More information about DsbB can be obtained based on the known information about SQR.

Table 2.2. DsbB Is Competitively Inhibited by 5-Halo-Q_0C_{10}

Q analogue	K_m (µM)	V_{max} (mol of Q/mol of DsbB/sec)	K_i (µM)
none	2.03 ± 0.19	5.06 ± 0.30	–
5-Br-Q_0C_{10}	5.50 ± 0.62	5.37 ± 0.91	5.08 ± 0.94
5-Cl-Q_0C_{10}	9.60 ± 1.08	5.02 ± 0.32	2.12 ± 0.57

Assay method is described in the Experimental Procedures of Chapter V and Figure 2.5A. Initial velocities of DsbB-catalyzed quinone reduction were measured at 275 nm. The assay buffer consists of 50 mM sodium phosphate, pH 6.0, 300 mM NaCl, 0.1% n-dodecyl maltoside, and 20 µM reduced DsbA. Q_0C_{10} was added to the concentrations ranging from 0 to 25 µM. In the cases of inhibition, 5~20 µM of 5-halo-Q_0C_{10} was added into the assay mixture. To start the reaction, DsbB was added to a final concentration of 1 nM. The data were fitted to a hyperbola. The apparent values for K_m (µM Q_0C_{10}) and V_{max} (nmol of ubiquinone per nmol of DsbB/s) were calculated from the fit.

Purified DsbB Contains Bound Coenzyme Q_8

Reduction of Native Quinone in Purified DsbB

The observation that DsbB catalyzes the reduction of quinones led us to analyze the quinone-binding properties of DsbB. We first decided to test if DsbB contains bound quinone after purification. Oxidized quinones can be detected by a decrement in absorption at 275 nm upon reduction into quinol with sodium borohydride (60). Figure 2.6 shows the UV spectra of purified DsbB before and after the addition of sodium borohydride ($NaBH_4$). An 11% decrease in the absorption at 275 nm was observed after $NaBH_4$ was added to the cuvette. We attributed this change in absorbance to the reduction of the ubiquinone bound to DsbB. The addition of the $NaBH_4$ did not change the absorbance of the buffer blanked against water or DsbA, which served as a negative control (data not shown). From this absorbance change and given that the absorbance coefficient of coenzyme Q is 12.25 mM^{-1} (60), we calculated that the purified DsbB contains 0.6 molar eq of bound quinone.

Identification of Quinone Component in DsbB by Solvent Extraction

In order to obtain additional proof for binding of ubiquinone to DsbB, we extracted DsbB with hexane, which should denature the protein and extract any bound quinones. The extract was analyzed by HPLC. The comparison of the elution profile of the DsbB extract (Figure 2.7a) with the elution profiles from known quinone standards (c and d) indicates that the sample extracted from DsbB contains coenzyme Q_8 (ubiquinone with 8 isoprenoid units in 6 position). Mixture of the DsbB extract and purified coenzyme Q_8 migrates as a single peak (Figure 2.7b). The identification of coenzyme Q_8 as the DsbB-bound quinone agrees very well with the fact that this quinone is the predominant quinone species present in *E. coli* membranes under aerobic growth conditions (53). From the peak area we calculated a molar ratio of 0.6 mol of coenzyme Q_8 bound per mol of DsbB, consistent with the value derived from the difference spectra shown in Figure 2.6.
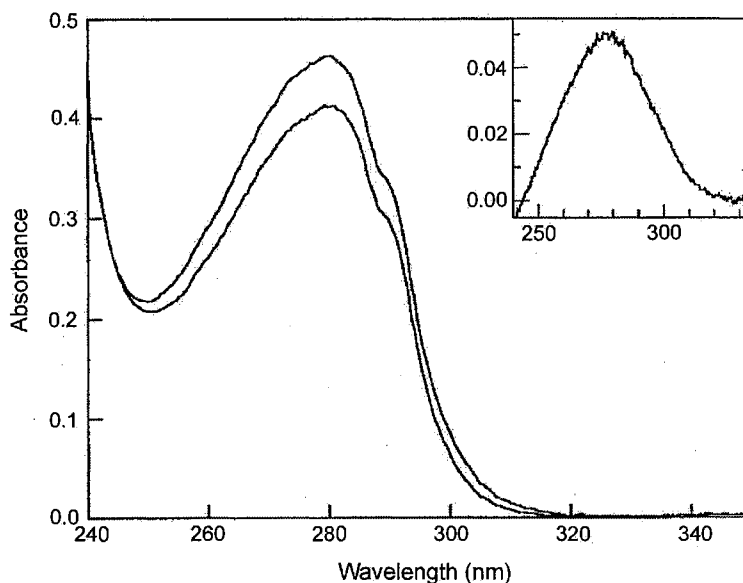
Figure 2.6. UV Spectra of DsbB Suggest That DsbB Contains Bound Ubiquinone.

The UV spectrum of DsbB was recorded from 240 to 340 nm in 50 mM sodium phosphate, pH 6.0, 300 mM NaCl, 0.1% n-dodecyl maltoside (upper trace). Solid sodium borohydride was added to the cuvette, and the spectrum of the reduced protein (lower trace) was recorded after 5 min of incubation at room temperature. The inset shows the difference spectra of oxidized minus reduced DsbB.
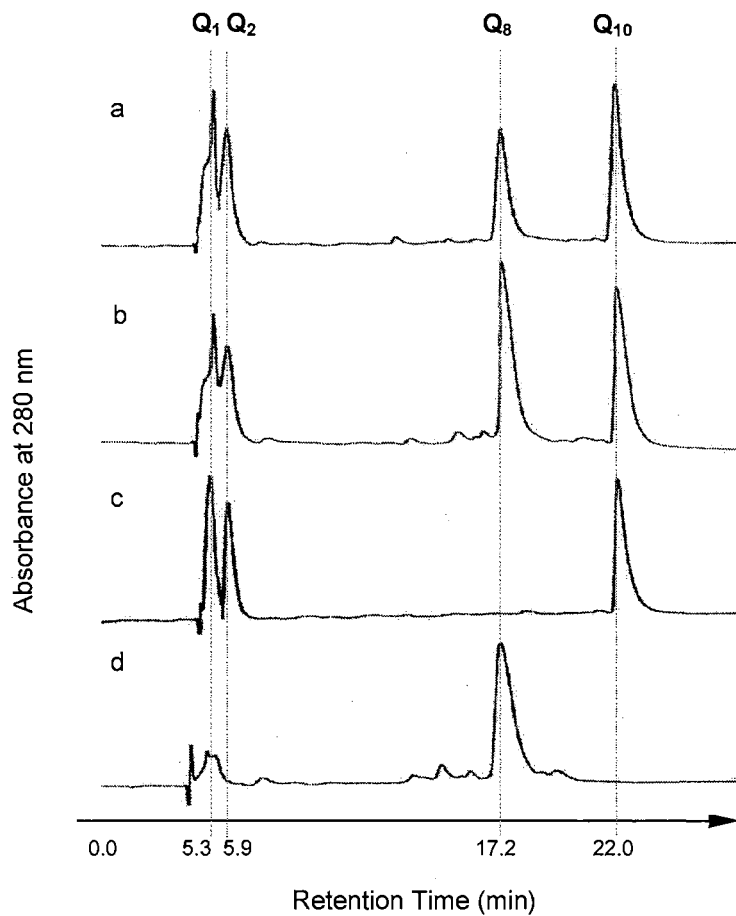
Figure 2.7. <u>Identification of Ubiquinone Q_8 as the Bound Quinone in DsbB.</u> DsbB was extracted with organic solvents as described in Experimental Procedures of Chapter V. The DsbB extract was dissolved in ethanol, mixed with various purified quinones, and loaded onto a reverse phase C8-HPLC column. Coenzymes Q_1, Q_2, Q_8, and Q_{10} served as standards. Profile a consists of Q_1, Q_2, DsbB extract, and Q_{10}. Profile b consists of Q_1, Q_2, DsbB extract + added Q_8, and Q_{10}. Profile c consists of Q_1, Q_2, and Q_{10}. Profile d is purified Q_8 only. The DsbB extract was judged to contain Q_8 based on the observations that the retention time for the DsbB-extracted sample is the same as for the Q_8 standard (a and d) and because a single, enhanced peak at the Q_8 position results when a mixture of the DsbB extract and Q_8 was applied (b). From the peak area of the known Q_8 standard a molar ratio of bound quinone to DsbB of 0.6 was calculated.

DsbB Binding of Ubiquinone Is Detergent Dependent

The amount of quinone associated with purified DsbB was found to vary with detergent used. Table 2.3 shows that the presence of 0.1% dodecyl-maltoside interferes the binding of quinone in DsbB. After the DsbB protein was extensively washed with 1.0% sodium cholate and passed through a desalting column equilibrated with 1.0% sodium cholate in phosphate buffer, the oxidized minus reduced difference spectra revealed only 0.3 moles of quinone bound. It suggests that the binding of the quinone to the isolated protein depends on the nature of detergent.

Titration of the DsbB's Ubiquinone-binding Site with Exogenous Quinone

We wanted to determine the number of high affinity quinone-binding sites that were present in DsbB. The specific quinone-binding in proteins can be titrated with external quinone. This is based on the assumption that specific binding would have an absorbance change, as compared to the non-specific quinone binding to the protein (46).

It was known that dodecyl-maltoside and other non-ionic detergent interfere with Q-binding to protein. Detergent in DsbB sample, 0.1% dodecyl-maltoside, was replaced by 1.0% sodium cholate. This was done because sodium cholate is more effective than 0.1% dodecyl-maltoside in removing endogenous Q and this improves the signal obtained during quinone titration. In fact, the signal observed for DsbB in the presence of 0.1% dodecyl maltoside was feeble as compared to that obtained with the sodium cholate detergent.

Figure 2.8 demonstrates that the presence of DsbB strongly affects the spectral property of externally added $Q_0C_{10}Br$, a synthetic ubiquinone analogue (54). The different spectral properties of $Q_0C_{10}Br$ in the presence of DsbB indicate the transfer of $Q_0C_{10}Br$ from an aqueous to a more hydrophobic environment. We attribute this absorbance change to the binding of ubiquinone to DsbB. The absorbance change of $Q_0C_{10}Br$ upon interaction with DsbB reaches a saturation level (open circles). After addition of 20 µM, $Q_0C_{10}Br$ showed the

Table 2.3. Detergent Dependence of DsbB Bound Ubiquinone

detergent	Ubiquinone/DsbB	Determined by
0.1% dodecyl-maltoside	0.6	asorbance
0.1% dodecyl-maltoside	0.6	HPLC
1.0% sodium cholate	0.3	asorbance

Assay method is described in Figure 2.6 and Figure 2.7 according to the Experimental Procedures in Chapter V.

Figure 2.8. <u>Titration on Quinone-Binding Site of DsbB.</u> DsbB was washed extensively with 50 mM sodium phosphate, 1% sodium cholate. After this procedure the amount of bound ubiquinone was 0.3 mol/mol DsbB. The titration was performed in the same buffer by adding $Q_0C_{10}Br$ in 1-μl increments from a 5 mM stock solution. After each addition, the sample was incubated for 5 min at room temperature, and the spectrum from 240 to 340 nm was recorded (panel A). Panel B is the buffer control. A change in absorption at 280 nm greater than that shown for the buffer control indicates the burial of ubiquinone in a protein environment. Panel C shows the absorbance changes *vs.* the amount of exogenous quinone according to panel A and B. This change is specific for ubiquinone-binding proteins. The cuvette containing DsbB at 25 μM (open circles) shows a greater change in absorbance than the buffer controls (solid circles) after quinone additions of up to 20 μM $Q_0C_{10}Br$. The DsbB contained 0.3 mol of quinone per mol of DsbB (8 μM of quinone bound) prior to any additions. We conclude that ~28 μM quinone is bound at saturation to 25 μM DsbB, a ~1:1 ratio.
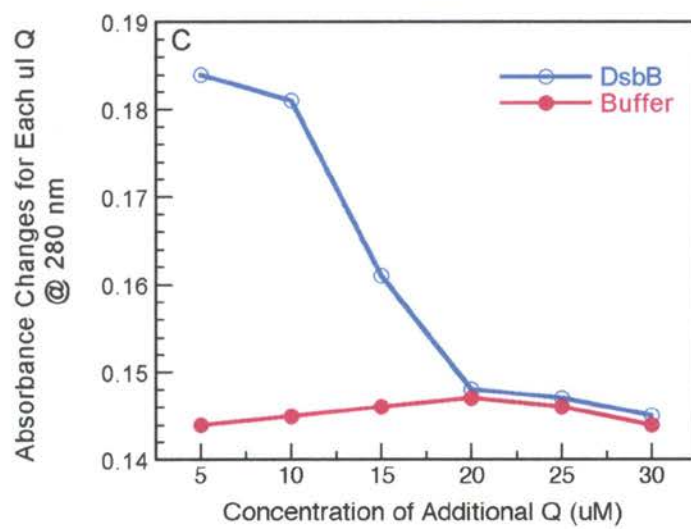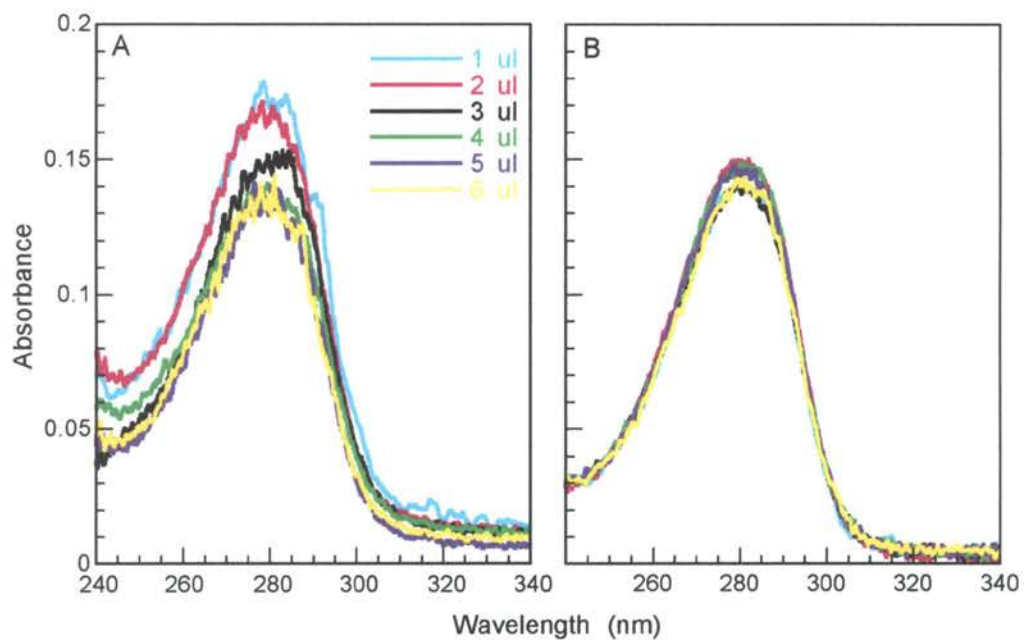
spectral properties that are typically observed for ubiquinone in the aqueous buffer control (closed circles). The DsbB concentration was 25 μM. By taking into account that the protein contained 0.3 mol (8 μM) of bound ubiquinone after the detergent exchange, the titration with external quinone provides evidence that the quinone site of DsbB can be titrated to a 1:1 molar ratio.

Mapping the Q Binding Fragment of DsbB

<u>Properties of [^{3}H]Azido-Q Derivatives</u>

Two radioactive azido-Q derivatives, 3-azido-2-methyl-5-methoxy-6-geranyl-1,4-benzoquinone ([^{3}H]3-N$_3$-5-MeO-PQ$_2$) and 5-azido-2,3-dimethoxy-6-decyl-1,4-benzoquinone ([^{3}H]5-N$_3$-Q$_0$C$_{10}$), were synthesized and characterized for identifying the Q-binding site in DsbB. According to their chemical structures shown in Scheme 2.6, there are three features in these compounds that are beneficial in the labeling experiment:

1. Overall structure are ubiquinone-like so that they can fit into the quinone specific binding site of DsbB.

2. Azido group (-N$_3$) can react nonselectively to form a covalent bond with nearby peptide when exposed to 250~460 nm ultraviolet light. It allows the azido-Q compounds to fix in the quinone site of DsbB.

3. ^{3}H makes the azido-Q compound traceable by following its radioactivity.

Unlike regular quinones which have absorption peak at ~275 nm, spectra of [^{3}H]3-N$_3$-5-MeO-PQ$_2$ and [^{3}H]5-N$_3$-Q$_0$C$_{10}$ (Figure 2.9) shows absorption peak at 306 nm and 315 nm, respectively. This absorption characteristic serves as an alternative reference in the spectral analysis to identify the quinone labeled peptides of DsbB. Maximum photolyzation was observed when the sample was illuminated for 7 minutes.

Both of the azido-Q derivatives exhibit partial electron acceptor activity for DsbB in dark, compared to the activity of Q$_2$ (Table 2.4). These azido-Qs can fit into the Q site and
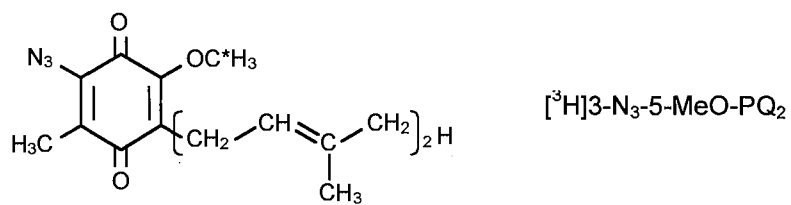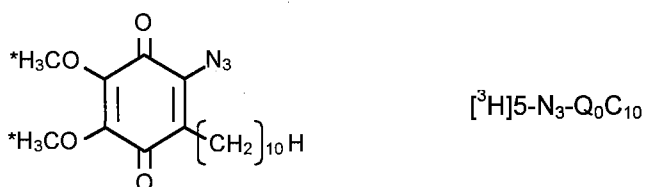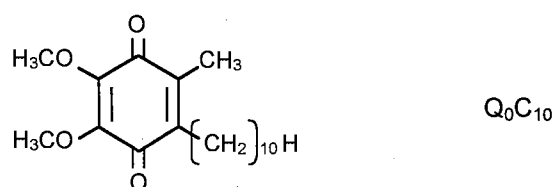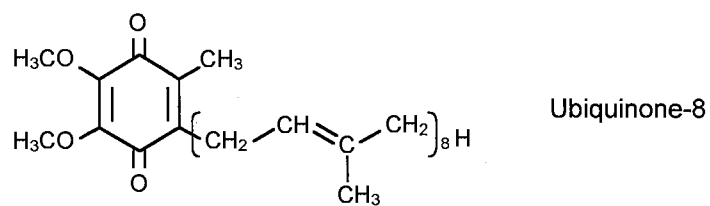
Scheme 2.6. Structural Formula of Ubiquinone-8 and Azido-Q Derivatives

3-N$_3$-5-MeO-PQ$_2$*

5-N$_3$-Q$_0$C$_{10}$
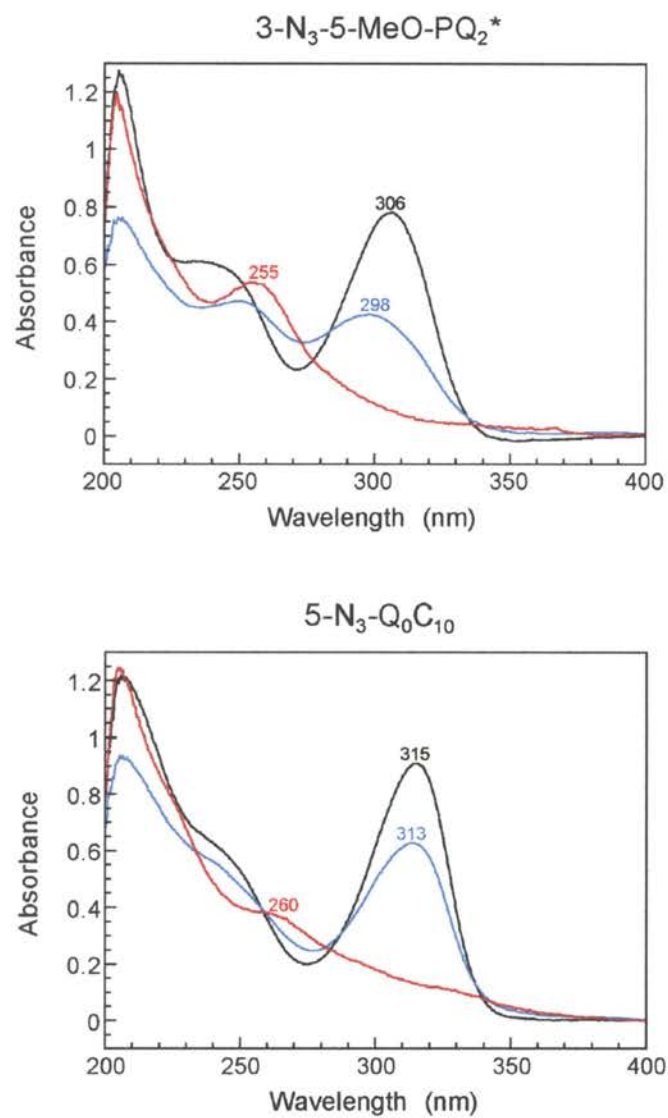
Figure 2.9. <u>Absorption Spectra of Azido-Q Derivatives</u>. The black curve represents the azido-Q in 95% ethanol in dark, the blue curves represents this azido-Q illuminated with long wavelength UV for 7 minutes, the red curve represents the azido-Q reduced by NaBH$_4$.

Table 2.4. Electron Acceptor Activity of [^{3}H]Azido-Q Derivatives for DsbB

Q Derivatives	Wavelength, nm	Activity, %
Q_2	278	100
Q_0C_{10}	278	72
$5\text{-}N_3\text{-}Q_0C_{10}$	315	35
[^{3}H]3-N_3-5-MeO-PQ_2	306	17

Assay method is described in Figure 2.6 and Figure 2.7 according to the Experimental Procedures in Chapter V. The activities of azido-Q derivatives were detected following the corresponding wavelength.

accept electron from DsbB with lower efficacy than Q_2. The [^{3}H]-azido-Q derivatives have the same electron acceptor activity for DsbB as the corresponding unlabeled cold compounds.

Correlation between Azido-Q Incorporation and Inactivation

Study of the quinone:protein interaction in DsbB using synthetic Q derivatives requires the prior removal of endogenous Q from the protein because the binding affinity of synthetic Q derivatives to the Q-binding sites is weaker than that of endogenous Q. Since a method for the reversible removal of Q from DsbB has not yet been developed, we replaced the detergent in DsbB with sodium cholate and decreased the native quinone-binding down to ~30% saturated (Table 2.3). The detergent or un-removed phospholipid in this DsbB sample could mask the Q-binding sites in DsbB. Therefore, the higher amount of azido-Q is required to attain the specific interaction between azido-Q and DsbB.

When purified DsbB was incubated with various concentration of [^{3}H]3-N$_3$-5-MeO-PQ$_2$, the activity decreased as the concentration of azido-Q increased. Maximum inactivation of approximately 40% were obtained when 10 mol azido-Q/mol of DsbB was used (Figure 2.10). This result suggests that the affinity of endogenous Q for its binding site is much stronger than that of the azido-Q derivatives. The DsbB inactivation was not due to inhibition of DsbB by photolyzed products of azido-Q, because when azido-Q was photolyzed in the absence of DsbB and then added to DsbB, no inhibition was observed.

On the other hand, according to the radioisotope incorporation for protein obtained from the paper chromatography, azido-Q uptake by protein increased as the concentration of Q increases (Figure 2.10). When azido-Q/DsbB molar ratio was higher than 10, the azido-Q uptake was at a much slower rate, suggesting that this slower incorporation is due to nonspecific binding of azido-Q to DsbB. The incorporation of the radioactivity in DsbB agrees with the inactivation of quinone reduction activity for the azido-Q labeled DsbB. It suggests that the inactivation observed results from the tight interaction of azido-Q to DsbB, which is not dissociated during the chromatography, even though DsbB may not covalently
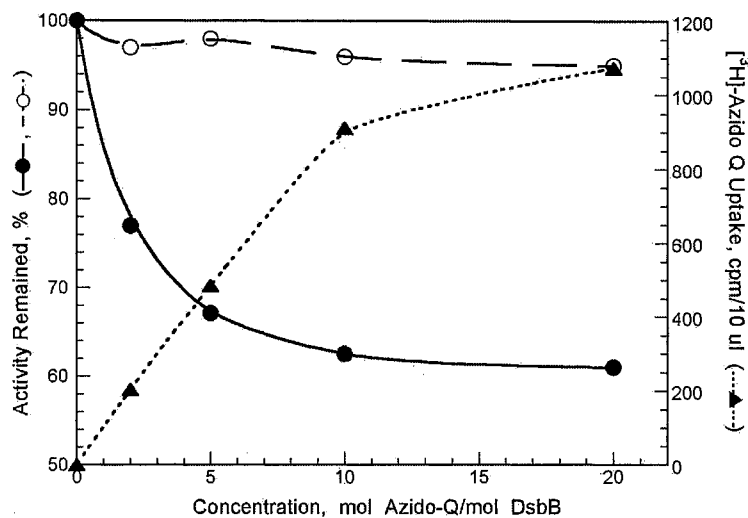
Figure 2.10. <u>Correlation between Incorporation and Inactivation of Azido-Q DsbB.</u>
Aliquots (50 µl) purified DsbB, 0.4 mg/ml (20 mM) in 50 mM phosphate buffer, pH 7.4, containing 1.0% sodium cholate, were incubated with indicated concentration of $[^3H]3\text{-}N_3\text{-}5\text{-MeO-PQ}_2$ (6×10^3 cpm/nmol) for 1 hour at 0 °C in the dark and then illuminated with long wavelength UV light for 7 minutes at a distance of 4 cm. DsbB activity was assayed following the method described in Figure 2.6 and Figure 2.7 (● ————). 100% activity is DsbB without treatment with azido-Q and without illumination. The activity assay for DsbB with indicated concentration of illuminated azido-Q serves as a control (O ————). $[^3H]$Azido-Q uptake of DsbB in 10 µl reaction mixture was determined by paper chromatography developing by $CHCl_3$-CH_3OH, 2:1 (▲ --------). The radioactivities of the protein origins were measured by liquid scintillation. According to the radioisotope incorporation, the ratio of azido-Q to DsbB was calculated to be 60:100.

link to all the azido-Q taken up. It could explain why we could not get up to 70%

inactivation after azido-Q labeling even though we started from the DsbB with 30%

endogenous Q.

The radioactivities of the filter paper after organic solvent chromatography showed

that 6% of the total cpm was incorporated with the DsbB protein in the origin. Based on the

10:1 molar ratio of azido-Q to DsbB in the labeling mixture, approximately 60% of DsbB

were labeled with azido-Q. The enzymatic inactivation result indicates most of the DsbB

associated azido-Qs were bound specifically to the Q-binding sites.

The azido-Q inactivation and radioactivity uptake by DsbB for $[^3H]5\text{-}N_3\text{-}Q_0C_{10}$ were

similar to those for $[^3H]3\text{-}N_3\text{-}5\text{-}MeO\text{-}PQ_2$, but the maximum inactivation is about 20% and

40% radioactive-Q incorporation. These results indicate that either $[^3H]$azido-Q is suitable

for studying the quinone:protein interaction for DsbB when 10 mol azido-Q/mol DsbB is used.

Identification of the Quinone Binding Peptide in DsbB

In order to identify the Q-binding domain in DsbB through isolation and sequencing

of an azido-Q-linked peptide, it is necessary that the isolated azido-Q-labeled DsbB be free

from contamination with unbound azido-Q. This is done by a gel filtration chromatography

in the presence of 1.0 % sodium cholate, and then concentrate by centricon-10. According

to the radioactivity of the filtrate and the retentate, most of the non-protein-bound azido-Q,

such as free azido-Q, or azido-Q linked to small molecule after photolysis, was removed after

this procedure. And the small amount of contamination can be subtracted based on the blank

control and the undigested $[^3H]$azido-Q labeled DsbB control.

Protease V8, which specifically cleaves peptide bonds on the carboxyl side of

glutamic acid or aspartic acid residues, and trypsin, which is highly specific toward positively

charged side chains with lysine and arginine, were selected to digest the $[^3H]$azido-Q-labeled

DsbB individually. One advantage of these protease in our system is that they are fully active

in the presence of up to 0.2 % (for V8) or 1.0 % (for trypsin) SDS (62,63). This detergent

condition is preferred in the digestion reaction for DsbB since it is a membrane protein.

Figure 2.11 shows the digestion pattern for [^{3}H]azido-Q- labeled DsbB protein. It appears that little intact DsbB exists in the trypsin-digested sample and about 40% of intact DsbB is present in the V8-digested protein. The digestion is not complete under our reaction conditions since the digested fragments are not in agreement with the calculated sizes according to the specific cutting sites of the DsbB sequence. The reason is that some of the cleavage sites in DsbB are not accessible for protease. They might also be masked by the detergent or aggregated with each other. In this case, the quinone binding amino acid residues which was labeled with [^{3}H]Q could be obtained in more than one piece of digested peptide fragments.

Because the protease digestions were not complete, we extracted the digested peptides from the reaction mixture with 45% acetonitrile before it is applied onto the HPLC column. The radioactivities of the supernatant and precipitate were checked to determine the recovery. It is found that more than 60% of the total radioactivity was in the acetonitrile extract, which means the digested peptides contained the azido-Q labeled fragment.

Figure 2.12 and Figure 2.13 show the distribution of radioactivity on the HPLC chromatography of [^{3}H]azido-PQ$_2$-labeled DsbB peptides digested by the protease V8 and trypsin, respectively. The majorities of the radioactivity are found in the fractions with retention time of 33.46 (PV-34) and 58.12 (PV-59) for V8 digestion; 32.58 (PT-33) and 58.11 (PT-59) for trypsin digestion. According to the undigested control, the P-59 corresponds to the intact or DsbB polypeptide, or the biggest polypeptide after protease digestion, which was labeled with azido Q. The PV-34 and PT-33 are V8 and trypsin digested fragments, respectively. The spectra of these peptides showed that their absorption red shifts to 287.8 and 288.2 nm while the normal absorption for tryptophan of peptide is at 280 nm. This observation provides another evidence for the quinone labeled peptide besides the radioactivity. The incomplete digestion of the labeled DsbB resulted in the relatively high radioactivity in several peptides other than the major peaks.
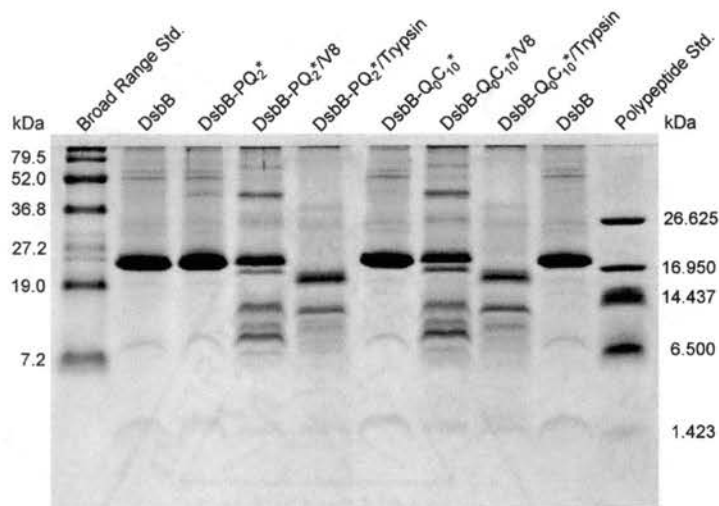
Figure 2.11. <u>Protease Digestion Pattern for Azido-Q Labeled DsbB by SDS-PAGE</u>. The electrophoresis was carried out in a Bio-Red Mini-gel apparatus with thickness 1.5 mm. The separation gel contained 16% acrylamide, 6% N,N'-methylene-bisacrylamide of acrylamide, 3.5 M urea, 10% glycerol, 1 M Tris-Cl pH 8.8, 5 mg/ml ammonium persulfate, 0.5 μl/ml N,N,N',N'-tetramethylethylenediamine. Protein samples were digested in 1% SDS, 0.4% β-mercaptoethanol, 3% glycerol and 10 mM Tris-Cl, pH 6.8 with 1 hour incubation in 37 °C. After addition of Coomassie brilliant blue R 250 as front marker, the electrophoresis was carried out at constant voltage (20V for stacking gel and 90V for separation gel).
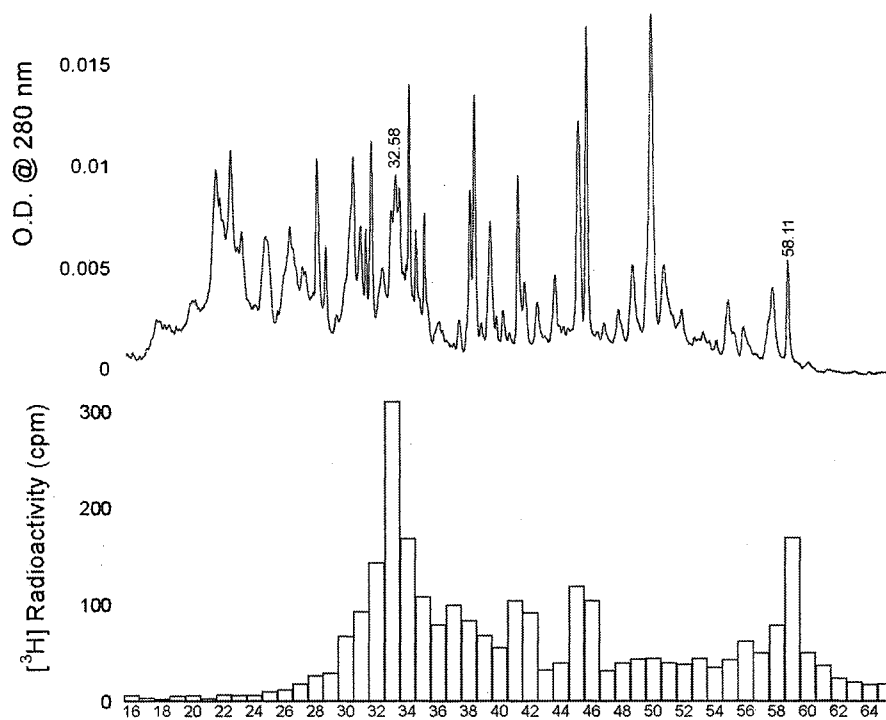
Figure 2.12. ³H Radioactivity Distribution on HPLC Chromatogram of Protease Trypsin Digested [³H]Azido-PQ₂-Labeled DsbB. The [³H]azido-PQ₂-labeled DsbB was mixed with trypsin, digested solution was extracted with acetonitrile and then subjected to HPLC separation as described in "Experimental Procedures". 100 μl aliquots were withdrawn from each fraction for radioactivity determination. The chromatography is displayed with retention time from 15 min to 65 min.
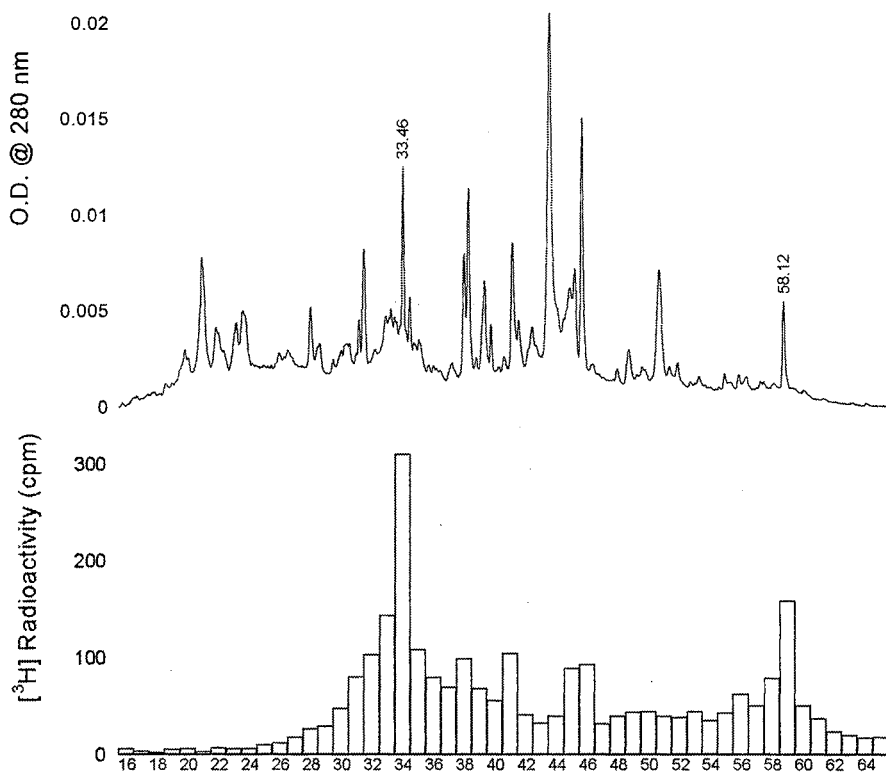
Figure 2.13. ^{3}H Radioactivity Distribution on HPLC Chromatogram of Protease V8 Digested [^{3}H]Azido-PQ$_2$-Labeled DsbB. The running conditions are the same as in Figure 2.12 except that the [^{3}H]azido-PQ$_2$-labeled DsbB was digested with V8 instead of trypsin.

Table 2.5 summarizes the Q-labeled peptide analysis. The partial NH_2-terminal amino acid sequence of PV-34 was found to be HTMLQLY-, corresponding to amino acid residues 91- of DsbB, while that of PT-33 is ATCDFMV-, corresponding to amino acid residues 102- of DsbB. This trypsin digestion fragment does not start from the specific cleavage site of trypsin (lysine or arginine). The sample could be unspecifically overdigested under our conditions.

By mass spectral analysis, we determined the sizes of these quinone-binding peptides, to be 2578.38 and 1315.53 for PV33 and PT34, respectively. These mass spectrometric results suggest that the Q labeled peptides are H91-E112 for V8 digestion and A102-E112 for trypsin digestion.

The sequencing results of $[^3H]5$-N_3-Q_0C_{10} labeled DsbB agree with that of $[^3H]3$-N_3-5-MeO-PQ_2 very well, which means either quinone labels the same peptide of DsbB.

According the proposed structure of DsbB (Scheme 2.3), the Q-binding sequence is ^{91}HTMLQLYPSPF^{102}ATCDFMVRFPE^{112}, located in starting region of the C-terminal periplasmic loop. One of the highly conserved amino acid residues for DsbB activity, Cys104 is in this Q-binding region. Although the identification of Q-binding peptide of DsbB according to $[^3H]$azido-Q photo-affinity labeling strongly indicates the involvement of a portion of DsbB in Q binding, it does not preclude the involvement of other segments in DsbB. It would not be surprising if the Q-binding site is a pocket formed from more than one segment of the DsbB polypeptide.

Simulation of Quinone Binding Pocket for DsbB

The study of quinone:protein interaction of DsbB eventually provides us the structural information to propose the mechanism of the electron transfer from DsbB to quinone. The availability of the three dimensional structure of other quinone binding protein allows us to simulate the quinone pocket of DsbB based on the alignment of the primary structure of DsbB to those of the well studied quinone proteins.

Table 2.5. Identification of Q-Binding Peptide for [^{3}H]PQ$_2$-DsbB

quota	Peptide data/parameter		method
Protease	V8	Trypsin	digestion
Retention time (min)	33.46	32.58	HPLC
CPM	308.5	316.0	Liquid scintillation
Absorption peak (nm)	287.8	288.2	spectrophotometry
N-terminal	HTMLQLY-	ATCDFMV-	Protein sequencing
MW (Da)	2578.38	1315.53	Mass spectrometry
Fragment position	91~112	102~112	Theoretical calculation based on the known sequence
Number of amino acid	21	11	
MW (Da)	2631.08	1315.52	

Crossing-linking Result Suggests That DsbB Is Dimer

Many of the well studied quinone-binding proteins, including NADH-quinone reductase (QR1), succinate-quinone reductase and fumarate reductase, are found to be homodimers and containing two Q sites with two polypeptide chains. It is not surprising that DsbB whose function is thiol-quinone reductase performs as a dimer. Even though DsbB is commonly thought to be a monomer in literature so far, there is no experimental evidence to support this idea. According to the SDS-PAGE without β-mercaptoethanol treatment, it is clear that no disulfide bond is formed between different DsbB polypeptides (Figure 2.14b, lane 6). However, DsbB can still exist as a dimer by non-covalent interaction between polypeptide chains. As a small membrane protein, it is hard to determine the DsbB's quaternary structure due to the association of detergent. In our study, a cross-linking agent APDP was used to stabilize the DsbB oligomers.

APDP is a cleavable, photoreactive, heterobifunctional crosslinker with a 21.02 Å spacer arm between the photoaffinity azido and pyridyldithio groups (Figure 2.14a). The 4 free thiol groups in a reduced form DsbB polypeptide allow the APDP to link DsbB with disulfide bonds and they are cleavable by β-mercaptoethanol. The SDS-PAGE (Figure 2.14b) showed a new band at about 40 kDa besides the original 20 kDa DsbB band after the crosslinking reaction (lane 2 and lane 4). Another Dsb protein, DsbA (in reduced form), which is a soluble protein and known to be a monomer, serves as negative control. Under the same condition for crosslinking reaction, no new band of twice the size for DsbA is observed (lane 8). Also, the crosslinking for DsbB is concentration independent (lane 2, lane 4). It indicates that the crosslinking reaction actually occurred in between two polypeptides spatially close to each other in the native DsbB conformation.

Accordingly, at least part of the DsbB polypeptides in the protein preparation are associated with each other to form homodimers.
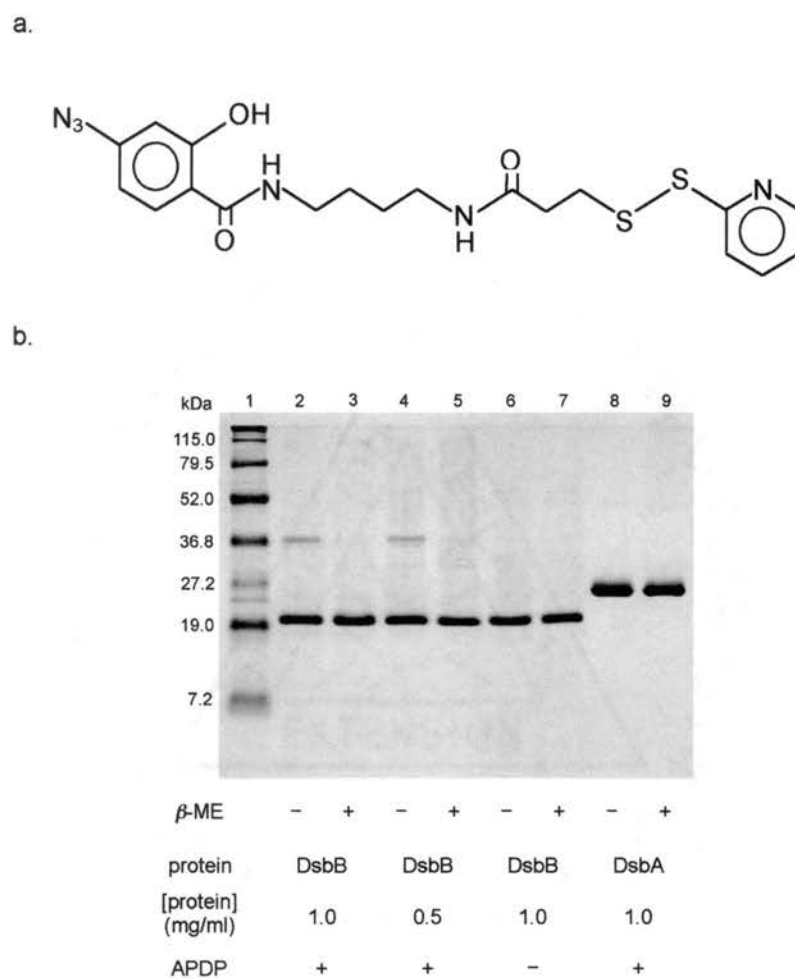
a.

b.

β-ME		−	+	−	+	−	+	−	+
protein		DsbB		DsbB		DsbB		DsbA	
[protein] (mg/ml)		1.0		0.5		1.0		1.0	
APDP		+		+		−		+	

Figure 2.14. <u>Cross-linking Reaction Suggests That DsbB Is Dimer</u>. a. Structural formula of
APDP (N-[4-(*p*-azidosalicylamido)butly]-3'(2'-pyridyldithio)propionamide) used
as the cross linker. b. High resolution SDS-PAGE for DsbB crosslinked by
APDP. The electrophoresis was carried out in a Bio-Red Mini-gel apparatus
with thickness 1.5 mm. The separation gel contained 12% acrylamide, 3%
N,N'-methylene-bisacrylamide of acrylamide, 3.5 M urea, 10% glycerol, 1 M
Tris-Cl pH 8.8, 5 mg/ml ammonium persulfate, 0.5 µl/ml N,N,N',N'-
tetramethylethylenediamine. The electrophoresis was carried out at constant
voltage (20V for stacking gel and 90V for separation gel). Lane 1 is
molecular weight standard. Lane 2 to lane 9 are described on the table
below the gel.

QR1 Acts as the Modeling Template

The recombinant human and mouse NADH:quinone acceptor oxidoreductase (QR1), a flavoenzyme that catalyzes the obligatory two-electron reduction of quinones to quinol, was used as our template to fit the quinone pocket of DsbB. The crystal structure of this enzyme with substrate duroquinone was reported in 1.7 Å earlier this year (42). It is a homodimer made of two interlocked monomers (Figure 2.15a). Duroquinone binds to the active site through a series of contacts involving several hydrophilic and hydrophobic residues. The quinone is hydrogen-bonded to a water molecule that bridges the Nε of His-161 and the -OH of Tyr-128'. In addition, five aromatic residues (Trp-105, Phe-106, Phe178', Tyr-126', Tyr-128') provide most of the hydrophobic contacts (Figure 2.15b).

In order to compare the quinone-binding pocket of DsbB and QR1, the activity of DsbB was assayed using duroquinone as the electron acceptor. As we expected, duroquinone which can be co-crystallized with QR1 serves as a substrate for DsbB. This indicates that duroquinone actually fits the quinone-binding pocket of both DsbB and QR1 very well.

The sequence alignment of DsbB to the QR1 is shown in Scheme 2.7. Even though the overall similarity of these two sequences is not high (27%), we found that the residues involved in Q pocket of QR1 are actually conserved in the sequence of the two periplasmic loops of DsbB. This result suggests that residues W31, F32, Y46, R48, H91, F106 might participate in the Q pocket in DsbB and could be crucial for its quinone reduction activity.

Summary

Our results further elucidate the mechanism of disulfide bond formation and how it is linked to the electron transport chain. By reducing ubiquinone, DsbB plays a central role in this pathway by creating disulfides from the reduction of quinone. Disulfide bonds are formed during the folding of many periplasmic proteins (14). By reconstituting the DsbA-DsbB system *in vitro*, we were able to identify the electron acceptor of DsbB to be quinones.
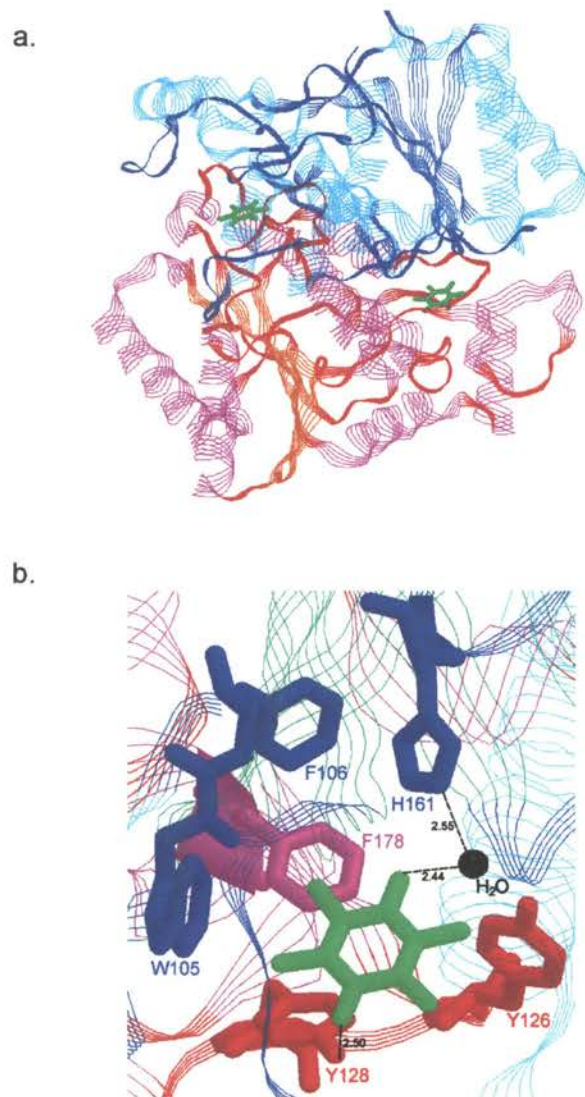
Figure 2.15. <u>Three Dimensional X-Ray Structure of NADH:Quinone Acceptor Oxidoreductase (Brookhaven Code: 1DXO)</u>. a. Overall structure: the blue and red colors indicate two identical polypeptide chains. The co-crystallized duroquinone molecules are shown in green color. b. Quinone-binding pocket of QR1. The hydrogen bonds between duroquinone and H161 or Y126 are illustrated with broken line. Other shown residues are involved to form the hydrophobic pocket for duroquinone.
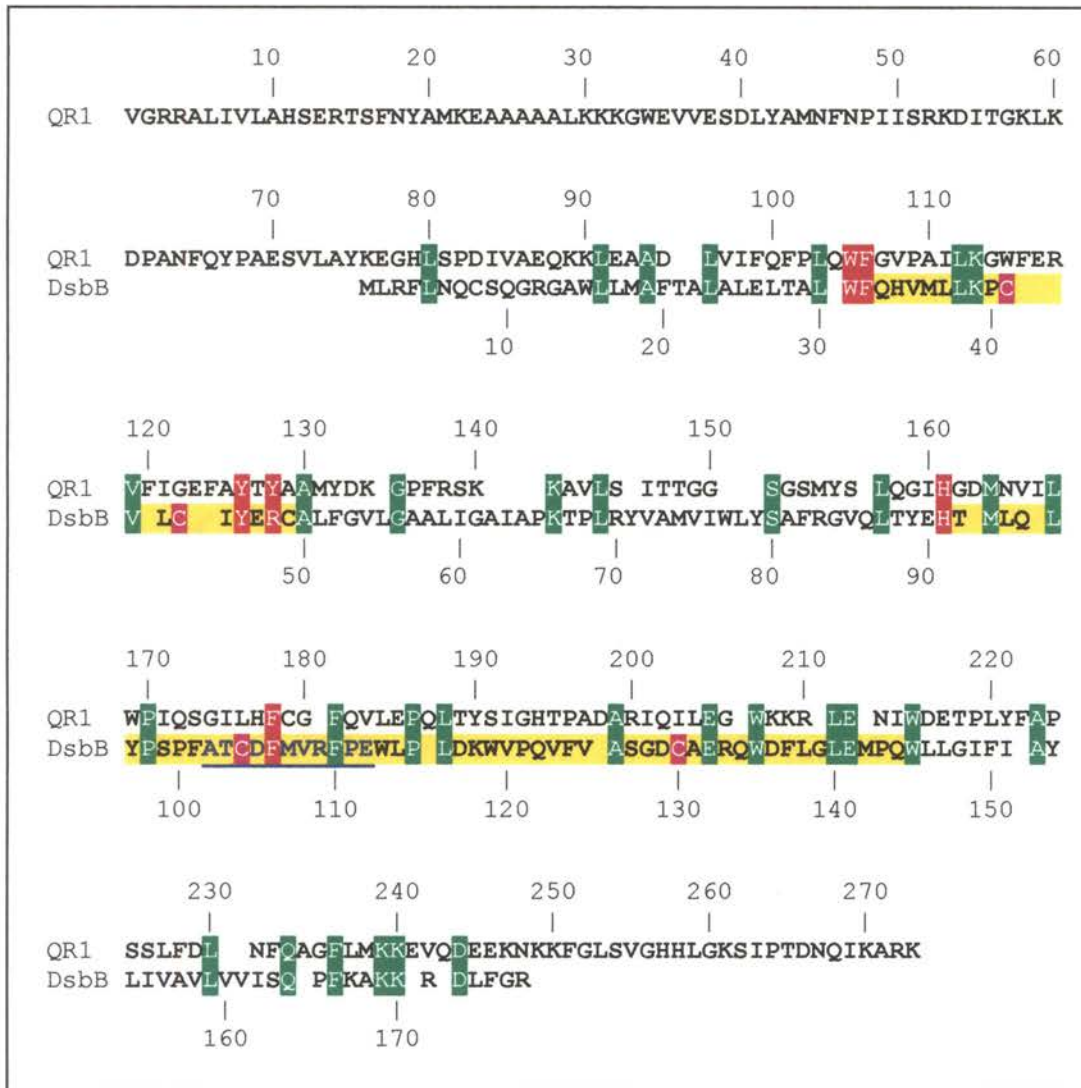
Scheme 2.7. <u>Sequence Alignment of QR1 and DsbB.</u> Periplasmic loops in DsbB are highlighted in yellow, **x**, conserved Q binding residues and functional cysteines are highlighted in red, x, other conserved residues are highlighted in green and in reversed font, x. The Q labeled sequence is underlined in blue, <u>x</u>.

101

Here we show that purified DsbB contains 0.6 mol of bound quinone per mol of protein. Since the DsbB purification protocol involves multiple columns and extensive dialysis, this implies that the quinone is rather tightly bound. The species of quinone bound to DsbB was determined to be coenzyme Q_8, the most abundant quinone found in the *E. coli* inner membrane under aerobic conditions. The ubiquinone-binding site can be titrated with externally added quinone to yield a 1:1 ratio.

The Q-binding domain in DsbB was identified by peptide sequencing and mass spectrometry of a trypsin or protease V8 digested [^{3}H]-Q peptide, which was obtained by HPLC separation of the protease digested [^{3}H]azido-Q labeled DsbB. The sequence of [^{3}H]azido peptide corresponds to residues 91-112 of DsbB sequence. The Q-binding domain is most likely located in the periplasmic interface of the cytoplasmic membrane, toward the periplasm side of the membrane. One of the highly conserved amino acid residues for DsbB activity, Cys104 is in this Q-binding region.

Simulation study of the Q-binding pocket for DsbB using QR1 as the modeling template suggests that residues W31, F32, Y46, R48, H91, F106, which are located in both periplasmic loops, might participate in the Q pocket in DsbB. Since it is found that DsbB forms homodimer in solution, the quinone pocket in DsbB would be involved in two polypeptide chains.

According to our findings from photo-affinity labeling and molecular modeling, several mutants including Y46F, R48H, H91A and Q95A have been constructed and purified by Dr. James Bardwell's lab at the University of Michigan. The kinetic study of these mutant shows that the apparent K_m value of R48H and Q95A for ubiquinone are 7-fold and 10-fold higher than the value obtained for the wild-type DsbB, respectively. In contrast, the apparent K_m of both mutants for DsbA was close to that of the wild-type enzyme. Thus, the alteration of Arg48 and Gln95 significantly reduced the affinity of the enzyme for ubiquinone without affecting its apparent K_m for DsbA.

Another mutant, H91A, had less than 10% activity of the wild-type protein. Since histidine is a common residue involved in Q-binding for many quinone proteins, it is reasonable to assume that H91 is another residue participating in the Q-binding in DsbB.

These mutagenesis studies support our Q-binding domain results based on the photo-affinity labeling and molecular modeling. However, not all residues based on the Q-pocket simulation are included in the Q-binding peptide based on the photo-affinity labeling. The Q-label peptide might not cover every residue of the Q-pocket which are located in different region of the polypeptide chain. Further explanation and data are required to figure out the quinone reductase function mechanism in DsbB.

Reference

1. Freedman, R.B. (1991) In Nall, B.T. and Dill, K.A. (eds), *Conformation and Forces in Protein Folding*. American Association for the Advancement of Science, Washington, DC, pp204~214

2. Saxena VP, Wetlaufer DB. (1970) *Biochemistry*, **9**, 5015~5022

3. Bardwell, J.C.A., McGovern, K. & Beckwith, J. (1991) *Cell*, **67**, 581~589

4. Raina, S., & Missiaka, D. (1997) *Annu. Rev. Microbiol.*, **51**, 179~202

5. Bardwell, J.C. (1994) *Mol. Microbiol.* **14**, 199~205

6. Hwang, C., Sinskey, A.J., Lodish, H.F. (1992) *Science*, **257**, 1496~1502

7. Derman, A.I., Beckwith, J. (1991) *J. Bacteriol.* **173**, 7719~7722

8. Holmgren, A. (1989) *J. Biol. Chem.*, **264**, 13963~13966

9. Russel, M. (1995) *Methods Enzymol.* **252**, 264~274

10. Weichsel, A., Gasdaska, J. R., Powis, G., Montfort, W. R. (1996) *Structure* **4**, 735

11. Creighton, T.E. (1980) *J. Mol. Biol.*, **142**, 43~62

12. Lamantia, M. & Lennarz, W.J. (1993) *Cell*, **74**, 899~908

13. Freedman, R.B., Hirst, T.R., and Tuite, M.F. (1994) *Trends Biochem. Sci.* **19**, 331~336

14. Rietsch, A. & Beckwith, J. (1998) *Annu. Rev. Genet*, **32**, 163~184

15. Kamitami, S., Akiyama, Y., Ito, K. (1992) *EMBO J.* **11**, 57~62

16. Mccarthy, A. A., Haebel, P. W., Torronen, A., Rybin, V., Baker, E. N., Metcalf, P. (2000) *Nat.Struct.Biol.* **7**, 196~199

17. Chung, J., Chen, T., Missiakas, D. (2000) *Mol. Microbiol.*, **35**, 1099~1109

18. Crooke, H., Cole, J. (1995) *Mol Microbiol.*, **15**, 1139-5110

19. Fabianek, R.A., Hennecke, H., & Thony-Meyer, L. (1998) *J. Bacteriol.*, **180**, 1947~1950

20. Bessette, P.H., Cotto, J.J., Gilbert, H.F., & Georgiou, G. (1999) *J. Biol. Chem.*, **274**, 7784~7792

21. Debarbieux, L., and Beckwith, J. (1999) *Cell* **99**, 117~119

22. Martin, J.L., Bardwell, J.C., Kunlyan, J. (1993) *Nature*, **365**, 464~468

23. Wunderlich, M., & Glockshuber, R. (1993) *Protein Science*, **2**, 717~726

24. Guddat LW, Bardwell JC, Glockshuber R, Huber-Wunderlich M, Zander T, Martin JL (1997) *Protein Sci* **6**, 1893~900

25. Grauschopf, U., Winther, J.R., Korber, P., Zander, T., Dallinger, P., *et al.* (1995) *cell* **83**, 947~955

26. Nelson, J.W., Creighton, T.E. (1994) *Biochemistry* **33**, 5974~5983

27. Kortemme, T., Creighton, T.E. (1995) *J. Mol. Biol.* **253**, 799~812

28. Jander, G., Martin, N.L., & Beckwith, J. (1994) *EMBO J.*, **13**, 5121~5127

29. Guilhot, C., Jander, G., Martin, N.L., & Beckwith, J. (1995) *Proc. Natl. Acad. Sci. USA*, **92**, 9895~9899

30. Kishigami, S., Kanaya, E., Kikuchi, M., & Ito, K (1995) *J. Biol. Chem.*, **270**, 17072~17074

31. Kishigami, S., Ito, K (1996) *Genes Cells*, **1**, 201~208

32. Gilbert, H.F. (1997) *J. Biol. Chem.* **272**, 29399~29492

33. Bader, M., Muse, W., Ballou, D.P., Gassner, C., & Bardwell, J. (1998) *Cell.*, **98**, 217~227

34. Bardwell, J.C., Lee, J.O., Martin, N.L., & Belin, D. (1993) *Proc. Natl. Acad. Sci. USA*, **90**, 1038~1042

35. Bader, M., Muse, W., Zander, T., & Bardwell, J. (1998) *J. Biol. Chem.*, **273**, 10302~10307

36. Kobayashi, T., Kishigami, S., Sone, M., Inokuchi, H., Mogi, T. (1997) *Proc. Natl. Acad. Sci. USA*, **94**, 11857~11862

37. Anraku, Y. (1998) *Annu. Rev. Biochem.* **57**, 101~132

38. Zeng, H., Snavely, I., Zamorano, P., & Javor, G.T. (1998) *J. Bacteriol.*, **180**, 3681~3685

39. Kobayashi, T. and Ito, K. (1999) *EMBO J.* **18**, 1192~1198

40. Glockshuber, R. (1999) *Nature*, **401**, 30~31

41. Xia, D., Yu, C.A., Kim, H., Xia, J.Z., Kachurin, A.M., Zhang, L., Yu. L., & Deisenhofe, J. (1997), *Science*, **277**, 60~66

42. Faig, M., Bianchet, M. A., Chen, S., Winski, S., Ross, D., Talalay, P., Amzel, L. M. (2000) *Proc. Natl. Acad. Sci. USA*, **97**, 3177~3182

43. Lee, G.Y., He, D.Y., Yu, L., and Yu, C.A. (1995) *J. Biol. Chem.,* **270**, 6193~6198

44. Shenoy, S.K., Yu, L., and Yu, C.A. (1997) *J. Biol. Chem.,* **272**, 17867~17872

45. Yang, X., Yu, L., He, D.Y., and Yu, C.A. (1998) *J. Biol. Chem.,* **273**, 31916~3192

46. Shenoy, S.K., Yu, L., and Yu, C.A. (1999) *J. Biol. Chem.,* **274**, 8717~8722

47. Yu, L., Yang, F.D., and Yu, C.A. (1985) *J. Biol. Chem.,* **260**, 963~973

48. Gu, L.Q., Yu, L., and Yu, C.A. (1990) *Biochim. Biophys. Acta.,* **1015**, 482~492

49. Darby, N.J., Raina, S., and Creighton, T.E. (1998) *Biochemistry*, **37**, 783~791

50. Riddle, P.W., Blakeley, R.L., and Zerner, B (1983) *Methods Enzymol..* **91**, 49~60

51. Redfearn, E.R. (1967).*Methods Enzymol.*, **X**, 381~384

52. Lee, G.Y. (1996) Ph.D. Thesis, Department of Biochemistry & Molecular Biology, Oklahoma State Univ.

53. Jonda, S., Huber-Wunderlich, M., Glockshuber, R. and Mossner, E. (1999) *EMBO J.*, **18**, 3271~3281

54. Wallace, B.J., and Young, I.G. (1977) *Biochim. Biophys. Acta.,* **461**, 84~100

55. Yu, C.A., and Yu, L. (1982) *J. Biol. Chem.,* **257**, 6127~6131

56. Mossner, E., Huber-Wunderlich, M. and Glockshuber, R. (1998) *Protein Sci.,* **7**, 1233~2020

57. Zapun, A., Missiakas, D., Raina, S., and Creighton, T. E. (1995) *Biochemistry* **34**, 5075-5089

58. Joelson, T., Sjoberg, B. M., and Eklund, H. (1990) *J. Biol. Chem.,* **265**, 3183-3188

59. Bessette, P.H., Cotto, J., Gilbert, H. and Georgiou, G. (1999) *J. Biol. Chem.,* **274**, 7784~7792

60. Lenaz, G. (1985) *Coenzyme Q*, John Wiley & Sons, Inc.1~144

61. Bader, M., Xie, T., Yu, C.A., & Bardwell, J. (2000) *J. Biol. Chem.,* **275**, 26082~26088

62. Drapoau, G.R. (1977) *Meth. Enzymol.,* **47**, 189

63. Compton, P.D., Coll, R.J. and Fink, A.L. (1986) *J. Biol. Chem.,* **261**, 1248~1252.

64. Iverson, T. M., Luna-Chavez, C., Cecchini, G., Rees, D. C. (1999) *Science* **284**, 1961~1966

65. Yu, C.A. and Yu, L. (1981) *Biochim. Biophys. Acta.,* **639**, 99~128

$\mathcal{2}$

VITA

Tong Xie

Candidate for the Degree of

Doctor of Philosophy

Thesis: STUDY ON PROTEIN-QUINONE INTERACTION

Major Field: Biochemistry and Molecular Biology

Biographical:

Education: Graduated from Guangdong Experimental High School, Guangzhou, China
in July 1986; received a Bachelor of Science degree and a Master of Science
degree in Chemistry from Zhongshan University, Guangzhou, China in July 1990
and July 1993, respectively. Completed the requirement for the Doctor of
Philosophy degree with a major in Biochemistry and Molecular Biology at
Oklahoma State University in December, 2000.

Experience: Employed as a teaching and research associate in the School of Life
Science, Zhongshan University from July 1993 to December 1995; employed by
Oklahoma State University, Department of Biochemistry and molecular Biology
as a graduate research associate from January 1996 to present.